DEGRADATION OF VINYL CHLORIDE AND 1,2-DICHLOROETHANE BY ADVANCED REDUCTION PROCESSES

A Dissertation

by

XU LIU

Submitted to the Office of Graduate Studies of
Texas A&M University
in partial fulfillment of the requirements for the degree of

DOCTOR OF PHILOSOPHY

Chair of Committee,	Bill Batchelor
Committee Members,	Ahmed Abdel-Wahab
	Bryan Boulanger
	Qi Ying
	Yongheng Huang
Head of Department,	Robin L. Autenrieth

August 2013

Major Subject: Civil Engineering

ABSTRACT

A new treatment technology, called Advanced Reduction Process (ARP), was developed by combining UV irradiation with reducing reagents to produce highly reactive species that degrade contaminants rapidly. Vinyl chloride (VC) and 1,2-dichloroethane (1,2-DCA) pose threats to humans and the environment due to their high toxicity and carcinogenicity. In this study, batch experiments were conducted under anaerobic conditions to investigate the degradations of VC and 1,2-DCA with various ARP that combined UV with dithionite, sulfite, sulfide or ferrous iron. Complete degradation of both target compounds was achieved by all ARP and the reactions were found to follow pseudo-first-order decay kinetics. The effects of pH, sulfite dose, UV light intensity and initial contaminant concentration on the degradation kinetics were investigated in the photochemical degradation of VC and 1,2-DCA by the sulfite/UV ARP. The rate constants were generally promoted by raising the solution pH. The optimal pH conditions for VC and 1,2-DCA degradation were pH 9 and pH 11,respectively. Higher sulfite dose and light intensity were found to increase the rate constants linearly for both target contaminants. A near reciprocal relation between the rate constant and initial concentration of target compounds was observed in the degradation of 1,2-DCA. The rate constant was observed to be generally independent of VC concentration, but with a slight increase at lower concentrations. A degradation mechanism was proposed that described reactions between target contaminants and reactive species such as the sulfite radical and hydrated electron that were produced in

the photolysis of sulfite solution. A mechanistic model that described major reactions in the ARP system was developed and explained the dependence of the rate constant on those experimental factors. Chloride ion and chloroethane were detected as the major degradation products at acid and neutral pH. An increase in pH promoted the extent of dechlorination with complete dechlorination being observed at pH 11 for both VC and 1,2-DCA. Due to the rapid degradation kinetics in these ARPs, this new treatment technology may be applied to remove various contaminants in water and wastewater.

ACKNOWLEDGEMENTS

I would like to express my deep appreciation and gratitude to my advisor, Dr. Bill Batchelor, for the patient guidance and mentorship he provided to me, all the way from the first day I started my study at Texas A&M University, through to completion of my Ph.D. degree. Dr. Batchelor provided an environment where it is a pleasure to conduct research and to take on scholarly responsibilities. His intellectual heft is matched only by his genuinely good nature and down-to-earth humility, and I am truly fortunate to have had the opportunity to work with him.

I would also like to thank my committee members, Dr. Ahmed Abdel-Wahab, Dr. Bryan Boulanger, Dr. Qi Ying and Dr. Yongheng Huang, for their friendly guidance, thought provoking suggestions, and the general collegiality that each of them offered to me over the years. I would like to thank Dr. Kung-Hui Chu, Dr. Roy Hann, Dr. Sandun Fernando and Dr. Michael Sherman, for contributions that each of them made to my intellectual growth during my years of study at Texas A&M University.

I wish to express my sincere gratitude to my Masters advisor, Dr. Paul T. Sun, for his continuous encouragement and guidance to my Ph.D. study and daily lives. I would also like to thank his wife, Jessie, who always treats me as a family member and help me overcome many difficulties.

I want to express my thanks to my colleagues, Dr. Bhanu Prakash Vellanki, Dr. Sunhee Yoon, Dr. Nasr Bensalah, for their hard work and warm help in preparing our papers.

I’d like to thank all my friends, Duan Yuhang, Vamsi Botlaguduru, Zhang Jingyuan, Luo Guofan, Wang Li, Kun-Ching Cho, Wang Baixin, Li Jingyi, Sri Harsha Kota, Chen Gang, Wang peng, Wu Li, Zheng Ce, Dong Yimai, Pang Chengzong and Deng Chunhua, who have shared with me both my gladness and my sadness in America. I also want to extend my gratitude to the Qatar National Research Fund, which provided the grant for this research, and to *Chemical Engineering Journal* and *Science of the Total Environment*, which published section 2 and 3 in my dissertation.

I especially thank my parents. My hard-working parents provided me unconditional love and care. I love them so much. I would not have made it this far without them. The best outcome from these past five years is finding my best friend, soul-mate, and wife, Yao Xing. There are no words to convey how much I love her. I truly thank Yao for her love, sacrifice, and kind indulgence. I feel that what we both learned a lot about life and strengthened our commitment and determination to each other and to live life to the fullest.

TABLE OF CONTENTS

Page

LIST OF FIGURES

Page

LIST OF TABLES

Page

1. INTRODUCTION

1.1. Introduction

Chlorinated organics in industrial discharge, surface water, groundwater and contaminated soils pose a great threat to humans and the environment. Full or partial dechlorination is required to transform hazardous chlorinated organics to non-toxic or less toxic compounds with more stability and less mobility. Nondestructive technologies such as adsorption, volatilization or liquid extraction have been used to change phase in which the contaminant exists, but they do not destroy the contaminant itself. Destructive technologies include both chemical oxidation-reduction and biological degradation and both are well developed to degrade chlorinated organics. However, most conventional treatment processes require long reaction times to achieve successful dechlorination due to slow degradation kinetics.

An example of a new set of treatment processes, called Advanced Reduction Processes (ARPs), is applied in this research. ARPs are similar to Advanced Oxidation Processes (AOPs), which combine an oxidant with various activating methods to produce highly reactive oxidizing radicals. ARPs combine different reductants with various activating methods to produce highly reactive reducing species. These reactive species can destroy target contaminants rapidly as they have great potential to overcome kinetic limitations.

Target contaminants, activation methods and appropriate reductants are the major components in ARPs. In this research, vinyl chloride (VC) and 1,2-dichloroethane (1,2-DCA) are chosen as the target chlorinated contaminant due to their hazardous properties and their resistance to being destroyed by conventional chemical or biological technologies. Ultraviolet light (UV) at 253.7 nm is chosen as the activation method, since previous research demonstrated its high efficiency in producing highly reactive compounds in AOPs. Dithionite, sulfite, sulfide and ferrous iron are selected as reductants since they can yield reactive species.

The overall goal of this research is to characterize the degradation of VC and 1,2-DCA by various ARPs, to investigate the effects of process variables on the degradation kinetics, to study the degradation mechanism and to develop a mechanistic model that can describes complex reaction in various ARPs.

1.2. Research Objectives and Methodology

The overall research can be divided into four tasks as described below:

1.2.1. Reagent screening based on the feasibility and effectiveness for removal of VC

Batch experiments were conducted with UV irradiation as the activation method and with various reductive reagents (dithionite, sulfite, sulfide and ferrous iron) in order to investigate the degradation extent of vinyl chloride. The effect of pH was also

considered, because at different pH values, the reagent existed in different forms. Three different pH values (3, 7, and 10) were applied for all reagents. Three control experiments were conducted in the first stage. First, a blank control experiment was conducted without a reagent and without irradiation. A solution of vinyl chloride was buffered at 3 pH values and kept in a quartz reactor inside anaerobic chamber in order to avoid oxygen and light. This experiment was conducted for a sufficient time to monitor any changes in the concentration of vinyl chloride. Second, a reagent control experiment was conducted with the presence of a reagent, but without irradiation. The selected reagent was added into a vinyl chloride solution and buffered at 3 pH values. The solution was kept in the dark and in an anaerobic chamber to avoid oxygen. Results could show how effectively the reagent reacted with and removed vinyl chloride without UV-L irradiation. Third, an irradiation control experiment was conducted without a reagent but with UV irradiation. The vinyl chloride solution was prepared at 3 pH values and put under UV-L irradiation. Vinyl chloride concentration was measured by GC-FID during the experiment. Results showed how effectively the UV-L irradiation destroyed vinyl chloride without any reagents. Results of all the control experiments results were compared with the results of experiments that combined reagents with UV-L irradiation.

In the experiments that combine reagents and UV-L irradiation, a selected reagent was added into VC solution and was buffered at 3 pH values before starting UV irradiation. The vinyl chloride degradation curve was developed and degradation effectiveness was compared at different pH values for different reagents. Results of these experiments are presented and discussed in Section 2.

1.2.2. Characterize kinetics of VC degradation in the sulfite/UV ARP

In the kinetic study of VC degradation by the sulfite/UV, a number of factors were evaluated for their abilities to affect the degradation kinetics of VC. These factors include light intensity, reductant dose, pH value and initial VC concentration. Each factor was tested at 4 levels. A total of 10 to 12 samples were taken during each experiment and appropriate sampling times were chosen to obtain about the same amount of VC removed in each sampling period. The VC degradation rate constants were used to compare the effects of process variables on VC removal at different experimental conditions. Results of kinetic experiments of VC degradation are presented and discussed in Section 3.

1.2.3. Degradation of 1,2-DCA by various ARPs and kinetic study

Similar reagent screening experiments were conducted for 1,2-DCA degradation by various ARPs and similar kinetic study was performed with the sulfite/UV ARP. Results of these experiments are presented and discussed in Section 4.

1.2.4. Quantum yield analysis in the degradation of VC and 1,2-DCA by the sulfite/UV ARP

The efficiency of sulfite/UV ARP in degrading VC and 1,2-DCA were investigated and expressed by the quantum yield. The effects of process variables such as solution pH, sulfite dose, UV light intensity and initial VC/1,2-DCA concentration on the initial quantum yield were studied and presented in Section 5.

1.2.5. Mechanistic model development for the degradation of VC and 1,2-DCA by the sulfite/UV ARP

A mechanistic model was developed based on the major reactions in the sulfite/UV ARP system. This model considered 76 reactions in the system and simulated the change of concentrations of 33 species. The effectiveness and accuracy were tested by comparing the model simulations with kinetic data collected in the degradation experiments of VC and 1,2-DCA by the sulfite/UV ARP. The development process and model validation are presented in Section 6.

2. PHOTOCHEMICAL DEGRADATION OF VINYL CHLORIDE WITH AN ADVANCED REDUCTION PROCESS (ARP) – EFFECTS OF REAGENTS AND PH*

A new treatment technology, called an Advanced Reduction Process (ARP), was developed by combining UV irradiation with reducing reagents to produce highly reactive reducing free radicals that degrade contaminants. Batch experiments were performed under anaerobic conditions to investigate the degradation of vinyl chloride (VC) by this ARP. All degradation reactions were found to follow a pseudo-first-order decay model and the rate constants (k_{obs}) were characterized for all experimental conditions. The influence of pH on k_{obs} was studied in experiments with direct photolysis as well as experiments with ARPs using reagents activated by ultraviolet (UV) light. Values for k_{obs} in direct photolysis were found to be 0.012, 0.011, and 0.018 min^{-1} at pH 3, 7 and 10, respectively. Values of most of the k_{obs} in experiments with ARP increased at all pH values compared with corresponding values obtained for direct photolysis. The increase in k_{obs} was due to the production of reactive species produced by photochemical reaction of the reducing reagents with UV light. The pH effect on k_{obs} observed with the ARP can be explained in terms of changes in the absorption spectra of the reagents at various pH. The rate of light absorption determines the rate of formation of the reactive

*Reprinted with permission from "Photochemical Degradation of Vinyl Chloride with an Advanced Reduction Process (ARP)–Effects of Reagents and pH" by Liu X, Yoon S, Batchelor B, Abdel-Wahab A., 2013. *Chem Eng J*, 215-216: 868–875.Copyright [2013] by Elsevier.

species which determines the rate of contaminant degradation. Chloride ion and chloroethane were detected as the products of VC degradation. The increase in pH value was shown to promote the transformation of VC to chloride.

2.1. Introduction

Large amounts of chlorinated organics are manufactured every year for industrial and commercial uses. Vinyl chloride (VC) is a chlorinated ethene that is present as a colorless gas with high toxicity and carcinogenicity toward humans. The major sources of VC contamination in surface water, ground water and air are releases from industrial plants that synthesize polyvinyl chloride (PVC) and other vinyl products (Kielhorn et al., 2000). Incineration of chlorinated plastic and landfill volatilization can also cause VC pollution. VC is always found at hazardous waste and landfill sites as a biodegradation product of chlorinated organics. In particular, VC is present as an accumulated intermediate during the reductive degradation of highly chlorinated solvents such as tetrachloroethene (PCE) or trichloroethene (TCE) (Lee et al., 1998). Drinking water can be contaminated by contact with PVC pipes, which can release VC under solar radiation (Al-Malack and Sheikheldin, 2001). VC is found at many contaminated sites that are listed in U.S. Environmental Protection Agency's National Priority List (ATSDR, 2006). The EPA has established regulations to control human exposure to VC. The Maximum Contaminant Level (MCL) for VC in drinking water is 0.002 mg/L and Maximum Contaminant Level Goal (MCLG) is zero.

Traditional treatment technologies have been widely used for chlorinated organics remediation. Nondestructive technologies such as adsorption, volatilization or liquid extraction has been used to transfer VC from the phase in which the contaminant exists, but they do not destroy the contaminant itself. Destructive technologies such as chemical oxidation-reduction and biological degradation are well developed to degrade chlorinated organics. Many studies have shown that the VC and other chloroethenes can be degraded by microorganisms under aerobic (Freedman and Herz, 1996; Koziollek P et al., 1999; Rasche et al., 1991) and anaerobic conditions (Cupples et al., 2003; He et al., 2003). The mechanisms of VC biodegradation involve both direct metabolism and cometabolism (Hartmans and Bont, 1992). The end products in VC biodegradation are found to be methane, ethene and carbon dioxide, as reported in several studies conducted by Bradley (Bradley and Chapelle, 1996; Bradley and Chapelle, 1998; Bradley and Chapelle, 1999; Bradley and Chapelle, 2000). Several studies (Andreas et al., 2009; Song and Carraway, 2005) have shown that chloroethenes (PCE, TCE, DCE and VC) can be degraded by zero-valent iron (ZVI). Most of this research shows a reductive dechlorination mechanism. The degradation pathways of VC involve both β-elimination and hydrogenolysis, as demonstrated by carbon isotope fractionation technology (Elsner et al., 2008). Non-chlorinated products including ethene, methane, ethane and acetylene have been identified and complete dechlorination of chloroethenes has been demonstrated, although most studies focus on PCE or TCE dechlorination (Butler and Hayes, 1999; Zhang, 2003). Direct photolysis of VC and other chloroethenes have been studied in both the gas phase and the liquid phase (Chu and Jia, 2009; Li et al., 2004; Lin

et al., 2009; Mertens and Sonntag, 1995). Acetylene, carbon monoxide, carbon dioxide, chloride ion, formyl chloride and monochloroacetaldehyde are the major products under 185 nm irradiation (Gurtler et al., 1994). Carbon monoxide, formic acid and phosgene ($COCl_2$) are reported as major byproducts in the studies that investigate the photodegradation of VC on porous TiO_2 pellets (Sano et al., 2002; Yamazaki et al., 2004).

Several chemicals, such as dithionite, sulfite, sulfide and ferrous iron, have been demonstrated to be able to yield highly reactive species when they are properly activated. These reactive species include sulfur dioxide radical (Makarov, 2001), sulfite radical, hydrated electrons (Buxton et al., 1988; Ranguelova et al., 2010; Shi and Shi, 1994) and hydrogen gas (Hara et al., 1999). Their reactions with inorganic and organic compounds have been well studied (Cheng et al., 2009a; Fischer and Warneck, 1996; Grodkowski and Neta, 2000; Melsheimer and Schlogl, 1997). Ultraviolet light (UV) in the UVC region (100~280nm) has been used for disinfection of drinking water and wastewater. Photons at shorter wavelength have higher energy so they have a greater potential to provide sufficient energy to break chemical bonds and yield free radicals. The low pressure UV lamp used in this research has an irradiation wavelength at 253.7 nm. It's already widely used as an activation method for advanced oxidation processes (AOPs) for treatment of organic pollutants in wastewater (Guo et al., 2009; Li et al., 2010; Zhao et al., 2010).

A new group of water and wastewater treatment technologies, called advanced reduction processes, have been developed by combining activation methods with

reducing reagents to yield reducing free radicals, which can destroy contaminants. In this study, UV irradiation at wavelength of 253.7 nm was used as activation method. Dithionite, sulfite, sulfide and ferrous iron were used as reducing reagents. The objective of this study is to investigate the VC degradation by combining UV irradiation with those reducing reagents. Direct photolysis (no reagents) is also studied in order to compare with the results obtained with ARP. Degradation kinetics was studied in all experimental conditions. The pH effect on the pseudo-first-order rate constant (k_{obs}) was investigated and a mechanism for pH dependence of k_{obs} was postulated. Both inorganic and organic degradation products were identified in this study.

2.2. Experimental Section

2.2.1. Reagents

All reagents were used as received. Vinyl chloride gas (1000 ppm in nitrogen), Vinyl chloride standard solution (200 μg/mL in 2-propanol) and sodium hydrosulfide (hydrate, 68%) were purchased from Sigma-Aldrich (St. Louis, MO, USA). Sodium dithionite (89%) and sodium sulfite (anhydrous, 98.6%) were purchased from Avantor Performance Materials (Center Valley, PA, USA). Ferrous sulfate (7-hydrate,99.4%) was purchased from Mallinckrodt chemicals (Hazelwood, MO, USA). Potassium phosphate (anhydrous, 97%), potassium hydrogen phosphate (anhydrous, 98%), potassium dihydrogen phosphate (99%) and phosphoric acid (85%) were purchased from

Alfa Aesar (Ward Hill, MA, USA). The vinyl chloride gas (1000 ppm in nitrogen) was used to prepare VC solution by sparging the gas into deoxygenated deionized water. Vinyl chloride standard solution (200 μg/mL in 2-propanol) was used for calibration.

2.2.2. Experimental procedure

All solution preparation and irradiation experiments were conducted in an anaerobic chamber (Coy Laboratory Products Inc., Grass Lake, MI, USA), which was filled by a gas mixture (95% nitrogen and 5% hydrogen) and equipped with an oxygen and hydrogen analyzer, fan boxes and palladium catalyst STAK-PAK (Coy Laboratory Products Inc., Grass Lake, MI, USA). The anaerobic chamber was flushed with gas mixture as required to keep the anaerobic condition. All UV irradiation experiments were carried out in 17-ml, cylindrical, UV-transparent quartz reactors purchased from Starna cells, Inc (Atascadero, CA, USA). The UV light source is a Phillips TUV PL-L36W/4P lamp which emitted short-wave UV radiation with a peak at 253.7 nm. The light intensity was adjusted by changing the distance between the UV lamp and the reactor and was measured by a UVC 512 light meter (Professional Measurement), which was calibrated by the modified method of ferrioxalate actinometer (Murov et al., 1993). The primary modification was to use the ferrozine method for the colorimetric analysis of iron (Stookey, 1970) using an Agilent 8453 UV-visible spectroscopy system.

Batch experiments were conducted with 4 reductive reagents separately and the extent of vinyl chloride degradation was measured. The effect of pH (pH 3, 7, 10) was

also investigated for all reagents. Three control experiments were conducted in the first stage. First, a blank control experiment was conducted without a reagent and without irradiation. A solution of VC was buffered at 3 pH values and kept in a quartz reactor inside anaerobic chamber in order to avoid oxygen and light. Second, a reagent control experiment was conducted with the presence of a reagent, but without UV irradiation. The selected reagent was added into the VC solution and buffered at 3 pH values. The solution was kept in dark and in an anaerobic chamber to avoid oxygen and light. Third, an irradiation control (direct photolysis) experiment was conducted without a reagent but with UV irradiation. The VC solution was buffered at 3 pH values and put under UV irradiation. Results of all the control experiments were compared with the results of ARP experiments (experiments that combined reagents with UV irradiation). In the ARP experiments, selected reagents were added into VC solution and buffered at 3 pH values before starting UV irradiation. The concentrations of sodium dithionite, sodium sulfite, sodium hydrosulfide and ferrous sulfate were 20, 12.5, 8.4 and 49 mg/L, respectively. During the experiment, a total of 6 samples were taken to measure the concentration of VC by gas chromatography.

2.2.3. Analytical methods

For all analysis of VC, a 5-mL sample was taken from the quartz reactor and injected into O.I. Analytical Eclipse 4660 purge and trap sample concentrator (O.I. Analytical, College Station, TX, USA), which was employed for sample pre-treatment.

The sample was purged for 11 minutes at 30°C and then desorbed for 2 minutes before injection into a HP 6890 gas chromatography (GC) (Agilent, Santa Clara, CA, USA). During the GC analysis, the trap was baked at 210 °C for 10 min. The HP 6890 GC equipped with a FID detector and a DB-5 column (30 m * 0.25 mm * 1 μm). The GC inlet temperature was set at 225°C. Helium was used as carrier gas and its flow rate was constant at 1.3 mL/min with spilt ratio of 50:1. The oven temperature program was employed with initial temperature of 35 °C for 3 min, followed by a ramp of 20 °C/min to 80 °C, followed by another ramp of 40 °C/min to 200 °C and held for 2 min. Chloride ion was expected as a VC degradation product and it was measured by an ion chromatography Dionex 500 (Thermo Fisher Scientific Inc, Bannockburn, IL, USA) equipped with AS-16 column and AS40 automated sampler following Standard Method 4110.

2.3. Result and Discussions

2.3.1. Reagents control for VC degradation

The results of reagent control (Figure 28 in Appendix A) showed that at all pH values there was little reaction between VC and the four reagents when no activation method was applied.

2.3.2. Direct photolysis - pH effect

Direct photolysis experiments with VC were performed at various pH values and results are shown in Figure 1. VC degradation kinetics under direct photolysis was found to follow a pseudo-first-order decay model:

$$-\frac{dC}{dt} = k_{obs} * C \quad (2.1)$$

With the analytical solution as

$$C_t = C_0 * e^{-k_{obs}*t} \quad (2.2)$$

where C_0 is the initial concentration of VC (mg/L), C_t is the VC concentration (mg/L) measured during the irradiation at time t, and k_{obs} is the pseudo-first-order rate constant (min^{-1}).

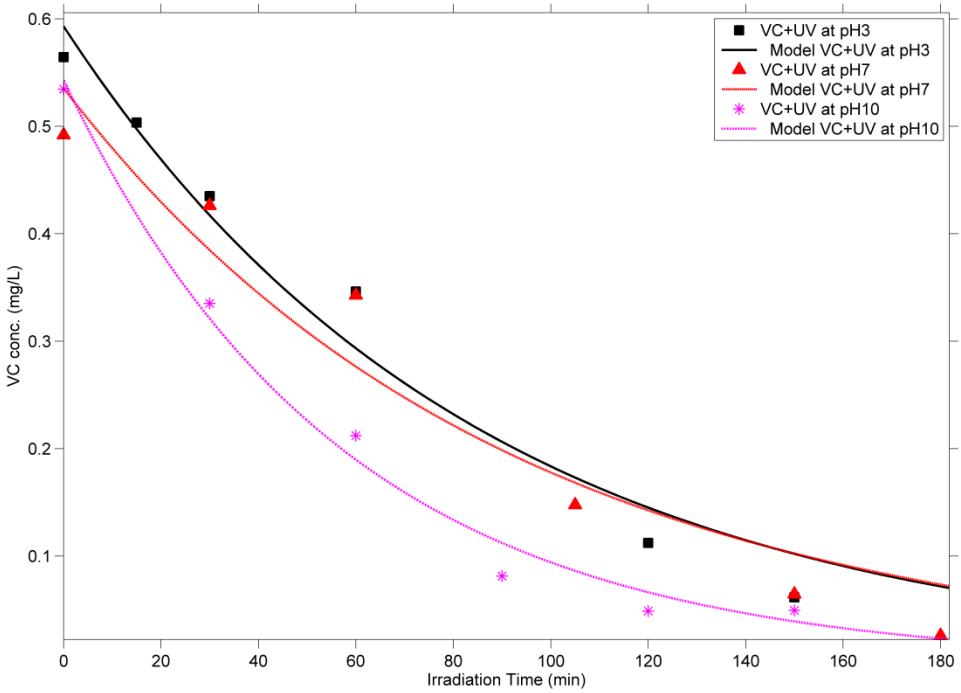

Figure 1. Pseudo first order decay of VC in direct photolysis at pH 3, pH 7 and pH 10.

At a UV light intensity of 2400 μw/cm^2 and initial VC concentration of 0.5 mg/L, the rate constants were found to be 0.012, 0.011, and 0.018 min^{-1} at pH 3, 7, and 10, respectively. This indicates that higher pH favors VC degradation by direct photolysis. Along with the degradation of VC, chloride ion was detected by IC as the only inorganic chlorine-containing end product. There are two possible pathways that could describe the transformation from VC to chloride, and they are shown in Figure 2. Pathway 1 (Klan and Wirz, 2009) is a photofragmentation and rearrangement process in which the vinyl and chlorine radicals are formed by hemolytic cleavage and then the chloride ion and acetylene are formed through a rearrangement process. This mechanism is called β-elimination. Pathway 2 shows a hydrogenolysis mechanism that involves a

single electron transfer in the first step that results in the formation of vinyl radical. Then the vinyl radical reacts with hydrogen ion to form ethene along with the release of chloride ion.

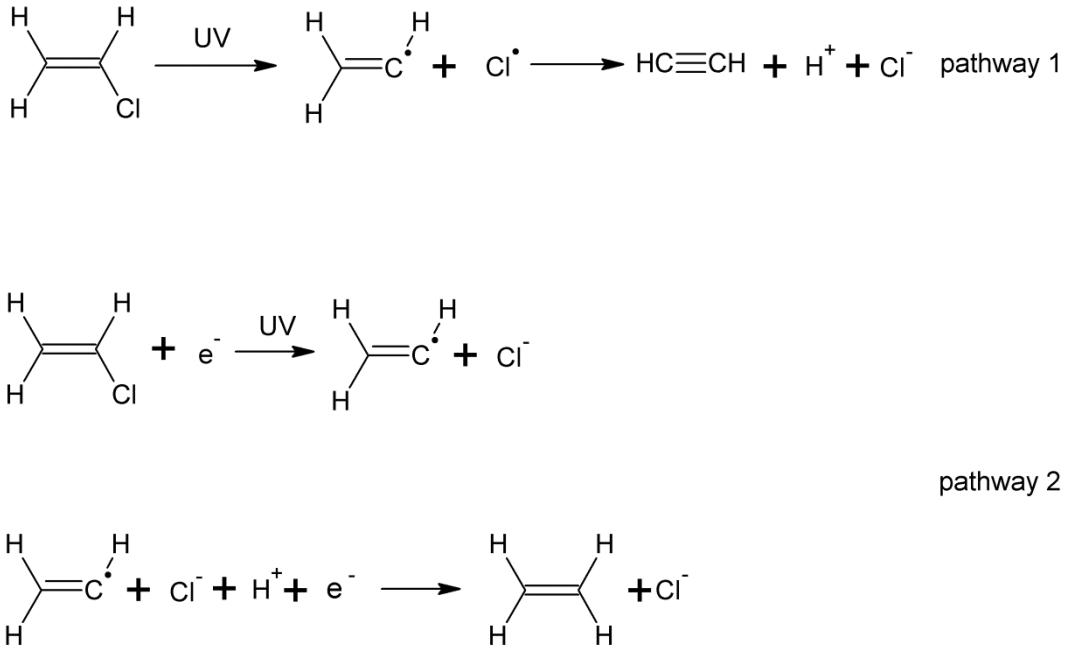

Figure 2. Pathways for VC transformation.

The direct photolysis reaction (pathway 1) produces a proton that would tend to lower solution pH, while the hydrogenolysis reaction (pathway 2) consumes a proton that would tend to raise solution pH. However, experiments on direct photolysis were conducted with a buffer so the pH was relatively constant through the reaction. To further identify the reaction mechanism of direct photolysis, another experiment was conducted without buffer to track the pH change during the reaction. Before UV irradiation at 4500 μw/cm^2 began, the pH of the VC solution was measured as 8.55 and

it decreased during the experiment to reach pH 7.31 after irradiation for 310 minutes. The drop in pH can be explained by the proton production shown in pathway 1. Further evidence is that gas-phase photolysis of VC with 185nm UV light has been reported to follow pathway 1 (Gurtler et al., 1994). In a similar study on photodissociation of the vinyl radical at 243 nm, acetylene has been reported to be the final product. In our experiments, the final organic product was not identified, but acetylene could be one of the organic products, since both pathway 1 and pathway 2 involve the production and dissociation of vinyl radical (Ahmed et al., 1999).

2.3.3. VC degradation in ARP - production of reactive species

VC degradation by various ARP was found also to follow the pseudo-first-order decay model. The rate constants for all experiments are summarized in Table 1. The rate constants for all ARP experiments, except the combination of UV with ferrous iron at pH 7, are larger than those obtained by direct photolysis, i.e. UV irradiation without reagents. The increase in rate constant could be explained by the production of highly reactive species, such as radicals or hydrated electrons, which are produced when the reagents are irradiated with UV light. These highly reactive species have the potential to greatly increase rates of VC degradation. The following paragraphs will discuss the reagents used and how they can produce reactive species.

Table 1. Comparison of k_{obs} (min^{-1}) in all experimental conditions

Combinations	Pseudo first-order decay rate constants (min^{-1})		
	pH3	pH7	pH10
UV only	0.012	0.011	0.018
UV+ dithionite	0.053	0.093	0.10
UV+ sulfite	0.025	0.030	0.059
UV+ sulfide	0.031	0.087	0.028
UV+ Fe^{2+}	0.058	0.0015	0.059

Dithionite has a long and weak S-S bond that can be broken to produce two sulfur dioxide radical anions ($SO_2^{\bullet-}$) (Makarov, 2001). This free radical is a strong and reactive reductant with a standard reduction potential of -0.66 v (Mayhew, 1978). Sodium dithionite is often used in physiology experiments as a means of lowering the redox potential of aqueous solutions. The absorption peak of dithionite is reported to have its maximum at 315 nm, so light with wavelength near this value may provide enough energy to break the S-S bond and yield free radicals (McKenna et al., 1991; Ohlsson et al., 1986; Pukhovskaya et al., 2005). A recent study reported that the sulfur dioxide radical could be produced by the UV irradiation of dithionite solution at 254 nm and demonstrated that the brilliant red X-3B was reduced by the sulfur dioxide radical (Fu et al., 2010). Thus the sulfur dioxide radical anion could be the reactive

intermediates that increased the degradation rates in the experiment of dithionite/UV ARP.

Sulfite also has the potential to produce reductive radicals when activated. Depending on the pH, the dominant species are sulfite (SO_3^{2-}), hydrogen sulfite (HSO_3^{2-}), and sulfurous acid (H_2SO_3). Free radicals can be produced when sulfite is under UV irradiation or through other mechanisms such as reaction with transition metals or human neutrophils (Buxton et al., 1988; Ranguelova et al., 2010; Shi and Shi, 1994), or though the irradiation of solution that contains ferric iron and sulfite under sunlight or UV-visible light(Zuo and Zhan, 2005; Zuo et al., 2005). Under UV irradiation, reactive species formed from sulfite are the sulfite radical anion ($SO_3^{\bullet-}$) and the hydrated electron, as shown in Eq. (2.3). The sulfite radical anion ($SO_3^{\bullet-}$) has both oxidizing and reducing ability as shown in Eq. (2.4) and (2.5). Its reaction with oxygen demonstrates its potential to be used as reductant.

$$SO_3^{2-} + h\nu \rightarrow SO_3^{\bullet-} + e^- \quad (2.3)$$

$$SO_3^{\bullet-} + e^- \rightarrow SO_3^{2-} \quad (2.4)$$

$$SO_3^{\bullet-} + O_2 \rightarrow SO_5^{\bullet-} \quad (2.5)$$

In addition, the aqueous electron can be produced with $SO_3^{\bullet-}$ under UV irradiation and can also act as a strong reductant (Chawla et al., 1973). The observed

increase in rates of VC degradation in the sulfite/UV ARP compared to rates during direct photolysis could be due to the sulfite radical or hydrated electron, or both of them. It was also observed that at the same pH value, the rate constants for the sulfite/UV ARP are smaller than those for the dithionite/UV ARP. This indicates some reactive intermediates in the sulfite/UV ARP are less reactive or are produced at lower rates than the sulfur dioxide radical that is produced in the dithionite/UV ARP. This is also supported by an electron spin resonance (ESR) study (Ozawa and Kwan, 1983) that concluded that the sulfite radical is a much weaker reductant than the sulfur dioxide radical.

Sulfide in solutions can absorb UV light with an absorption peak at 230 nm (Dzhabiev and Tarasov, 1993; Kotonarou et al., 1992; Melsheimer and Schlogl, 1997). The UV irradiation of sulfide solutions produces reactive species such as excited state bisulfide ion (HS^{-*}) (Linkous et al., 2004) or hydrogen atom (Khriachtchev et al., 1998), as shown in Eqs. (2.6) and (2.7). These reactive species could promote degradation of VC.

$$HS^- + h\nu \rightarrow HS^{-*} \tag{2.6}$$

$$H_2S + h\nu \rightarrow H + SH \tag{2.7}$$

Many studies show that reductive dechlorination with zero-valent iron involves a mechanism in which ferrous iron complexes are formed from zero-valent iron and act as

reductants for chlorinated organics. Some studies (Airey and Dainton, 1966; Borowska and Mauzerall, 1987; Korolev and Bazhin, 1978; Zuo and Deng, 1997) have reported that UV irradiation of ferrous iron solutions produces hydrated electrons or hydrogen atom which reacts to form hydrogen gas. Therefore, the hydrated electron is probably the species that causes the rate of VC degradation to be higher for the ferrous iron/UV ARP than for direct photolysis.

2.3.4. VC degradation by ARP - effect of pH

Solution pH had a great influence on rate constants in all experiments with ARP and there are at least two explanations for these pH effects. First, the formation rate of reactive species, such as radicals or hydrated electrons, could be different at different pH. Second, those reactive intermediates could degrade VC at various reaction rates at different pH values.

The rate of formation of reactive intermediates should be proportional to the rate of light absorption. Light absorption would depend on the wavelength and the concentrations of light-absorbing species present, which can change with pH. The absorption spectra for all reagents were measured by UV-visible spectrophotometer and the results are shown in Figure 3.

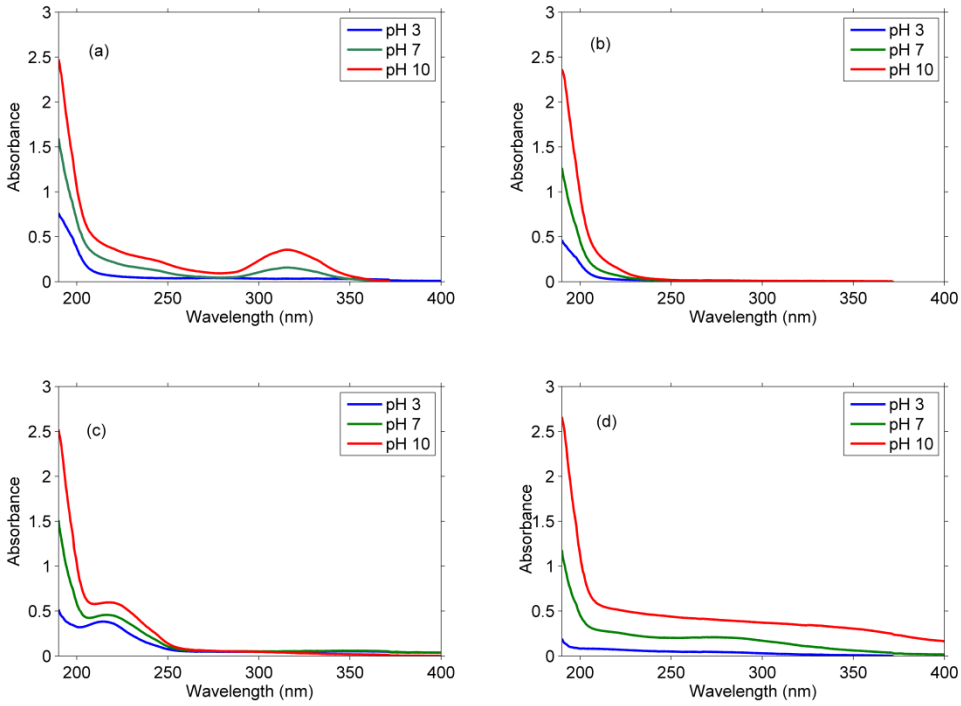

Figure 3. Absorption spectra in 10 mM buffer solution at different pH values of (a) dithionite, (b) sulfite, (c) sulfide, and (d) ferrous iron.

The total concentrations of each reagent and the buffer were the same as those used in reagent/UV ARP experiments. Generally the absorbances of all solutions decrease with an increase in wavelength. The solution with dithionite has an absorption peak around 315 nm and the solution with sulfide has an absorption peak around 220 nm. The absorbances at 253.7 nm of solutions of dithionite, sulfide or ferrous iron increased with pH, as shown in Figure 4. At a concentration of 20 mg/L, the absorbances of sodium sulfite solution at all pH values were too low to show real differences. However, literature has reported that the absorbance of sulfite solution increased with increase in pH at this wavelength (Deister et al., 1986).

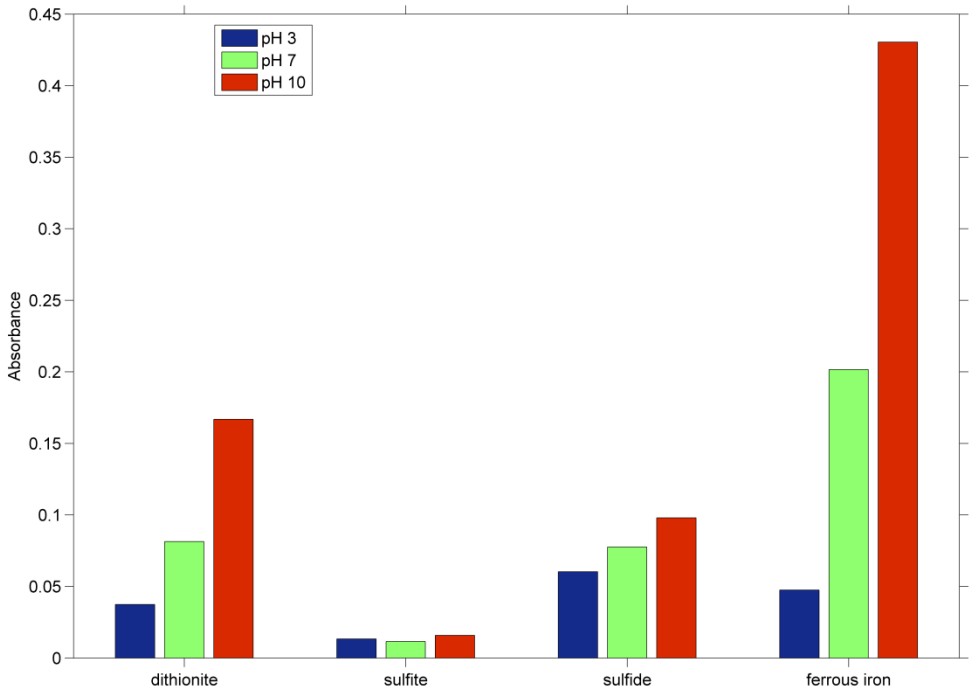

Figure 4. Absorbance of all reagents at 253.7 nm at different pH values.

In order to explain the effect of the change in absorbance on the production rate of reactive species, a simple kinetic model was developed to describe the rate of the reaction in which a reagent (A) photolyze to form a radical (R) (Eq. (2.8)). A detailed derivation of the rate equation is described in Appendix A and the result is shown in Eq. (2.9). A is the reagent, R is radical, φ is the quantum yield of the reagent, I_0 is the light intensity entering the reactor, $\varepsilon_{ln,A}$ is the molar absorptivity of reagent, $\varepsilon_{ln,vc}$ is the molar absorptivity of VC, C_A is the molar concentration of the reagent, C_{vc} is the molar concentration of VC and L is the thickness of reactor in direction of light path. Sulfite is an example of a reagent that can exist in different forms as a function of pH, e.g. H_2SO_3,

HSO_3^-, SO_3^{2-}. If the C_A is taken to be the total concentration (sum of individual species), then the molar absorptivity must be a weighted average of the values for each individual species. Therefore, when pH is changed, the value of C_A would remain constant, but the average molar absorptivity would change when the molar absorptivities of individual species are different. Therefore, a change in pH would result in a change in rate of production of radicals by changing the concentrations of reagent species, which would absorb different amounts of light and potentially produce radicals at different efficiencies.

$$A+h\nu \rightarrow R \tag{2.8}$$

$$r = \frac{\varphi \varepsilon_{\ln,A} C_A I_0 \left(1-\exp\left(-(\varepsilon_{\ln,A} C_A + \varepsilon_{\ln,VC} C_{VC})L\right)\right)}{(\varepsilon_{\ln,A} C_A + \varepsilon_{\ln,VC} C_{VC})L} \tag{2.9}$$

The effect of pH on light absorption in the dithionite/UV and sulfite/UV ARPs can explain the pH dependence of VC degradation rate constant, because when pH increases, the absorbance of dithionite or sulfite solution increases, which increases the rate of degradation and this is what was observed. However, the effects of pH on light absorption in the other ARP were not consistent with the effects on the rate constants.

Some studies (Sun et al., 2008; Xie and Cwiertny, 2010) had demonstrated that the sulfur dioxide radical, which would be produced by irradiation of dithionite is more reactive at higher pH, which could also explain the behavior in the dithionite/UV ARP.

The sulfite radical is one of the reactive intermediates that could be produced by irradiation of sulfite solutions. At higher pH, the sulfite ion (SO_3^{2-}) dominates and at lower pH the hydrogen sulfite ion (HSO_3^-) dominates. The quantum yields for sulfite radical by photolysis of the sulfite ion (SO_3^{2-}) at 253.7 nm and for hydrogen sulfite ion (HSO_3^-) at 213.9 nm were reported by Fischer (Fischer and Warneck, 1996) to be 0.39±0.04 and 0.19±0.03, respectively. The quantum yield for HSO_3^- solution at 253.7 nm was not identified but could have a value around 0.19, which would be smaller than the quantum yield of the sulfite ion at 253.7nm. Therefore, the pH effect on the VC degradation rate constant for the sulfite/UV ARP could be explained by the different formation rate of sulfite radical at various pH values. In addition, the hydrated electrons that were produced with the sulfite radical could also act as the reactive specie that causes VC degradation. It was found that in the range pH 4 to pH 5, the hydrated electron concentration was 4 to 5 orders of magnitude lower than at pH 9 (Fischer and Warneck, 1996), which could explain the pH dependence of the rate constant.

In the sulfide/UV ARP, pH 7 gave the highest degradation rate constant. In this study, the dominant species of sulfide at pH 3 would be H_2S and at pH 10 it would be HS^-. At pH 7, the two species (H_2S, HS^-) would be about equal in concentration, as calculated by Visual MINTEQ (http://www2.lwr.kth.se/English/OurSoftware/vminteq/). The reactive intermediate formed from photolysis of sulfide would be the excited state bisulfide ion (HS^{-*}) or the hydrogen atom (H). However, no studies were found to discuss the pH effect on the rate of formation of the reactive species or on the rates of they react with other compounds. In this study, the favorable neutral pH condition for

VC degradation with the sulfide/UV ARP could not be well explained by the rates of formation or reaction of reactive intermediates.

In the ferrous iron/UV ARP, similar values of the degradation rate constant were observed at pH 3 and pH 10, but a much smaller value was obtained at pH 7. Hydrated electrons were the reactive intermediates that could cause VC degradation and their formation by photolysis of ferrous iron is shown in Eq. (2.10) (Airey and Dainton, 1966).

$$Fe^{2+} + h\nu \rightarrow Fe^{3+} + e_{aq}^{-} \qquad (2.10)$$

A Study (Borowska and Mauzerall, 1987) has shown that the formation rate of hydrogen gas in irradiated solutions of ferrous iron reached a minimum near pH 5, and they proposed a mechanism in which absorption of lower wavelengths by Fe^{2+} causes hydrogen production at low pH and absorption of higher wavelengths by $FeOH^{+}$ causes hydrogen production at higher pH. The results presented here are similar, in that a minimum rate is observed, but it was observed at a higher pH (pH 7 in this study). These differences could be caused by the differences in the wavelengths of light used or by the presence of phosphate buffer. Table 2 shows the equilibrium distribution of soluble species of Fe(II) calculated by Visual MINTEQ. It shows that iron-phosphate complexes dominate at all pH values, but that there are substantial differences in concentrations of Fe^{2+} and $Fe(OH)^{+}$ at the different pH values. Therefore, the pH effects observed for VC degradation could be the result of two photolysis reactions: one of Fe^{2+}

at low pH and the other of $Fe(OH)^+$ at high pH. Figure 4 shows the solutions of ferrous iron absorb more 253.7 nm light at pH 10 than pH 3, so the reaction at pH 3 would have to be more efficient (higher quantum yield) to result in a similar rate of VC degradation.

Table 2. Species distribution for dissolved ferrous iron at pH 3, pH 7 and pH 10*

	pH3	pH7	pH10
Fe^{2+}	23.7%	9.86%	6.03%
$FeH_2PO_4^+$	75.8%	16.4%	0.018%
$FeHPO_4$ (aq)	0.035%	73.5%	76.4%
$FeOH^+$	-	0.028%	15.9%
$Fe(OH)_2$ (aq)	-	-	1.10%
$Fe(OH)_3^-$	-	-	0.405%
$FeSO_4$ (aq)	0.515%	0.176%	0.087%

* 0.18 mM ferrous sulfate with 10 mM phosphate buffer

2.4. VC Degradation Products

The degradation products of VC were also investigated in this study. Chloride ion was the only chlorine-containing inorganic product identified by IC. In order to better quantify the chloride production under all experimental conditions, additional experiments were conducted at pH 7 with higher initial VC concentrations. The chlorine

transformation extent (R) measures the fraction of VC removed over the entire experiment that was converted to chloride ion and was calculated with Eq. (2.11).

$$R=(C_{\text{cl, in final chloride}})/(C_{\text{cl, in initial VC}}-C_{\text{cl, in final VC}}) \quad (2.11)$$

where R is the chlorine transformation extent, $C_{\text{cl, in final chloride}}$, $C_{\text{cl, in initial VC}}$ and $C_{\text{cl, in final VC}}$ are the final chloride ion concentration (mM), initial chlorine concentration (mM) in VC, and the final chlorine concentration in VC, respectively. The chlorine transformation extents are 76.2% in direct photolysis, 15.4% in dithionite/UV ARP, 13.6% in sulfite/UV ARP, 60.6% in sulfide/UV ARP and 51.4% in ferrous iron/UV ARP.

The similar chlorine transformation extents observed with dithionite and sulfite indicate that they may degrade VC with similar mechanisms. Some organic products from VC degradation were also identified. Chloroethane was identified as one of the major organic products in the dithionite/UV, sulfite/UV and sulfide/UV ARPs at all pH values, and with the ferrous iron/UV ARP at pH 3. However, the concentration of chloroethane was not quantified in this study. There was another major organic product shown in the chromatograms but was not identified in this study, due to overlap of its mass spectrum with that of nitrogen and oxygen in the background. By comparing of the peak area in the chromatograms, it was also noticed that at pH 10 in all ARPs, the peak area of the unidentified organic product was larger than the peak area of chloroethane. While at pH 3 and pH 7, the peak area of chloroethane was much larger than this

unidentified product. This indicates that when pH increased, the production of chloroethane decreased and the production of the unidentified product increased. To further investigate the pH influence on product distribution, another experiment was conducted with the sulfite/UV ARP at pH 9 and the chlorine transformation extent was compared to its value at pH 7. Results showed that R increased from 13.6% at pH 7 to 50.9% at pH 9. Therefore, the increase in pH promoted the transformation of chlorine in VC to chloride ion. This result also indicates that the unidentified organic product could be a non-chlorinated compound, because when it dominated the products at high pH, the chlorine transformation extents was higher.

2.5. Conclusion

In summary, complete degradation of VC was achieved with both direct photolysis and various ARP and degradation kinetics followed a pseudo-first-order decay model. Rates of degradation of VC by most ARP were higher than observed for direct photolysis (UV only) at all pH values. The improved ability of ARP to degrade VC was due to the production of highly reactive intermediates such as reducing radicals and hydrated electrons. The pH had a strong influence on degradation kinetics of VC and this was mainly due to pH changing the speciation of reagents and the resulting changes in production of reactive species. Higher pH also promoted the transformation of chlorine in VC to chloride ion and lowered the transformation from VC to chloroethane.

Due to the rapid degradation kinetics of VC, the reagents/UV ARP has the potential to degrade other chlorinated organics.

3. DEGRADATION OF VINYL CHLORIDE (VC) BY THE SULFITE/UV ADVANCED REDUCTION PROCESS (ARP): EFFECTS OF PROCESS VARIABLES AND A KINETIC MODEL*

Vinyl chloride (VC) poses a threat to humans and environment due to its toxicity and carcinogenicity. In this study, an advanced reduction process (ARP) that combines sulfite with UV light was developed to destroy VC. The degradation of VC followed pseudo-first-order decay kinetics and the effects of several experimental factors on the degradation rate constant were investigated. The largest rate constant was observed at pH 9, but complete dechlorination was obtained at pH 11. Higher sulfite dose and light intensity were found to increase the rate constant linearly. The rate constant had a little drop when the initial VC concentration was below 1.5 mg/L and then was approximately constant between 1.5 mg/L and 3.1 mg/L. A degradation mechanism was proposed to describe reactions between VC and the reactive species that were produced by the photolysis of sulfite. A kinetic model that described major reactions in the system was developed and was able to explain the dependence of the rate constant on the experimental factors examined. This study may provide a new treatment technology for the removal of a variety of halogenated contaminants.

*Reprinted with permission from "Degradation of Vinyl Chloride by the Sulfite/UV Advanced Reduction Process (ARP): Effects of Process Variables and a Kinetic Model" by Liu X, Yoon S, Batchelor B, Abdel-Wahab A., 2013. *Sci Total Environ*, 454-455: 578-583. Copyright [2013] by Elsevier.

3.1. Nomenclature

The following abbreviations are used in the paper:

ARP	Advanced Reduction Process
Sulfite/UV	The ARP that combines sulfite with UV irradiation
UV	Ultraviolet
VC	Vinyl Chloride (CH_2CHCl)

The following symbols are used in the paper:

R	reactive species that were produced when sulfite receives UV irradiation, including sulfite radical, hydrated electron and hydrogen atom
S	scavengers that could react with reactive species
P_1, P_2, P_3	products of reaction (b), (c) and (d) in Table 1.
r_1, r_2, r_3, r_4	reaction rates of reactions (a) ~ (d) in Table 1.
φ_1, φ_2	quantum yield of sulfite or VC
$\varepsilon_{ln,sulfite}$, $\varepsilon_{ln,VC}$	molar absorptivity of sulfite or VC ($M^{-1}cm^{-1}$, defined on natural logarithm basis, differs from molar absorptivity used with Beer-Lambert law for absorbance by factor of 2.303, $\varepsilon_{ln} = 2.303\ \varepsilon_{bl}$, where ε_{bl} is the decadic molar absorptivity used with the Beer-Lambert law, i.e. $I=I_0 10^{-\varepsilon Cx}$)
$C_{sulfite}$, C_{VC}, C_R, C_s	molar concentrations of sulfite, VC, reactive species and scavenger (mol/L)
I_{avg}	average light intensity in the solution ($\mu w/cm^2$)

I_0 Light intensity entering the top surface of quartz reactor ($\mu w/cm^2$)

k_3, k_4 second order rate constant of reaction (c) and (d) in Table 1. ($M^{-1}s^{-1}$)

k_{obs} the observed pseudo-first-order rate constant in VC degradation (min^{-1})

3.2. Introduction

Vinyl chloride (VC) is a chlorinated ethene that is of a concern due to its toxicity and carcinogenicity. VC is classified as a priority pollutant and has been found at many National Priority List sites established by US Environmental Protection Agency (ATSDR, 2006). The compound is produced at a large scale by the chemical industry in order to synthesize polyvinyl chloride (PVC) and the releases from those facilities are the major source of VC pollution in the atmosphere. VC contamination is also found in surface water and groundwater that were originally contaminated by chlorinated solvents such as tetrachloroethene (PCE) and trichloroethene (TCE), because their biodegradation can result in accumulation of VC (Lee et al., 1998).

Some technologies have been developed to destroy VC. Biodegradation of VC has been reported under aerobic (Begley et al., 2012; Freedman and Herz, 1996; Tiehm et al., 2008; Zhao et al., 2011) and anaerobic conditions (Hata et al., 2004; Popat and Deshusses, 2011; Smits et al., 2011), with VC acting as sole carbon and energy source or being degraded through cometabolism. Zero-valent iron (ZVI) has been used to reduce chloroethenes including PCE, TCE and VC, both in lab scale (Andreas et al., 2009) and in field study (Wei et al., 2010). Abiotic degradation of VC by nanoscale ZVI has been

reported to involve β-elimination and hydrogenolysis mechanisms with ethene, ethane and acetylene as major products (Elsner et al., 2008). VC can be absorbed from the gas phase by room-temperature ionic liquids (Cheng et al., 2009b) and it can be degraded by direct photolysis at 185nm producing both non-chlorinated and chlorinated organics (Gurtler et al., 1994). Other gas-phase VC degradation technologies involve the application of radio-frequency-powered plasma with a $Pt/\gamma\text{-}Al_2O_3$ catalyst (Yuan et al., 2011) and photocatalytic degradation by TiO_2 pellets (Sano et al., 2002; Yamazaki et al., 2004).

Sulfite species (SO_3^{2-} and HSO_3^-) have been used in the removal of chlorination byproducts but the dechlorination reactions are often slow and incomplete (Croue and Reckhow, 1989; MacCrehan et al., 1998; Yiin et al., 1987). However, sulfite has been reported to yield highly reactive species such as sulfite radical and hydrated electron when it is properly activated (Fischer and Warneck, 1996; Neta and Huie, 1985; Zuo and Zhan, 2005; Zuo et al., 2005). Ultraviolet light (UV) at 253.7 nm has been widely applied in disinfection of drinking water and wastewater and it is also used as an activation method in advanced oxidation processes (AOPs) (Li et al., 2010; Zhao et al., 2010).

A new group of water and wastewater treatment technologies, called advanced reduction processes (ARPs), have been developed by combing activation methods and reducing reagents to produce reactive species which can destroy many contaminants. One recent article describes application of the sulfite/UV ARP to the degradation of monochloroacetic acid (Li et al., 2012). To the best of our knowledge, there has been no

report on the degradation of chloroethenes with sulfite/UV treatment process. The objective of this study was to investigate the effects of solution pH, sulfite concentration, UV light intensity and initial VC concentration on the degradation kinetics of VC. A kinetic model that described the major photochemical reactions in the sulfite/UV ARP was developed to explain the influence of experimental factors on the degradation rate constants.

3.3. Materials and Methods

3.3.1. Reagents

All reagents were purchased from commercial source and used as received. Vinyl chloride gas (1000 ppm in nitrogen), vinyl chloride standard solution (200 µg/mL in 2-propanol) were purchased from Sigma-Aldrich (St. Louis, MO, USA). Sodium sulfite (anhydrous, 98.6%) was supplied by Avantor Performance Materials (Center Valley, PA, USA). Potassium phosphate (anhydrous, 97%), potassium hydrogen phosphate (anhydrous, 98%), potassium dihydrogen phosphate (99%) and phosphoric acid (85%) were purchased from Alfa Aesar (Ward Hill, MA, USA). The vinyl chloride gas was used to prepare VC solution by sparging the gas into deoxygenated deionized water. Vinyl chloride standard solution (200 µg/mL in 2-propanol) was used for calibration.

3.3.2. Experimental procedure

All experiments were conducted in an anaerobic chamber (Coy Laboratory Products Inc., Grass Lake, MI, USA), which was filled by a gas mixture (95% nitrogen and 5% hydrogen) and equipped with an oxygen and hydrogen analyzer, fan boxes and palladium catalyst STAK-PAK (Coy Laboratory Products Inc., Grass Lake, MI, USA). The anaerobic chamber was flushed with the gas mixture periodically. All UV irradiation experiments were carried out in sealed, 17-ml, cylindrical, UV-transparent, quartz reactors purchased from Starna cells, Inc. (Atascadero, CA, USA). The UV light source was a Phillips TUV PL-L36W/4P lamp, which emitted UV radiation with a monochromatic wavelength at 253.7 nm. The quartz reactor that contained samples was placed inside the anaerobic chamber and received UV irradiation perpendicular to its top surface (19.6 cm^2). The light path (reactor thickness) was 1 cm. The light intensity that entered the top surface of quartz reactor was adjusted by changing the distance between the reactor and the UV lamp and its value was recorded as I_0. Temperature was controlled around 34 ± 2 ºC by an air circulation fan box. Phosphate buffers were used to control a constant pH during all experiments.

Batch experiments were conducted as a blank control (VC only), reagent control (VC and sulfite) and irradiation control (direct photolysis of VC by UV) in order to compare with the results obtained with the sulfite/UV ARP. Batch experiments also were conducted to investigate several experimental factors that affected the degradation kinetics of VC with the sulfite/UV ARP. These factors included pH value, light

intensity, sulfite dose and initial concentration of VC. During each experiment, 10 to 12 samples were taken to measure the concentration of VC by gas chromatography. Since there was little reaction between sulfite and VC (less than 5% of initial VC depletion in 9 hours), VC samples were directly measured after irradiation without quenching the residual sulfite in solution.

3.3.3. Analytical methods

The light intensity was measured by a UVC 512 light meter (Professional Equipment, Janesville, WI, USA), which was calibrated by the modified ferrioxalate actinometer (Murov et al., 1993). The primary modification was to use the ferrozine method for the colorimetric analysis of iron (Stookey, 1970) using an Agilent 8453 UV-visible spectroscopy system (Agilent, Santa Clara, CA, USA). To analyze VC, a 5-mL sample was taken from the quartz reactor and injected into a O.I. Analytical Eclipse 4660 purge and trap sample concentrator (O.I. Analytical, College Station, TX, USA). The sample was purged for 11 minutes at 30°C and then desorbed for 2 minutes before injection into a HP 6890 gas chromatography (GC) (Agilent, Santa Clara, CA, USA). During the GC analysis, the trap was baked at 210 °C for 10 min. The GC equipped with a FID detector and a DB-5 column (30 m * 0.25 mm * 1 μm). The GC inlet temperature was set at 225 °C. Helium was used as carrier gas with a constant flow at 1.3 mL/min and the spilt ratio was 50:1. The oven temperature started at an initial temperature of 35 °C for 3 min, followed by a ramp of 20 °C/min to 80 °C, followed by another ramp of 40

°C/min to 200 °C and held for 2 min. Chloride ion was detected by an ion chromatography (Dionex 500) equipped with AS-19 column and AS40 automated sampler following Standard Method 4110.The volatile degradation products were analyzed using static head space gas chromatography-mass spectrometry (SHGC-MS). SHGC-MS was performed on Ultra GC/DSQ (ThermoElectron, Waltham, MA, USA). First, a 5-ml sample was transferred to a 10-mL vial and immediately capped with silicone rubber Teflon cap. This sample was equilibrated at 80 ^{o}C for 10 min in the static headspace sampler. A Rxi-5ms column was used with dimensions of 60 m length, 0.25 mm i.d., and 0.25 μm film thickness (Restek; Bellefonte, PA, USA). A split (1:20) injection was used with helium as the carrier gas at constant flow of 1.5 ml/min. The transfer line and ion source were held at 250 °C. The column temperature was maintained at 30 °C for 3 min; raised to 80 °C at 10 °C/min; and then raised to 200 ^{o}C at 40 ^{o}C/min. Electron impact mass spectra were recorded in the 10-100 m/z range at 70 eV ionization energy.

3.4. Results

The degradations of VC under direct photolysis and UV/sulfite ARP were found to follow a pseudo-first-order decay model, which is shown for a batch reactor in Eq. (3.1).

$$dC_{vc} / dt = -k_{obs} C_{vc} \quad (3.1)$$

where C_{vc} is the VC concentration (mg/L) measured at irradiation time t and k_{obs} is the observed pseudo-first-order rate constant (min^{-1}). Values of these rate constants and their 95% confidence intervals were determined by nonlinear least squares regression with Matlab routine nlinfit and nlparci, respectively.

The pH had no apparent influence on the direct photolysis rate constant (range from 0.0021 to 0.0052 min^{-1}), but it had a noticeable effect on kinetics in the UV/sulfite ARP, as shown in Figure 5 (a) and (b). In the sulfite/UV ARP, the rate constant increases when pH changes from 5 to 9, but it drops when pH moves from 9 to 11. The rate constants in the sulfite/UV ARP were much higher than those in direct photolysis. The rate constants in the sulfite/UV ARP exceeded those in direct photolysis by factors of 0.001, 0.025, 0.042 and 0.016 min^{-1} at pH 5, 7, 9, and 11, respectively.

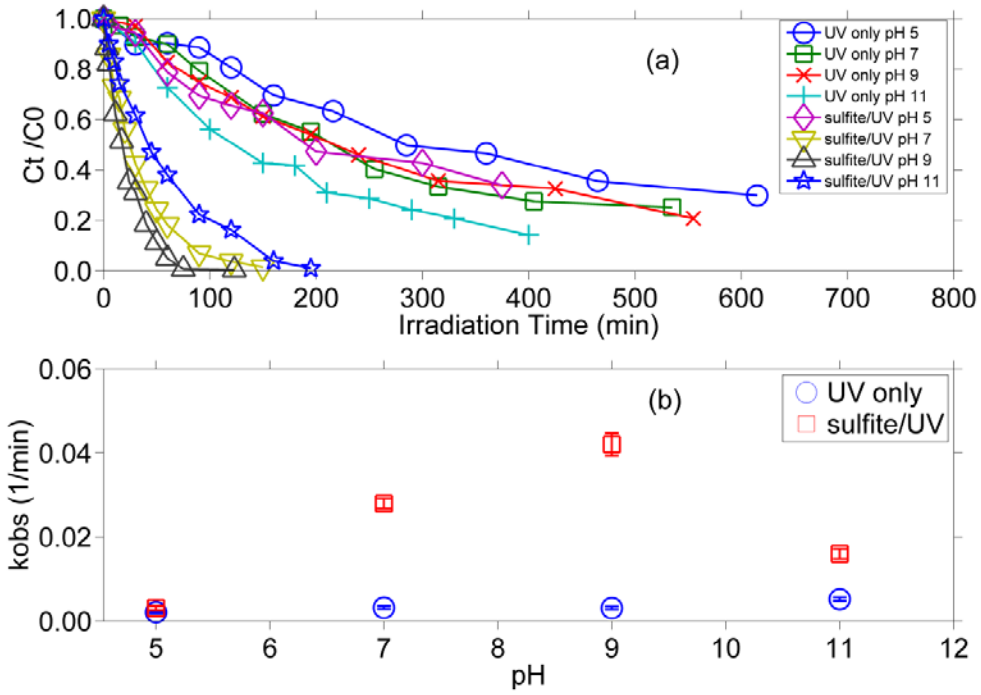

Figure 5. (a) Effect of pH on the degradation rate constant of VC in direct photolysis and sulfite/UV ARP. Conditions: $[VC]_0$=1.0 mg/L, $[Na_2SO_3]_0$=20 mg/L, light intensity= 4000 μw/cm^2. (b) The degradation rate constant versus pH. (Error bars represent 95% confidence intervals)

Figure 6 (a) and (b) show the degradation of VC with various sulfite doses and they demonstrate that the rate constant increases with sulfite concentration in an approximately linear manner.

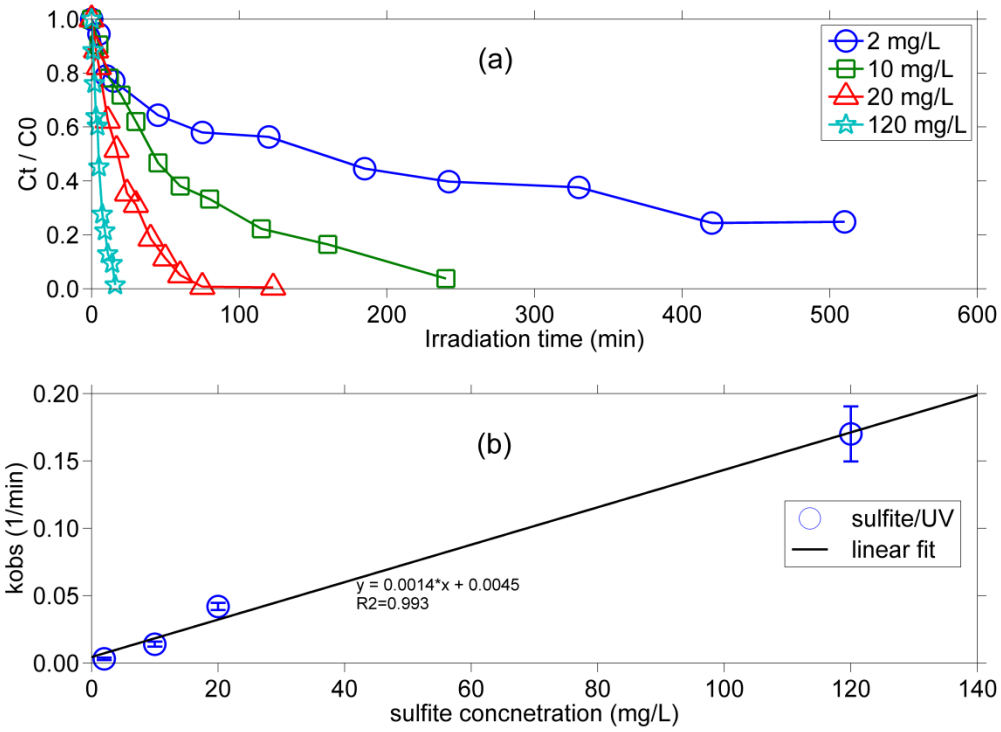

Figure 6. (a) Effect of sodium sulfite concentration on the degradation rate constant of VC in the sulfite/UV ARP. Conditions: $[VC]_0$=1.0 mg/L, pH=9.0, light intensity= 4000 μw/cm^2. (b) The degradation rate constant versus sodium sulfite concentration. (Error bars represent 95% confidence intervals)

The effect of light intensity on the degradation rate constant was determined for direct photolysis as well as in the sulfite/UV ARP and the results are shown in Figure 7 (a) and (b). In direct photolysis, the rate constant increases when higher light intensity is applied. A similar but greater influence of light intensity was observed in the sulfite/UV ARP. Rate constants in the sulfite/UV ARP were greater than those in direct photolysis by factors of 0.024, 0.043, 0.047 and 0.057 min^{-1} at light intensities of 2000, 4000, 6000 and 8000 μW/cm^2, respectively.

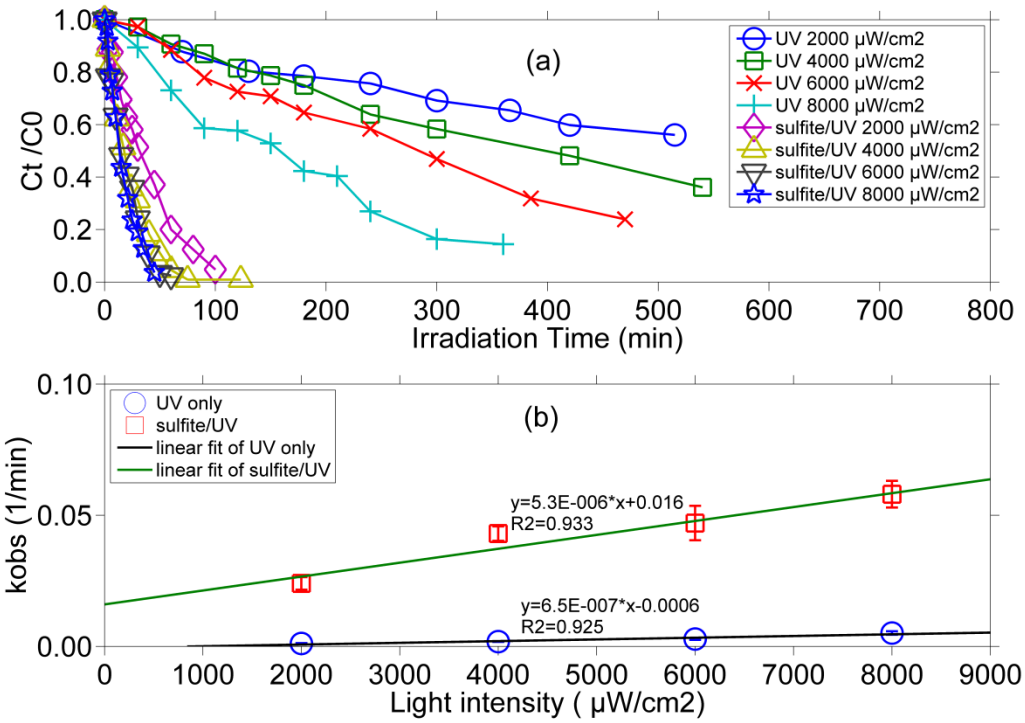

Figure 7. (a) Effect of light intensity on the degradation rate constant of VC in direct photolysis and sulfite/UV ARP. Conditions: $[VC]_0$=1.0 mg/L, pH=9.0, $[Na_2SO_3]_0$=20 mg/L. (b) The degradation rate constant versus light intensity. (Error bars represent 95% confidence intervals)

The effect of initial VC concentration on the rate constant in the sulfite/UV ARP is shown in Figure 8 (a) and (b). As the initial VC concentration rises from 1.1 mg/L to 1.5 mg/L, the rate constant decreases a little, and remains relatively constant from 1.5 mg/L to 3.1 mg/L.

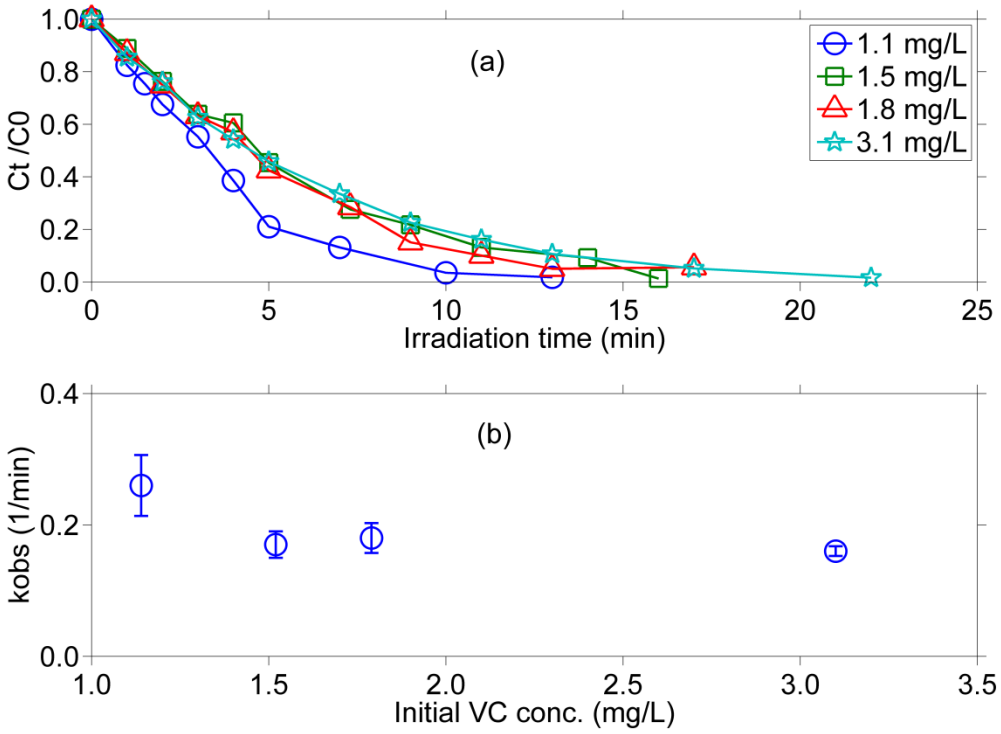

Figure 8. (a) Effect of initial concentration of VC on the degradation rate constant of VC in the sulfite/UV ARP. Conditions: pH=9.0, $[Na_2SO_3]_0$=120 mg/L, light intensity= 4000 μw/cm^2. (b) The degradation rate constant versus initial concentration of VC. (Error bars represent 95% confidence intervals)

3.5. Discussion

3.5.1. Degradation mechanisms

The major mechanism of VC degradation in direct photolysis is believed to involve the β-elimination pathway (Eq. (3.2)), which has been reported for VC photolysis in the gas phase (Gurtler et al., 1994). This mechanism is also supported by

production of chloride and hydrogen ions during the reaction. The pH was observed to decrease and more than 76% of initial chlorine in VC was transformed to chloride ion.

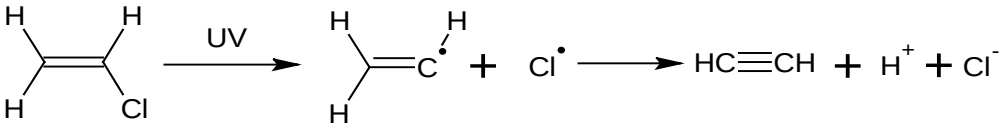

(3.2)

Degradation of VC in the sulfite/UV ARP was accomplished by reactive species such as sulfite radical, hydrated electron and hydrogen atom (Fischer and Warneck, 1996) produced by sulfite photolysis, as shown in Eqs. (3.3) and (3.4).

$$SO_3^{2-} + h\nu \rightarrow SO_3^{\bullet -} + e_{aq}^- \quad (3.3)$$

$$HSO_3^- + h\nu \rightarrow SO_3^{\bullet -} + H^\bullet \quad (3.4)$$

The sulfite radical has been reported to attach to unsaturated bonds (C=C, C=N and C≡C) and to be more active in acidic conditions (Neta and Huie, 1985; Ozawa and Kwan, 1986). The degradation of VC at lower pH could be caused by the sulfite radical following the pathways shown in Eqs. (3.5) and (3.6). First, the sulfite radical adds to the C=C bond in VC and forms a secondary radical (the product in Eq. (3.5)). Then the secondary radical can react with HSO_3^- to form sulfonate (product in Eq. (3.6)) and another sulfite radical. The sulfonate is not stable under UV irradiation and could undergo other reactions such as breaking the C-S bond, because it is weaker than the C-

Cl and C-H bonds (Luo, 2012). In this case, the product would be chloroethane (CH_3CH_2Cl), which was identified as the major organic product by GC-MS analysis at pH 5 and pH 7.

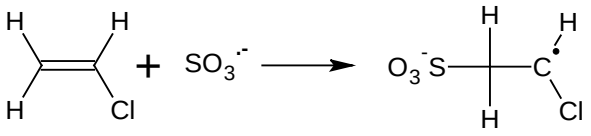

(3.5)

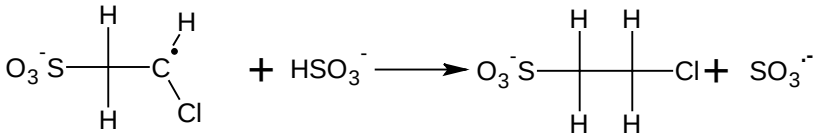

(3.6)

Eq. (3.7) shows the reaction between hydrated electron and vinyl chloride to produce a vinyl radical and a chloride ion (Koester and Asmus, 1971) with a rate constant reported as $2.5 * 10^8\ M^{-1}s^{-1}$. The ability of the hydrated electron to degrade VC has also been demonstrated with the ferrous iron/UV ARP in a previous study (Liu et al., 2013b).This reaction results in complete dechlorination of VC.

$$e_{aq}^- + H_2C{=}CHCl \rightarrow CH_2CH^{\bullet} + Cl^- \qquad (3.7)$$

The hydrogen atom has been reported to react with chlorinated organics such as chloroacetic acid to produce secondary radicals and hydrogen gas (Buxton et al., 1988) and this could be a mechanisms for VC degradation by the sulfite/UV ARP. The extent

of dechlorination was also investigated at various pH conditions and was defined as the percentage of chlorine atoms transform to chloride ions relative to the total originally in VC. At initial VC concentration of 1 mg/L, chloride analysis showed that the extent of dechlorination was small at pH 5 (11.4%) and pH 7 (17.6%), but was much higher at pH 9 (88.9%) and pH 11 (94.1%). These results indicate that the sulfite radical addition mechanism could play the major role in VC degradation at lower and neutral pH, since this mechanism involves the production of chloroethane and this would lower the extent of dechlorination. At higher pH, it seems that the degradation mechanism involves the hydrated electron reacting with VC, since it does result in dechlorination.

3.5.2. Kinetic model

A basic kinetic model was developed in order to explain the effect of pH, sulfite dose, light intensity and initial VC concentration on the degradation rate constant of VC. The model is shown in Table 3 and the details of the derivation are shown in the Appendix B.

The first two steps of this model are the photolysis of the target compound (VC) and the photolysis of the reagent (sulfite) to produce reactive species such as the sulfite radical, hydrated electron and hydrogen atom. The third and fourth steps are the reactions of the radical with the target compound and with scavengers. The model assumes that the rates of reaction of the radical are fast, so their concentrations will be very low and therefore, the derivatives of their concentrations with time will be

negligible. Applying these assumptions provides the following Eqs. that describe how process variables affect the loss of VC.

Table 3. Process kinetics and stoichiometry for VC degradation by sulfite/UV ARP

	Reactions	Rate equations	Sulfite	R	VC	S
(a)	$Sulfite+h\nu \rightarrow R$	$r_1=\varphi_1 I_{avg} \varepsilon_{ln,sulfite} C_{sulfite}$	-1	1		
(b)	$VC+ h\nu \rightarrow P_1$	$r_2= \varphi_2 I_{avg} \varepsilon_{ln,VC} C_{VC}$			-1	
(c)	$VC+R \rightarrow P_2$	$r_3=k_3 * C_{VC} * C_R$		-1	-1	
(d)	$S+R \rightarrow P_3$	$r_4=k_4 * C_s * C_R$		-1		-1

$$dC_{VC} / dt = -[\varphi_2 I_{avg} \varepsilon_{ln,VC} + k_3 (\varphi_1 I_{avg} \varepsilon_{ln,sulfite} C_{sulfite}) / (k_3 C_{VC} + k_4 C_S)] C_{VC} \quad (3.8)$$

This relationship can be used to explain the effect of process variables on the observed pseudo-first-order rate constant (k_{obs}) by combining Eqs. (3.1) and (3.8).

$$k_{obs}= \varphi_2 I_{avg} \varepsilon_{ln,VC} + k_3 \varphi_1 I_{avg} \varepsilon_{ln,sulfite} C_{sulfite} / (k_3 C_{VC} + k_4 C_S) \quad (3.9)$$

The solutions used in these experiments had UV light transmittances above about 90%, so the average light intensity (I_{avg}) can be assumed to be the same as the light intensity entering the reactor (I_0) as shown in Eq. (3.10).

$$k_{obs} = \varphi_2 I_0 \varepsilon_{ln,VC} + k_3 \varphi_1 I_0 \varepsilon_{ln,sulfite} C_{sulfite} / (k_3 C_{VC} + k_4 C_S) \quad (3.10)$$

3.5.3. Effect of pH

The pH dependence of rate constant in the sulfite/UV ARP can be explained by changes in the average molar absorptivity ($\varepsilon_{ln,sulfite}$) and quantum yield (φ_1) of sulfite, both of which affect k_{obs} (Eq. (3.10)). The molar absorptivities for sulfite solutions were measured over a range of pH and the results are shown in Table 4. These values are consistent with a model that calculates the solution absorptivity as the sum of the ionization fractions for bisulfite and sulfite times molar absorptivities for those species (Table 4).

The increase in $\varepsilon_{ln,sulfite}$ would result in an increase in the rate of light absorption and therefore, in the rate of formation of reactive species ($r_1 = \varphi_1 I_{avg} \varepsilon_{ln,sulfite} C_{sulfite}$). This would result in an increase in the concentration of reactive species and an increase in the rate of degradation of VC. Changes in absorptivity can explain the increases in k_{obs} over the range from pH 5 to pH 9, but cannot explain the decrease between pH 9 and pH 11, since there is little difference in absorptivity over that pH range. One possible explanation for the decrease at the highest pH could be that a higher concentration of scavengers (C_S) exists at pH 11, which would lower the degradation rate constant (Eq. (3.10)).

Table 4. Species distribution in sulfite solution* and molar absorptivities at different pH values (ionization fractions calculated by Visual MINTEQ)

pH	Fraction HSO_3^- (α_{hso3}^-)	Fraction SO_3^{2} (α_{so3}^{2-})	Measured $\varepsilon_{ln,sulfite}$ ($M^{-1}cm^{-1}$)	Model** $\varepsilon_{ln,sulfite}$ ($M^{-1}cm^{-1}$)
5.2	0.980	0.010	17.5	17.5
7.5	0.317	0.682	35.0	34.1
9.0	0.014	0.986	40.1	41.6
10.9	0.0001	0.999	41.9	41.9

*0.16mM sodium sulfite solution

** $(\varepsilon_{ln,sulfite})_{model} = \alpha_{hso3}^- (17.4) + \alpha_{so3}^{2-} (42.0)$

The change of pH could also change the quantum yields of reactive species (sulfite radical, hydrated electron, hydrogen atom). In particular, a change to lower pH would shift from production of the hydrated electron to production of the hydrogen atom (Fischer and Warneck, 1996) and these species would probably have different reactivities with VC. Other unknown changes in production or scavenging of reactive species could occur at the higher pH and cause the observed decrease in observed rate constant.

3.5.4. Effect of sulfite dose

The change of sulfite dose could influence the degradation rate constant in at least two ways, depending on whether VC is being degraded by direct photolysis or by radicals produced by photolysis of sulfite. If direct photolysis of VC is the dominant degradation mechanism, the effect of an increase in sulfite concentration would be to decrease k_{obs} due to the increased absorbance of solution, which determines the averaged light intensity in solution. The averaged light intensity can be expressed by Eq. (3.11) with detailed derivations in Appendix B. Eq. (3.11) shows that when sulfite concentration ($C_{sulfite}$) increases with other factors kept constant, the averaged light intensity will decrease. The decrease of averaged light intensity then would lower the first term in Eq. (3.9), which represents the impact of direct photolysis on the degradation rate constant (k_{obs}).

$$I_{avg} = \frac{I_0\left(1-\exp\left(-(\varepsilon_{\ln,sulfite}C_{sulfite} + \varepsilon_{\ln,VC}C_{VC})L\right)\right)}{(\varepsilon_{\ln,sulfite}C_{sulfite} + \varepsilon_{\ln,VC}C_{VC})L} \tag{3.11}$$

However, if VC degradation is dominated by reaction with radicals produced by the photolysis of sulfite, then increasing the concentration of sulfite will tend to increase the rate of light absorption and the rate of radical formation, thereby increasing the rate of VC degradation. This promotion effect is limited when the concentration of sulfite is so large that substantially all of the light is absorbed in the solution. In that case,

additional sulfite will not result in significant increase in VC degradation. In this study, the experimental results showed that the rate constant increased with sulfite concentration and a linear fit was conducted in Figure 6 (b). This result indicates that the primary mechanism of VC degradation is reaction with radicals produced by sulfite photolysis. In Figure 6 (b), the intercept of the linear fit was calculated as 0.0045 min^{-1}, which is a prediction for the value of the observed first-order rate constant for the direct photolysis of VC. This value is reasonably close to the value of 0.0031 min^{-1}, which was measured in direct photolysis experiments without addition of sulfite.

3.5.5. Effect of influent light intensity

The kinetic model predicts that k_{obs} will be proportional to influent light intensity (I_0). Higher light intensity results in proportionally higher rates of formation of reactive species (r_1) and a higher rate of direct photolysis of VC (r_2). Thus, k_{obs} should increase proportionally with I_0, as long as a constant fraction of radicals that are produced to react with VC. The results shown in Figure 7 (b) indicate that k_{obs} was very nearly proportional to I_0 for direct photolysis, as indicated by the near-zero intercept. However, the intercept of the regression line for the sulfite/UV ARP was substantial, so that k_{obs} was not proportional to I_0. This non-zero intercept could indicate that sulfite can react with VC in the absence of UV light. However, this is not the case, since the reagent control experiments showed little reaction between VC and sulfite without UV irradiation. Another possible explanation is that a smaller fraction of radicals produced

by sulfite photolysis were effective in reacting with VC at higher light intensities. The actual degradation mechanism is likely a complex one with many reactions among radicals and scavengers. However, the kinetic model simplifies the degradation mechanism and so it may not be able to fully predict the effect of light intensity.

3.5.6. Effect of initial VC concentration

Figure 8 shows the results of experiments to evaluate the effect of initial VC concentration on VC degradation kinetics. The observed first-order rate constant was generally constant with a slight decrease observed after the lowest concentration. The way the kinetic model predicts the effect of VC concentration on the first-order rate constant can be seen more clearly by simplifying Eq. (3.10) as shown in Eq. (3.12). In this equation, C_1 is $\varphi_2 I_0 \varepsilon_{ln,VC}$, C_2 is $k_3\varphi_1 I_0 \varepsilon_{ln,sulfite} C_{sulfite}$ and C_3 is $k_4 C_S$.

$$k_{obs} = C_1 + C_2/(k_3 C_{VC} + C_3) \quad (3.12)$$

The kinetic model predicts that the rate constant would be constant when VC concentration is high ($k_{obs}=C_1$). This would occur when photolysis of VC dominates reaction with reactive species as the main degradation mechanism. Experimental measurements show that this is not the case. The kinetic model also predicts that k_{obs} will be constant when C_3 is much larger than $k_3 C_{VC}$, which would occur when scavenging is high ($k_{obs}=C_1+C_2/C_3$). The importance of scavenging can be seen in

quantum yield for the reaction that degrades VC. This can also be considered the efficiency (φ_r) of the degradation reaction and is defined as the moles of VC degraded per mole of reactive species produced. When assuming that sulfite radical is the only reactive species to cause VC degradation, the values of φ_r were calculated to be 0.28±18%, 0.25±12%, 0.28±13% and 0.47±4.6% with the initial VC concentration at 1.14, 1.52, 1.79 and 3.10 mg/L, respectively. The details of this calculation are provided in the Appendix B. The results indicate that about 50%~70% of reactive species react with compounds other than VC, i.e. scavengers. If the hydrated electron or H atom also reacts with VC, the value of φ_r would be even lower. Therefore, it appears that the scavenging effect is important, which supports the observation that the degradation rate constant for VC is not sensitive to the change of initial concentration of VC in the studied range.

3.6. Conclusion

Complete degradation of VC was observed during direct photolysis and during application of the sulfite/UV ARP and both systems followed pseudo-first-order decay kinetics. The dependence of the rate constant on pH was mainly due to the effect of pH on distribution of sulfite species, which affected the rate of light absorption and the types of reactive species produced. The observed rate constant increases linearly with an increase in sulfite dose and influent light intensity. The rate constant was observed to be generally independent of VC concentration, but with a slight increase at lower

concentrations. The faster degradation rates observed in the sulfite/UV ARP were due to the production of reactive species such as the sulfite radical, hydrated electron and hydrogen atom. A basic kinetic model was developed and applied to explain the effects of experimental variables on the degradation kinetics. Considering the rapid degradation kinetics observed in the sulfite/UV ARP, this technology has the potential to degrade other oxidized organic contaminants.

4. DEGRADATION OF 1,2-DICHLOROETHANE WITH ADVANCED REDUCTION PROCESSES (ARPS): EFFECTS OF PROCESS VARIABLES AND MECHANISMS

1,2-dichlroroethane (1,2-DCA) is a widely used chemical with potential to harm the environment and human health. In this study, successful degradation of 1,2-DCA was achieved with various advanced reduction processes (ARPs) that combine ultraviolet (UV) irradiation with various reagents (dithionite, sulfite, sulfide, ferrous iron). The degradation kinetics in the sulfite/UV ARP was found to follow a pseudo-first-order decay model and the effects on kinetics of several factors were studied. More than 90% of initial 1,2-DCA was removed within 20 minutes in alkaline conditions (pH 8.2, 9.0 and 11.0) while it took 130 minutes to reach same removal at pH 7.0. Increasing the sulfite dose and UV light intensity caused the rate constant to increase linearly, but higher initial 1,2-DCA concentrations resulted in lower rate constants. Scavenging experiments with nitrate and nitrous oxide demonstrated the aqueous electron is the major species causing 1,2-DCA degradation in the sulfite/UV ARP, while the sulfite radical appears to be more important in degradation of vinyl chloride. The dechlorination of 1,2-DCA to chloride ion was enhanced by raising the solution pH with more than 90% dechlorination obtained at pH 11. This work supports application of ARPs to degradation of other chlorinated organics.

4.1. Introduction

1,2-dichloroethane (1,2-DCA) is one of several chlorinated aliphatic hydrocarbons that are often found in air, water and soils. The predominant use of 1,2-DCA is in the synthesis of polyvinyl chloride (PVC) pipes, but it is also widely used as a solvent to remove lead from gasoline (ATSDR, 2001) or extract oil from pesticides and pharmaceuticals(Gwinn et al., 2011) . The contamination by 1,2-DCA is frequently found in surface and ground water near locations where vinyl products are manufactured. Due to its high volatility, 1,2-DCA can be released to the air during its manufacture and transport. 1,2-DCA has been determined to be a probable human carcinogen by the U.S. EPA and the international Agency for Cancer Research (IARC). The maximum contamination level (MCL) for 1,2-DCA in the drinking water is set as 5 µg/L by U.S. EPA and the Maximum Contaminant Level Goal (MCLG) is set as zero (EPA, 2011).

Due to its adverse effects on human health and its persistence in the environment, many treatment technologies have been applied to remove 1,2-DCA from water. Biodegradation of 1,2-DCA has been studied intensively and it has been demonstrated that 1,2-DCA can be degraded under both aerobic and anaerobic conditions(Dinglasan-Panlilio et al., 2006; Kocamemi and Cecen, 2010; Smidt and de Vos, 2004). However, the incomplete biodegradation of 1,2-DCA leads to the accumulation of more hazardous byproducts such as vinyl chloride (Le and Coleman, 2011). Physical or chemical treatment of 1,2-DCA has also been investigated. Several studies have shown that 1,2-

DCA can be successfully degraded by a number of methods: nanoscale zero-valent-iron/copper (Huang et al., 2011; Wei et al., 2012), hydrogen sulfide (Barbash and Reinhard, 1989), the electrochemical degradation on stainless-steel electrodes (Bejankiwar et al., 2005) or the Fenton's oxidation process (Vilve et al., 2010). Atmospheric contamination by 1,2-DCA draws more attention because of its high volatility. Decomposition of 1,2-DCA in the gas phase usually employs surface catalytic reactions and the reactions generally follow the hydrodechlorination mechanism(Aochi and Farmer, 1997; Pirard et al., 2011; Shalygin et al., 2011). Photolysis (Yano and Tschuikowroux, 1979), radio frequency plasma(Li et al., 2003) and photo-catalytic reactions(Lin et al., 2011) also have been reported to effectively degrade 1,2-DCA in the gas phase.

Advanced Reduction Processes (ARPs) have been developed in our previous study to degrade chlorinated organic contaminants such as vinyl chloride (VC) (Liu et al., 2013a; Liu et al., 2013b). ARPs combine reducing reagents with activation methods to produce highly reactive species that are capable of rapid and effective dechlorination. In this study, ultraviolet light (UV) at 253.7 nm was used as the activation method, since it was widely used in the treatment of organic contaminants by Advanced Oxidation Processes (AOPs) (Guo et al., 2009; Li et al., 2010; Zhao et al., 2010). A number of reducing reagents (dithionite, sulfite, sulfide, ferrous iron) were tested for their abilities to produce reactive species that could degrade 1,2-DCA. The objective of this study is to investigate: (1) the effectiveness of these ARPs in the degradation of 1,2-DCA; (2) the effects of system variables (pH, UV light intensity, reagent dose and initial 1,2-DCA

concentration) on degradation kinetics; (3) the degradation mechanism; (4) the dechlorination efficiency; and (5) development of a basic kinetic model that can describe the assisted photochemical degradation of 1,2-DCA.

4.2. Materials and Methods

4.2.1. Materials

1,2-DCA (analytical standard, ≥99.0%), chloride standard (1000 mg/L), nitrate standard (1000 mg/L), nitrous oxide (99%) and sodium hydrosulfide (hydrate, 68%) were purchased from Sigma-Aldrich (St. Louis, MO, USA). Sodium dithionite (89%) and sodium sulfite (anhydrous, 98.6%) were purchased from Avantor Performance Materials (Center Valley, PA, USA). Ferrous sulfate (7-hydrate,99.4%) was purchased from Mallinckrodt chemicals (Hazelwood, MO, USA). Phosphate buffers (5 mM) were prepared using potassium phosphate (anhydrous, 97%), potassium hydrogen phosphate (anhydrous, 98%), potassium dihydrogen phosphate (99%) and phosphoric acid (85%) that were purchased from Alfa Aesar (Ward Hill, MA, USA). All solutions were prepared in deoxygenated ultrapure water that was obtained from Barnstead Ultrapure Water Purification Systems (Thermo Scientific, Asheville, NC, USA) and was deoxygenated by spiking N_2 gas into the ultrapure water.

4.2.2. Experimental procedure

All experiments were conducted in an anaerobic chamber (Coy Laboratory Products Inc., Grass Lake, MI, USA), which was filled by a gas mixture (95% nitrogen and 5% hydrogen) and equipped with an oxygen and hydrogen analyzer, fan boxes and palladium catalyst STAK-PAK (Coy Laboratory Products Inc., Grass Lake, MI, USA). The anaerobic chamber was flushed with the gas mixture periodically. The UV light source was a Phillips TUV PL-L36W/4P lamp, which was fixed in a cabinet horizontally and emitted UV radiation with a monochromatic wavelength at 253.7 nm. In all UV irradiation experiments, the solutions were contained in sealed quartz reactors (cylindrical, 17mL, 4.7 cm in diameter and 1 cm in thickness) purchased from Starna cells, Inc. (Atascadero, CA, USA). A quartz reactor was placed under the UV lamp and received UV irradiation perpendicularly to its top surface (around 19.6 cm^2). The light intensity was adjusted by changing the distance between the reactor and the UV lamp. Temperature was controlled around 34 ± 2 ºC by an air circulation system. Phosphate buffers were used to control a constant pH during experiments.

4.2.3. Experimental plan

First, the reagents screening experiments were carried out to investigate the effectiveness of reducing reagents in producing reactive species and degrading 1,2-DCA. A blank control (only 1,2-DCA, no reagents, no UV), a reagent control (1,2-DCA with

only a reagent, no UV) and an irradiation control (1,2-DCA with only UV, no reagent) were performed. Then the ARP experiments that combined UV with dithionite, sulfite, sulfide or ferrous iron were carried out at different pH values in order to study their ability to degrade 1,2-DCA compared with control experiments. In each experiment, 3 or 4 samples were taken at different times and the concentration of 1,2-DCA was measured by GC-FID.

Second, the results of the first set of experiments were used to identify the sulfite/UV ARP as the most promising ARP for further kinetic study. The effects of pH, sulfite dose, UV light intensity and initial concentration of 1,2-DCA on the degradation kinetics of 1,2-DCA with sulfite/UV ARP were investigated. In each kinetic experiment, 10 to 12 samples were taken at different times and 1,2-DCA concentrations were measured. Due to the lack of significant degradation of 1,2-DCA in the reagent control (less than 2.5% of initial 1,2-DCA depleted in 5 hours), the regent was not quenched before analysis. The samples were also analyzed for chloride by ion chromatography in order to determine the extent of dechlorination.

Third, scavenging experiments were conducted to explore the mechanism of degradation of both 1,2-DCA and vinyl chloride (VC) with the sulfite/UV ARP. Nitrous oxide (N_2O) or nitrate (NO_3^-) was used to quench the aqueous electron (e_{aq}^-). The results of these experiments were compared with the experiments that were conducted at the same experimental conditions but without a scavenger.

4.2.4. Analytical methods

The light intensity (I_0) was measured on the top surface of the quartz reactor by a UVC 512 light meter (Professional Equipment, Janesville, WI, USA), which was calibrated by the modified ferrioxalate actinometer (Murov et al., 1993). The primary modification was to use the ferrozine method for the colorimetric analysis of iron (Stookey, 1970) with an Agilent 8453 UV-visible spectroscopy system (Agilent, Santa Clara, CA, USA). GC-FID was employed to analyze 1,2-DCA with the same settings that were used for measurement of VC in our previous studies (Liu et al., 2013a; Liu et al., 2013b). The chloride ion was detected by an ion chromatograph (Dionex 500) equipped with an AS-19 column and an AS40 automated sampler following Standard Method 4110. The volatile degradation products were analyzed using static head space gas chromatography-mass spectrometry (SHGC-MS). SHGC-MS was performed on Ultra GC/DSQ (ThermoElectron, Waltham, MA, USA). First, a 5-ml sample was transferred to a 10-mL vial and immediately capped with silicone rubber Teflon cap. This sample was equilibrated at 80 ^{o}C for 10 min in the static headspace sampler. A Rxi-5ms column was used with dimensions of 60 m length, 0.25 mm i.d., and 0.25 μm film thickness (Restek; Bellefonte, PA, USA). A split (1:20) injection was used with helium as the carrier gas at constant flow of 1.5 ml/min. The transfer line and ion source were held at 250 °C. The column temperature was maintained at 30 °C for 3 min; raised to 80 °C at 10 °C/min; and then raised to 200 ^{o}C at 40 ^{o}C/min. Electron impact mass spectra were recorded in the 10-100 m/z range at 70 eV ionization energy.

4.3. Results and Discussion

4.3.1. Reagents screening

The results of reagent control and irradiation control experiments showed that there was little reaction between 1,2-DCA and the reducing reagents or UV light in 5 hours (depletion of initial 1,2-DCA<2.5%). The results of 1,2-DCA screening experiments using various ARPs are shown in Figure 9.

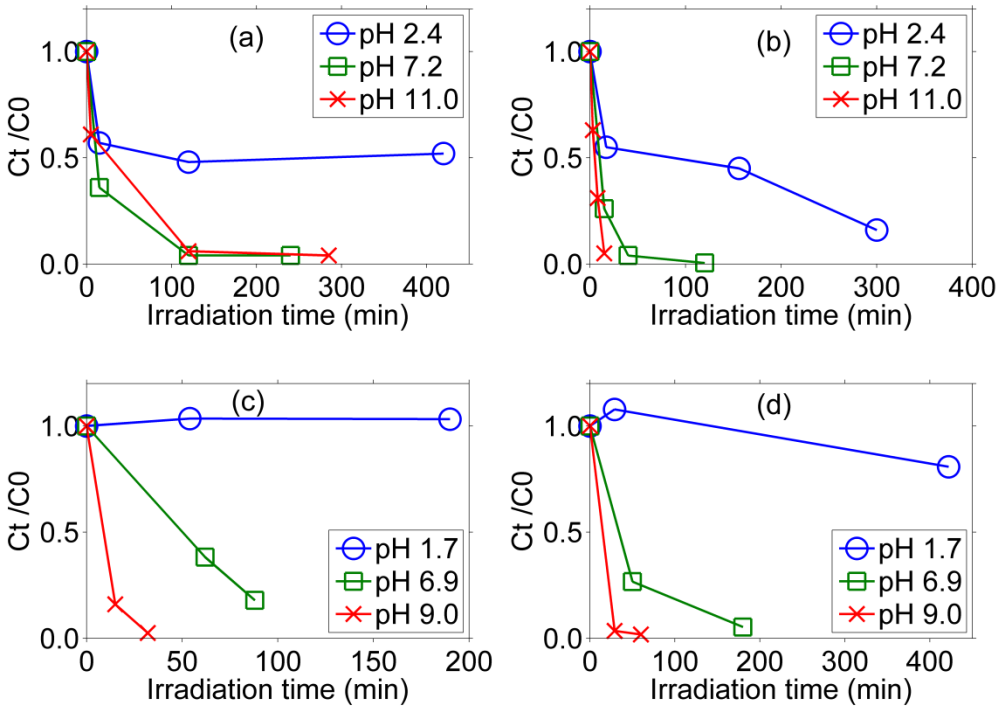

Figure 9. Degradation of 1,2-DCA at different pH values with various ARPs. (a) dithionite/UV ARP. (b) sulfite/UV ARP. (c) sulfide/UV ARP. (d) ferrous iron/UV ARP

Conditions: $[1,2\text{-DCA}]_0$=0.02 mM, incident UV light intensity= 7000 μw/cm^2, $[Na_2SO_3]_0$=1 mM, $[Na_2S_2O_4]_0$=1.2 mM, $[Na_2S]_0$=0.4 mM, $[Fe^{2+}]_0$=4 mM.

1,2-DCA was successfully degraded over a wide range of pH by most of the ARPs, except the sulfide/UV and Fe^{2+}/UV ARPs were not effective at pH 1.7. Comparing these results with the results of control experiments indicates that degradation is mainly due to the reaction between 1,2-DCA and the reactive species produced when the reducing reagents receive UV irradiation. These reactive species include the sulfur dioxide radical ($SO_2^{\bullet-}$) (Fu et al., 2010), sulfite radical ($SO_3^{\bullet-}$) (Fischer and Warneck, 1996), aqueous electron (e_{aq}^-) (Airey and Dainton, 1966; Fischer and Warneck, 1996; Zuo and Deng, 1997), hydrogen atom (H) (Khriachtchev et al., 1998)and excited state bisulfide ion (HS^{-*}) (Linkous et al., 2004). Their production under UV irradiation is summarized by Eqs. (4.1-4.5).

dithionite/UV ARP $$S_2O_4^{2-} + h\nu \rightarrow 2\ SO_2^{\bullet-} \quad (4.1)$$

sulfite/UV ARP $$SO_3^{2-} + h\nu \rightarrow SO_3^{\bullet-} + e_{aq}^- \quad (4.2)$$

sulfide/UV ARP $$HS^- + h\nu \rightarrow HS^{-*} \quad (4.3)$$

$$H_2S + h\nu \rightarrow H^{\bullet} + HS^{\bullet} \quad (4.4)$$

Fe^{2+}/UV ARP $$Fe^{2+} + h\nu \rightarrow Fe^{3+} + e_{aq}^- \quad (4.5)$$

The degradation rate of 1,2-DCA was affected by pH, with higher rates generally observed at higher pH. However, fewer samples were taken in the screening experiments, so the effect of pH will not be discussed further in this section, but will be explained in more detail in the following discussion of results of the more detailed kinetic experiments.

4.3.2. Kinetic experiments with sulfite/UV ARP

The degradation of 1,2-DCA by the sulfite/UV ARP probably followed a second order reaction with respect to the concentrations of 1,2-DCA and relevant reactive species (sulfite radical or aqueous electron). However, it is difficult to quantify the concentration of reactive species during the experiment, so a pseudo-first-order decay model was used to fit the experimental data and provide a means of evaluating effects of process variables. This rate equation can be combined with a material balance equation for a batch reactor as shown in Eq. (4.6).

$$dC_{DCA} / dt = -k_{obs} C_{DCA} \quad (4.6)$$

where C_{DCA} is the 1,2-DCA concentration (mM) measured at irradiation time t and k_{obs} is the observed pseudo-first-order rate constant (min^{-1}). The values of k_{obs} and their 95% confidence intervals were determined by nonlinear least squares regression using the Matlab routines nlinfit and nlparci. The pseudo-first-order rate constants (k_{obs}) at

different pH values, sulfite doses, UV light intensities and initial 1,2-DCA concentration are compared to show how these factors affect 1,2-DCA degradation kinetics.

4.3.2.1 Development of a basic kinetic model

A basic kinetic model was developed to support analysis of the effects of process variables on degradation kinetics as represented by the pseudo-first-order rate constant (k_{obs}). This model greatly simplifies the complex reactions of the reactive species in these ARPs, but it does describe the fundamental processes. The major reactions considered in the model are shown in Table 5 and a detailed derivation of the model is provided in the Appendix C.

Table 5. Process kinetics and stoichiometry for 1,2-DCA degradation by UV-activated ARP

	Reactions	Rate equations	Reagent	R	DCA	S
(a)	Reagent+hν→R	$r_1=\varphi_1 I_{avg} \varepsilon_{ln,reagent} C_{reagent}$	-1	1		
(b)	DCA+R→P_1	$r_2=k_2 * C_{DCA} * C_R$		-1	-1	
(c)	S+R→P_2	$r_3=k_3 * C_s * C_R$		-1		-1

Table 5. Continued

Nomenclature:

Reagent=reagent that produces reactive species

R= reactive species such as sulfite radical or hydrated electron

DCA= the target contaminant of 1,2-DCA

S= scavengers that could react with sulfite radicals or hydrated electrons

P_1, P_2=products

r_1, r_2, r_3= reaction rates of reactions (a) ~ (c)

$\varphi_{1=}$quantum yield of reagent

$\varepsilon_{ln,reagent}$= molar absorptivity of reagent (defined on natural logarithm basis, differs from molar absorptivity used with Beer-Lambert law for absorbance by factor of 2.303, ε_{ln} = 2.303 ε_{bl}, where ε_{bl} is the decadic molar absorptivity used with the Beer-Lambert law, i.e. $I=I_0 10^{-\varepsilon Cx}$)

$C_{reagent}$, C_{DCA}, C_R, C_s= molar concentrations of reagent, 1,2-DCA, reactive species and scavenger

k_2, k_3=second order rate constant of reaction (b) and (c)

Reaction (a) describes the production of reactive species (R) by the photolysis of sulfite. The reactive specie in the sulfite/UV ARP could be the sulfite radial or the aqueous electron and both would be produced in the same reaction (reaction (a) in Table 5) and have same quantum yield (φ_1). It is possible that both compounds could be

reactive species, or one could be reactive with 1,2-DCA and the other could be consumed by various scavenging reactions. Reaction (b) is the reaction of the reactive specie with the target compound (1,2-DCA). The model assumes that the reactive specie can react with a number of scavengers (S) as shown in reaction (c). These scavenging reactions may include reactions of the reactive specie with itself or other radicals as well as reactions of the reactive specie with other compounds in the solution. This kinetic model is derived with the assumption of stationary conditions, i.e. that the time derivative of the concentration of the reactive specie is negligible with respect to the rates of production and consumption of the reactive specie. This assumption is reasonable, because the rates of reaction of reactive species are very fast, so its concentration in solution is very low and the time derivative of its concentration is also low. The absorbances of solutions in all experimental conditions were measured to be below 0.05, which indicates that the light intensity leaving the reaction was about 90% of the light intensity entering the reaction. Thus, the average light intensity (I_{avg}) can be reasonably approximated as the light intensity entering the top surface of the reactor (I_0). Applying these assumptions produces Eq. (4.7), which describes the dependence of k_{obs} on various factors. The definitions of parameters shown in Eq. (4.7) are described in Table 5.

$$k_{obs} = k_2 \varphi_1 I_0 \varepsilon_{ln,reagent} C_{reagent} / (k_2 C_{DCA} + k_3 C_S) \quad (4.7)$$

4.3.2.2. Effect of the solution pH

The influence of the solution pH on kinetics of 1,2-DCA degradation by the sulfite/UV ARP was studied over the range from 4.3 to 11.0 and the results are illustrated in Figure 10.

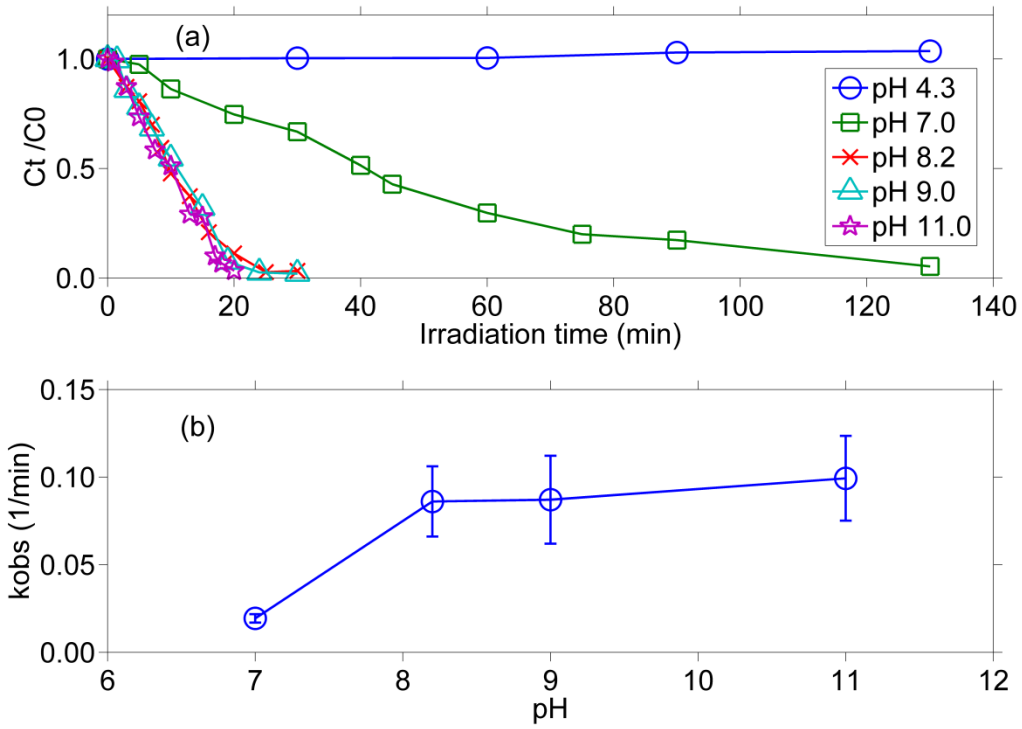

Figure 10. (a) Effect of pH on the degradation of 1,2-DCA by the sulfite/UV ARP. Conditions: $[1,2\text{-DCA}]_0$=0.02 mM, $[Na_2SO_3]_0$=0.2 mM, incident UV light intensity= 6000 μw/cm^2. (b) The pseudo-first-order rate constant versus pH. (Error bars represent 95% confidence intervals)

At low pH (pH 4.3), the degradation of 1,2-DCA was negligible throughout the experiment. At high pH (pH 8.2-11.0), degradation was rapid and at rates that were not

affected by pH. At intermediate pH (pH 7.0), degradation was intermediate between that observed for high and low pH. This behavior is shown in Figure 10 (b) and can be explained by the basic kinetic model. The effect of pH on degradation kinetics is probably due to changes in the distribution of sulfite species with pH. The sulfite ion (SO_3^{2-}) dominates the total sulfite species at pH values greater than the pK_a (7.2) and it can absorb light to produce the sulfite radical and the aqueous electron. At lower pH, the relative importance of bisulfite ion (HSO_3^-) and metabisulfite ion ($S_2O_5^{2-}$) increase. Hayon(Hayon et al., 1972) reports that the bisulfite ion absorbs little light and does not produce reactive species. Dogliotti(Dogliott.L and Hayon, 1968) also reports that no transients are formed on photolysis of bisulfite solution at room temperature. Hayon(Hayon et al., 1972) also mentions that the metabisulfite ion absorbs UV light and produces sulfite radical and sulfur dioxide radical. However, at the total sulfite concentration used in our research (0.2 mM), the fraction of metabisulfite ion is negligible (1.2% at pH 4.3, 0.4% at pH 7.0 and < 0.01 % at pH 8.2, 9.0 and 11.0) and thus it is not likely to be responsible for degradation of 1,2-DCA in these experiments.

Therefore, we believe the production of reactive species (sulfite radical and aqueous electron) is only attributed to the sulfite ion in solution, and the terms of $\varepsilon_{ln,reagent}$ and $C_{reagent}$ in Eq. (4.7) represent the molar absorptivity of sulfite ion ($\varepsilon_{ln,SO3}^{2-}$, measured as 41.7 M^{-1} cm^{-1}) and sulfite ion concentration (C_{SO3}^{2-}) for the sulfite/UV ARP. In addition, the concentration of sulfite ion can be expressed as a function of its ionization fraction value (α_{SO3}^{2-}) and total sulfite species concentration ($C_{sulfite}$). Thus the rate constant (k_{obs}) can be expressed by Eq. (4.8).

$$k_{obs} = k_2 \varphi_1 I_0 \varepsilon_{ln,SO3^{2-}} \alpha_{SO3^{2-}} C_{sulfite} / (k_2 C_{DCA} + k_3 C_S) \quad (4.8)$$

The ionization fractions of sulfite ions at pH values used in experiments are summarized in Table 6. The increase in solution pH from 4.3 to 8.2 leads to a substantial increase in $\alpha_{SO3^{2-}}$. The kinetic model predicts that this should increase the production rate of reactive species ($r_1=\varphi_1 I_{avg} \varepsilon_{ln,SO3^{2-}} \alpha_{SO3^{2-}} C_{sulfite}$, where $C_{sulfite}$ is the total concentration of all sulfite species in solution, i.e. $C_{sulfite} = C_{h2so3} + C_{hso3} + C_{so3}$) and thus promote the overall degradation rate of 1,2-DCA,. When pH is above 7.2, the sulfite ion (SO_3^{2-}) dominates the bisulfite ion and there is only slight difference in $\alpha_{SO3^{2-}}$ between pH 8.2 and pH 11 (from 0.915 to 0.998). Therefore, there would be little change in the degradation rate constant.

Table 6. Sulfite species distribution in 0.2 mM sulfite solution at different pH values (ionization fractions calculated by Visual MINTEQ)

pH	Fraction HSO_3^- (α_{HSO3^-})	Fraction SO_3^{2-} ($\alpha_{SO3^{2-}}$)
4.3	0.983	0.0014
7	0.587	0.407
8.2	0.082	0.915
9	0.014	0.984
11	0.00014	0.998

4.3.2.3. Effect of the sulfite dose

Various sulfite doses were applied to evaluate their effects on 1,2-DCA degradation and the results are shown in Figure 11.

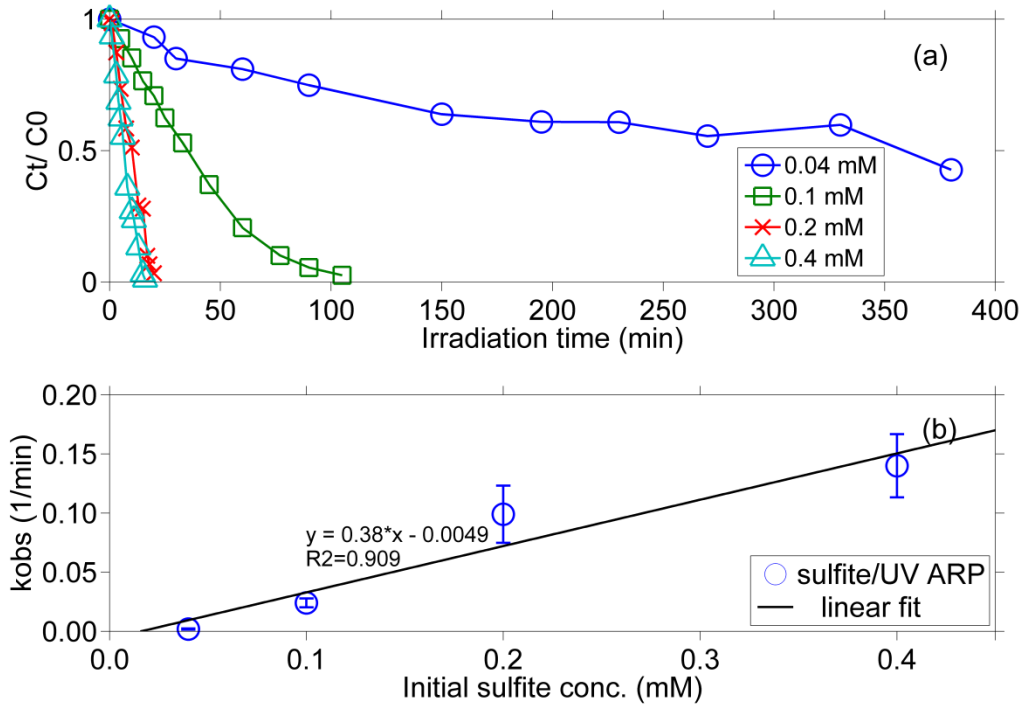

Figure 11. (a) Effect of initial sulfite concentration on the degradation of 1,2-DCA by the sulfite/UV ARP. Conditions: $[1,2\text{-DCA}]_0$=0.02 mM, pH 11.0, incident UV light intensity= 6000 μw/cm^2.(b) The pseudo-first-order rate constant versus initial sulfite concentration. (Error bars represent 95% confidence intervals)

Concentrations of 1,2-DCA appear to flatten out at the lowest initial concentration (Figure 11(a)), which could be due to the concentration of sulfite approaching zero resulting in no production of active species. The observed effect of

sulfite concentration on k_{obs} (Figure 11(b)) approximates the proportionality predicted by the model. However, the model uses the actual concentration of sulfite, while Figure 11(b) uses the initial sulfite concentration. The actual concentration of sulfite would decrease during the course of the experiment and the relative decrease would be greatest for lower initial concentrations. This would tend to cause a non-proportional relationship between k_{obs} and initial sulfite concentration. The lack of strict proportionality could also be caused by production in intermediates that would act as scavengers of active species during the course of the reaction.

4.3.2.4. Effect of the UV light intensity

The degradation of 1,2-DCA was studied at various incident UV light intensities (I_0) and the results are illustrated in Figure 12. Higher UV light intensities enhance the removal of 1,2-DCA, because the higher UV light intensity results in a higher production rate of reactive species ($r_1=\varphi_1\ I_{avg}\ \varepsilon_{ln,SO3}{}^{2-}\ \alpha_{SO3}{}^{2-}\ C_{sulfite}$) and thus promotes the overall degradation rate. The simple model predicts that the observed rate constant should be proportional to the light intensity (Eq. (4.7)) and the data agree reasonably well. The small non-zero intercept that was observed may be the result of the simple model not taking into account all reactions of active species.

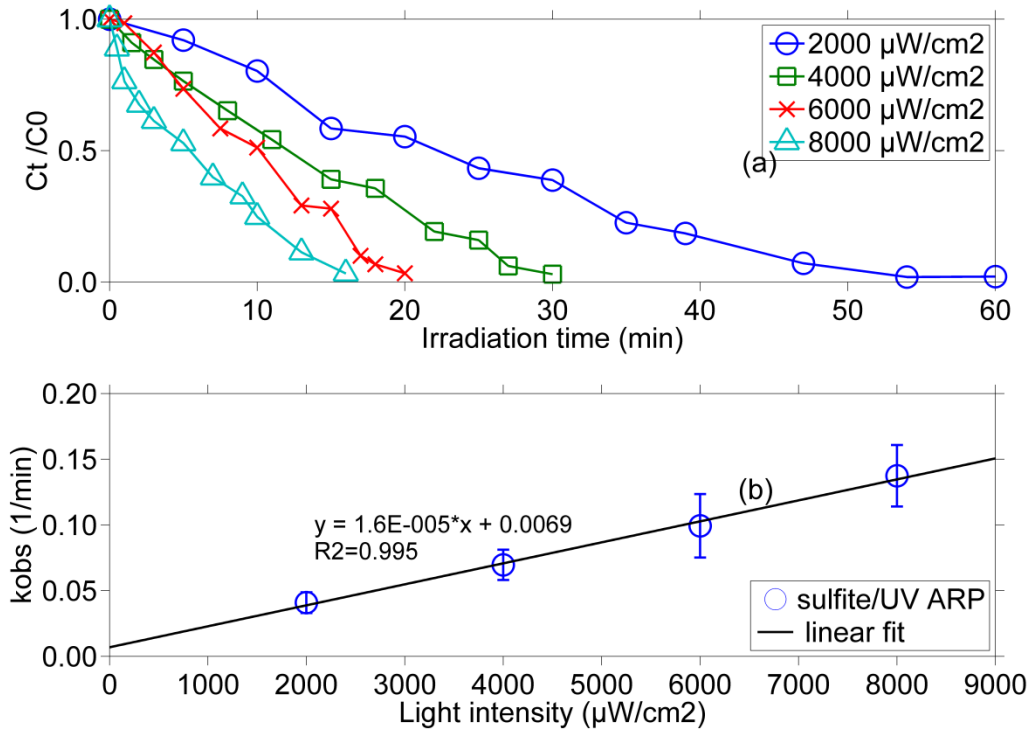

Figure 12. (a) Effect of UV light intensity on the degradation of 1,2-DCA by the sulfite/UV ARP. Conditions: $[1,2\text{-DCA}]_0$=0.02 mM, pH 11.0, $[Na_2SO_3]_0$=0.2 mM. (b) The pseudo-first-order rate constant versus incident UV light intensity. (Error bars represent 95% confidence intervals)

4.3.2.5. Effect of the initial 1,2-DCA concentration

The effect of initial concentration of 1,2-DCA on the degradation kinetics is shown in Figure 13. When the dose of 1,2-DCA increases, the value of the pseudo-first-order rate constant decreases. The model (Eq. 4.7) predicts that the first order rate constant will decrease when the actual concentration increases as long as scavenging (k_3C_s) is not excessive. Since the average concentrations of 1,2-DCA will be related to

the initial concentrations, the model generally predicts the observed behavior if there is not excessive scavenging, but the extent of agreement cannot be accurately determined.

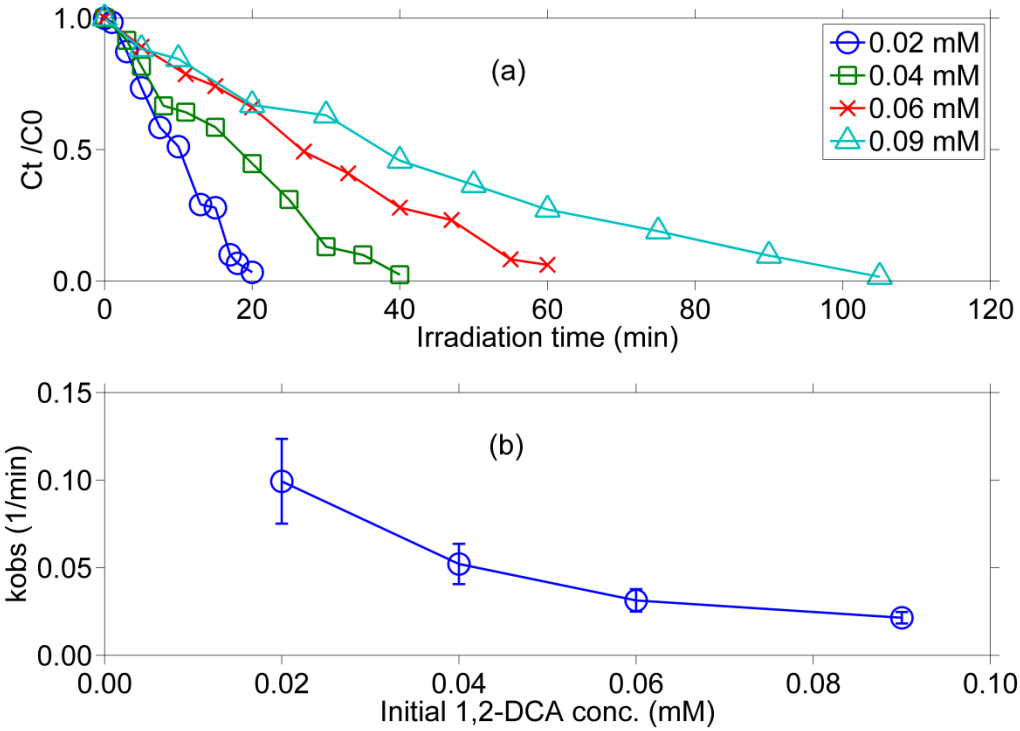

Figure 13. (a) Effect of initial concentration of 1,2-DCA on the degradation of 1,2-DCA by the sulfite/UV ARP. Conditions: pH 11.0, $[Na_2SO_3]_0$=0.2 mM, incident UV light intensity= 6000 μw/cm^2. (b) The pseudo-first-order rate constant versus initial concentration of 1,2-DCA. (Error bars represent 95% confidence intervals)

The extent of scavenging can be evaluated using the efficiency (φ) of reactive species for 1,2-DCA degradation which is defined in terms of the quantum yield for 1,2-DCA degradation divided by the quantum yield of reactive species. Values of φ were calculated as 0.45, 0.46, 0.39 and 0.42 at initial 1,2-DCA concentration of 0.02, 0.04, 0.06 and 0.09 mM, respectively. Information on how these calculations were performed

is provided in supplementary data. The values of φ indicate that the scavenging effects are important, but do not dominate. Therefore, the behavior of the rate constants with initial concentration of 1,2-DCA is consistent with the model prediction.

4.3.3. Degradation mechanism in the sulfite/UV ARP

The sulfite/UV ARP produces the sulfite radial and the aqueous electron and either or both could be responsible for degradation of 1,2-DCA. To evaluate which of them is responsible for 1,2-DCA degradation, scavenger experiments were conducted with nitrous oxide (N_2O) and nitrate (NO_3^-), both of which scavenge the aqueous electron. The aqueous electron has also been reported to degrade 1,2-DCA and all of these reactions are summarized by Eqs. (4.9-4.11).

$$e_{aq}^- + ClCH_2CH_2Cl \rightarrow Cl^- + \cdot CH_2CH_2Cl \qquad k_9 = 6.4E8\ M^{-1}s^{-1} \qquad \text{(Getoff, 1990)} \qquad (4.9)$$

$$e_{aq}^- + NO_3^- \rightarrow (NO_3^{\bullet})^{2-} \qquad k_{10} = 9.2E9\ M^{-1}s^{-1} \qquad \text{(Chen et al., 1994)} \qquad (4.10)$$

$$e_{aq}^- + N_2O + H_2O \rightarrow N_2 + OH^{\bullet} + OH^- \qquad k_{11} = 9.1E9\ M^{-1}s^{-1} \qquad \text{(Buxton et al., 1988)} \qquad (4.11)$$

The effectiveness of scavenging can be determined using these rate constants and the initial concentrations used in the experiments. The ratio of the rate of the scavenging reaction to the rate of the reaction between e_{aq}^- and 1,2-DCA ($r_{DCA+eaq-}$) was calculated as 288 for nitrate and 17,700 for nitrous oxide. Therefore, almost all of the aqueous electrons that are generated should be scavenged and not be available to react with 1,2-DCA.

Figure 14 shows that degradation of 1,2-DCA was negligible when nitrous oxide or nitrate was present, which indicates that the aqueous electron (e_{aq}^-) is the compound that is primarily responsible for 1,2-DCA degradation. Since addition of N_2O promotes production of sulfite radicals (Fischer and Warneck, 1996; Li et al., 2012), the scavenging experiment results with N_2O provide additional evidence that the sulfite radical is not important and the aqueous electron is responsible for degradation of 1,2-DCA.

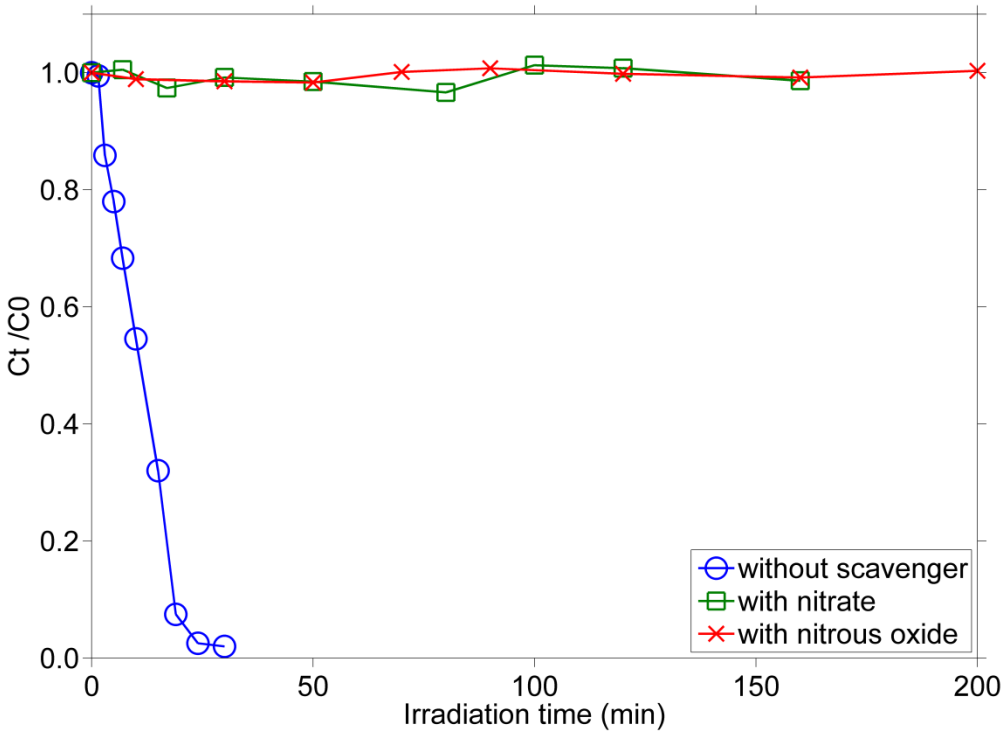

Figure 14. Effects of aqueous electron scavengers on the degradation of 1,2-DCA by the sulfite/UV ARP. Conditions: pH 9.0, $[1,2\text{-DCA}]_0$=0.02 mM, $[Na_2SO_3]_0$=0.2 mM, incident UV light intensity= 6000 μw/cm^2, $[NO_3^-]_0$=0.4 mM, $[N_2O]_0$≈25 mM (near saturation).

Although the sulfite radical is not important for 1,2-DCA degradation, it may play a role in degradation of other compounds, so similar scavenging experiments were conducted to evaluate the degradation mechanism of vinyl chloride (VC) by the sulfite/UV ARP. The aqueous electron has been reported to be able to degrade VC, as shown in Eq. (4.12). Using the reported rate constants and initial concentrations, the ratio of the scavenging rate to the rate of degradation of VC would be 736 with nitrate and 18,200 with nitrous oxide. Therefore, both are effective scavengers of aqueous electrons in this experimental system.

$e_{aq}^- + H_2C{=}CHCl \rightarrow$

$CH_2CH\cdot + Cl^-$ $\quad k_{12}=2.5E8M^{-1}s^{-1}$ (Koester and Asmus, 1971) (4.12)

The results of these scavenging experiments are illustrated in Figure 15 and rate constants are summarized in Table 7.

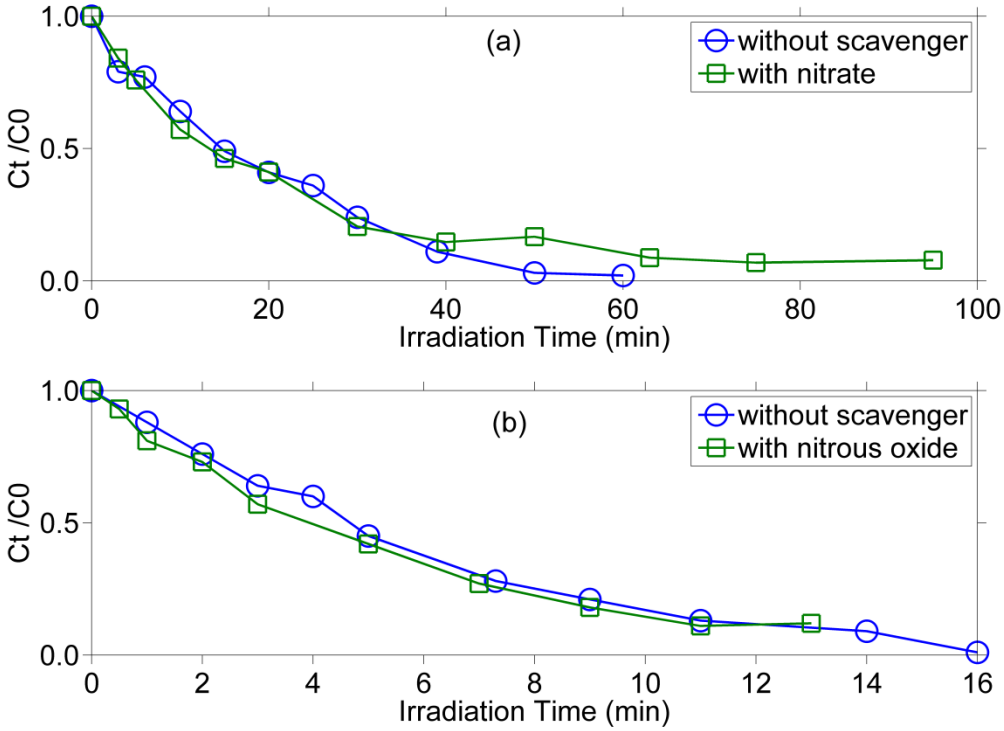

Figure 15. Effects of aqeuous electron scavengers on the degradation of VC by the sulfite/UV ARP (a) with and without NO_3^- as scavenger. (b) with and without N_2O as scavenger. Conditions: (a) pH 9.0, $[VC]_0$=0.02 mM, $[Na_2SO_3]_0$=0.2 mM, UV light intensity= 6000 μw/cm^2, $[NO_3^-]_0$=0.4 mM. (b) pH 9.0, $[VC]_0$=0.02 mM, $[Na_2SO_3]_0$=1 mM, UV light intensity= 4000 μw/cm^2, $[N_2O]_0\approx$10 mM.

Table 7. Pseudo-first-order rate constant (k_{obs}) for scavenging experiments with VC and the sulfite/UV ARP

	k_{obs} (min^{-1})	Products in GC-FID chromatograms
VC+sulfite/UV+ NO_3^-	0.046±0.0069[*]	No product peaks were shown in GC-FID
VC+sulfite/UV (control) [**]	0.047±0.0066	Chloroethane and a unidentified peak
VC+sulfite/UV+ N_2O	0.18±0.014	No product peaks were shown in GC-FID
VC+sulfite/UV (control) [***]	0.17±0.020	Chloroethane and a unidentified peak

[*] The values of k_{obs} and 95% confidence intervals were determined by nonlinear least squares regression with Matlab routine nlinfit and nlparci.

[**]The experiment with NO_3^- as scavenger and its control experiment (without NO_3^- added) were conducted in the following conditions: pH 9 (buffered), UV light intensity =6000 μw/cm^2, $[VC]_0$= 0.02mM, $[SO_3^{2-}]_0$= 0.2mM , $[NO_3^-]_0$=0.4mM.

[***] The experiment with N_2O as scavenger and its control experiment (without N_2O added) were conducted in the following conditions: pH 9 (buffered), light intensity =4000 μw/cm^2, $[VC]_0$= 0.02mM, $[SO_3^{2-}]_0$= 1mM , $[N_2O]_0$≈10 mM.

The presence of the scavengers shows little effect on VC removal, so the aqueous electron probably plays little role in VC degradation by the sulfite/UV ARP. This means that the sulfite radical alone is probably responsible for VC degradation by the sulfite/UV ARP. This conclusion is supported by reports that the sulfite radical attacks

unsaturated bonds (C=C, C=N and C≡C) (Neta and Huie, 1985; Ozawa and Kwan, 1986) such as are found in VC.

Further insight into the degradation mechanism of VC can be seen in the intermediate products formed in these scavenger experiments. Without a scavenger, the degradation products were chloroethane and an unidentified product, which was probably a hydrocarbon as discussed in the following section. However, in the experiments with a scavenger no organic products were observed. Therefore, the degradation pathway of VC is likely to be that the sulfite radical first reacts with the C=C bond of VC to form a radical intermediate ($^{-}O_3S\text{-}CH_2\text{-}C^{\bullet}HCl$), which then reacts with the aqueous electron to produce products (chloroethane and another unidentified product). However, when scavengers are present, VC is still removed by reaction with the sulfite radical, but there are no aqueous electrons to react with the radical intermediate, so it further reacts with itself or the sulfite radical to form undetected organic products or inorganic products. Non-volatile organic intermediates would not be detected by the head-space procedure used. One unexplained aspect of this mechanism is why an enhancement in VC degradation was not observed when N_2O was used as scavenger. N_2O reacts with the aqueous electron and forms the hydroxyl radical, which then can react with sulfite to form a sulfite radical (Fischer and Warneck, 1996). This would enhance degradation rates of VC in experiments with N_2O, but that was not observed. The lack of enhancement could be explained by side reactions that consume the hydroxyl radical so that additional production of the sulfite radical is minimized and

the rate of 1,2-DCA degradation remains near values observed in the absence of N_2O scavenging.

4.3.4. Dechlorination efficiency

The major inorganic product in the degradation of 1,2-DCA by the sulfite/UV ARP is the chloride ion (Cl^-). The "dechlorination efficiency" (R_{dech}) was used to quantify the chloride production efficiency and was defined as the fraction of chlorine atoms in 1,2-DCA that was degraded and converted to chloride ions.

$$R_{dech} = (C_{Cl,\ chloride\ ion\ released})/ (C_{Cl\ in\ initial\ 1,2\text{-}DCA} - C_{Cl,\ in\ final\ 1,2\text{-}DCA}) \quad (4.13)$$

The dechlorination efficiency was investigated in experiments at various pH conditions and sulfite doses and results are shown in Table 8. The results show that the solution pH has a great influence on the dechlorination efficiency. At pH 4.3, little 1,2-DCA was degraded and no chloride was detected. In the pH range from 7.0 to 11.0, the dechlorination efficiency increases and this increase is much like the increase observed for degradation rate constant. The value of R_{dech} has a substantial increase from pH 7.2 to 8.2, but increases slowly from pH 8.2 to 11.0. The examination of organic degradation products reveals the dependence of dechlorination efficiency on the solution pH. Chloroethane (C_2H_5Cl) was detected as a major organic product at pH 7.0 and another product peak was shown but not identified. The peak area of chloroethane decreases

substantially when pH rises from 7.0 to 8.2, and only has a slightly decrease from pH 8.2 to 9.0, and it disappears at pH 11.0. Along with the change in the peak area of chloroethane, the peak area of the unidentified product increases when pH rises. The ratio of the peak area of chloroethane to the peak area of unidentified product is 4.0, 0.34, 0.03 and 0 at pH 7.0, 8.2, 9.0 and 11.0 respectively. Therefore, chloroethane is the major product at low pH and the unidentified, but probably non-chlorinated, product dominates at high pH.

Table 8. Dechlorination efficiency at various pH* and sulfite doses**

	dechlorination efficiency (R_{dech})
pH 4.3	Cl^- not detected
pH 7.0	23.6%
pH 8.2	79.9%
pH 9.0	86.7%
pH 11.0	92.6%
$[SO_3^{2-}]_0$= 0.04mM	90.5%
$[SO_3^{2-}]_0$= 0.1mM	93.4%
$[SO_3^{2-}]_0$= 0.2mM	92.6%
$[SO_3^{2-}]_0$= 0.4mM	93.1%

Table 8. Continued

*The experiments at various pH were conducted in the following conditions: UV light intensity =6000 μw/cm^2, [1,2-DCA]$_0$= 0.02mM, [SO_3^{2-}]$_0$= 0.2mM.

** The experiments at various sulfite doses were conducted in the following conditions: UV light intensity =6000 μw/cm^2, [1,2-DCA]$_0$= 0.02mM, pH 11.

Table 8 also shows that changing the sulfite concentration at pH 11 does not cause much change in the dechlorination efficiency. All the values of R_{dech} are higher than 90%, which indicates nearly complete dechlorination is achieved with various sulfite doses.

4.4. Conclusion

This study demonstrated the ability of many ARPs to rapidly degrade 1,2-DCA, but the sulfite/UV ARP was selected for detailed kinetic study. Degradation of 1,2-DCA generally followed a pseudo-first-order decay model and the rate constant was determined at all experimental conditions. An increase in solution pH at acidic and neutral conditions increases the degradation rate, but it has little effect at alkaline conditions. Higher sulfite doses and light intensities promote 1,2-DCA degradation linearly generally as predicted by the simple model. The pseudo-first order rate constants decrease slightly at higher initial 1,2-DCA concentrations, as predicted by the model that considers the influence of scavengers of reactive species. Experiments with scavengers

of aqueous electrons showed that the degradation of 1,2-DCA is mainly due to the aqueous electron and that degradation of VC initiated by the sulfite radical, but the aqueous electron probably reacts with intermediate products, thereby affecting distribution of products. The affinity of the sulfite radical for VC is probably associated with its double bond, which implies that it will probably be important in degrading other chlorinated alkenes while the aqueous electron will be more important in degrading chlorinated alkanes. The dechlorination efficiency varies with the solution pH and more than 90% dechlorination was achieved at pH 11.0.

The technology of advanced reduction process has been applied to both VC and 1,2-DCA and the results demonstrate the ability of these processes to effectively degrade chlorinated aliphatic compounds. Application of these ARP in treatment systems is promising given the rapid degradation kinetics and detoxification efficiency. It will be important in such applications to consider the effects of scavengers of reactive species that are present in water to be treated. It may be advantageous to apply appropriate pretreatments to remove scavengers (such as nitrate or dissolved oxygen), otherwise either the degradation efficiency of 1,2-DCA will be compromised or more reagent (e.g. sulfite) will be consumed. The basic kinetic model developed in this study was able to describe many aspects of the observed kinetics; however, a more complex mechanistic model that describes individual reactions of reactive species is needed to more fully characterize ARP kinetics and this work is underway.

5. QUANTUM YIELD ANALYSIS FOR THE DEGRADATION OF VINYL CHLORIDE (VC) AND 1,2-DICHLOROETHANE (1,2-DCA) BY THE SULFITE/UV ADVANCED REDUCTION PROCESS (ARP)

5.1. Quantum Yield Calculation

The energy utilization efficiencies in the degradation of VC and 1,2-DCA by the sulfite/UV ARP can be evaluated though analysis of quantum yields. The quantum yield is defined as being equal to the number of degraded VC or 1,2-DCA molecules divided by the number of photons absorbed by light absorbing species (sulfite). In this study, the initial quantum yield (Φ) is used to compare effectiveness of various ARPs .It can be expressed as the ratio of initial degradation rate of a target (VC or 1,2-DCA) to the rate of photon absorption, as shown in Eq. (5.1).

$$\emptyset = \frac{-r_R}{\frac{I_0}{L} * (1 - 10^{-\varepsilon_{sulfite} * C_{sulfite} * L}) * \frac{\lambda_{253.7}}{N_A * h * c}} \tag{5.1}$$

where r_R= initial degradation rate of target (VC or 1,2-DCA), I_0 = incident UV light intensity measured entering the quartz reactor (J/m^2-s), L= light path length (thickness) in reactor (m), $\varepsilon_{sulfite}$ = molar absorptivity of sulfite ion(decadic, m^2/mol), $C_{sulfite}$= concentration of sulfite ion (mol/m^3), $\lambda_{253.7}$ =wavelength of UV light (m), N_A =

Avogadro's number, $6.02*10^{23}$ (1/mol), h = Planck's constant, $6.626*10^{-34}$ (J-s), c = speed of light, $3*10^{8}$ (m/s).

5.2. Quantum Yield Analysis for VC Degradation by the Sulfite/UV ARP

Quantum yields for VC degradation by the sulfite/UV ARP and the influence of process variables on them are illustrated in Figure 16 (a) – (d). The quantum yield drops substantially when the solution pH rises from 5 to 7. There is no obvious change in the quantum yield when solution pH changes from 7 to 9. The quantum yield at pH 11 is smaller compared to the value obtained at pH 7 and 9. The change of pH will change the fractions of individual sulfite species (i.e. sulfite ion or bisulfite ion), which will change the rate of light absorption and the rate of sulfite radical production. However, it is not clear whether the quantum yield will follow the same pattern as the pH effect on the degradation rate, because the quantum yield represents the fraction of photons absorbed that eventually results in degradation of VC. Radicals produced at different pH may or may not be as effective in degrading VC, depending on how pH affects reactions of the radicals with VC and scavengers.

The similar quantum yield at pH 7 and pH 9 indicates that the increase in sulfite radical production rate at pH 9 (as shown in Figure 5 in section 3) leads to a similar increase in the rate between sulfite radical and VC when compared to the rate increase between sulfite radical and intermediates. The drop in the quantum yield at pH 11 indicates that this ratio of rates does not remain constant when pH is raised from 9 to 11.

The quantum yield at pH 5 was calculated to be greater than 1 and was much higher than values obtained at other pH conditions. One possible explanation for this is that certain intermediates are formed during VC degradation at low pH and they are able to react with VC so that its rate of degradation is higher. If this is true, the system efficiency in utilizing each photon is enhanced, thus the quantum yield is increased.

The quantum yield does not change substantially at with sulfite dose, although the pseudo-first-order degradation rate constant increases linearly (Figure 6) when higher sulfite dose is applied. The higher sulfite concentration would increase the production rate of sulfite radical but if the utilization efficiency of the sulfite radical remained constant, the rate of degradation would increase proportionally and the quantum yield would be similar.

Higher light intensity is found to result in lower quantum yield, since the regression analysis shows a negative slope ((-1.58±0.5)E-5 $cm^2/\mu W$) in Figure 16 (c). The higher light intensity can enhance the reaction by increasing the rate of production of the sulfite radical, which would increase the reaction rate constant (Figure 7). However, the behavior of the quantum yield indicates that the efficiency of sulfite radical in degrading VC decreases when higher light intensity is applied. This could be caused by different scavenging effects at various light intensities where a larger fraction of sulfite radical reacts with VC at lower light intensities while a smaller fraction of sulfite radical reacts with VC at higher light intensities..

The initial VC concentration has little effect on quantum yield in the range from 0.018 to 0.029 mM, but the quantum yield does increase at initial VC concentration of

0.050 mM. In section 3, the analysis of sulfite radical efficiency indicated that the effective fraction of sulfite radical in degrading VC is 0.28 ±18%, 0.25 ± 12%, 0.28 ± 13% and 0.47 ± 4.6% with the initial VC concentration at 0.018, 0.024, 0.029 and 0.050 mM, respectively. These values are consistent with the quantum yield behavior at various initial VC concentrations.

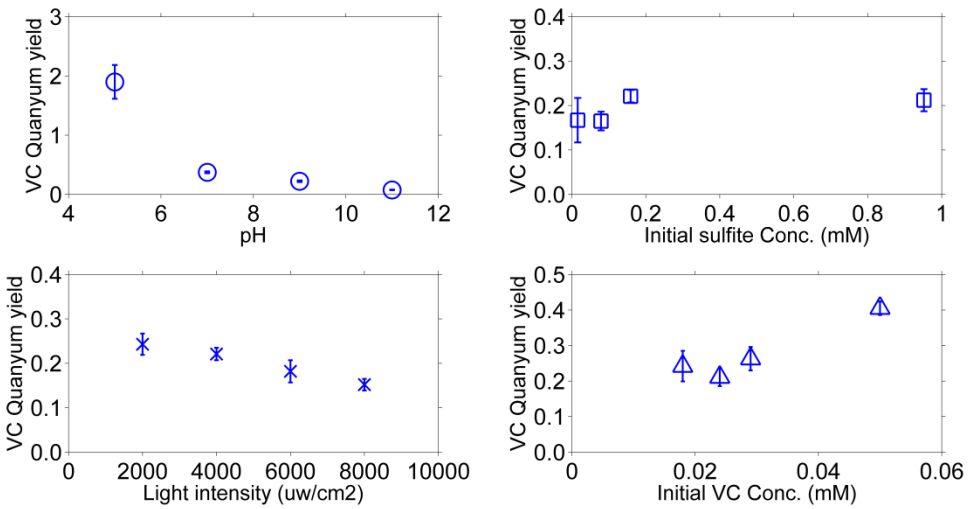

Figure 16. The effects of process variables on the quantum yield of VC degradation by the sulfite/UV ARP.

5.3. Quantum Yield Analysis for 1,2-DCA Degradation by the Sulfite/UV ARP

Results of quantum yields for 1,2-DCA degradation by the sulfite/UV ARP and the effects of process variables on them are illustrated in Figure 17 (a) – (d). The quantum yield is zero at pH 4.3, since negligible aqueous electron can be produced at this pH and thus no degradation of 1,2-DCA is observed. The quantum yield increases

when the solution pH rises from 7.0 to 8.2 and then is constant at higher pH. Since the aqueous electron is the major species causing the degradation of 1,2-DCA and it is only produced by the photolysis of sulfite ion (SO_3^{2-}) , it is reasonable to observe the lower quantum yield at pH 7.0 than other higher pH values, because the fraction of sulfite ion in total sulfite species rises from 40.7% at pH 7 to more than 90% at pH ≥8.2. Little change in the concentration of sulfite ion occurs when pH is raised above 8.2, so the solution pH should not affect the quantum yield at higher pH. The effect of solution pH on the quantum yield of 1,2-DCA degradation is different from that observed for the quantum yield for VC degradation. In VC degradation, similar quantum yields were observed at pH 7 and pH 9, but it dropped at pH 11. The difference in pH effects could be due to different reactive species in degrading the two targets. The sulfite radical that causes VC degradation and the aqueous electron that causes 1,2-DCA degradation may react with scavengers differently at the same solution pH and this would lead to the different pH effects on the quantum yield.

An obvious increase in the quantum yield is observed when sulfite dose rises from 0.04 mM to 0.2 mM, and then it tends to be constant between 0.2 mM and 0.4 mM (Figure 17 (b)). This indicates that the increases in sulfite dose below 0.2 mM not only enhances the reaction rate (Figure 11) but also improves the utilization of sulfite radical.

The quantum yield is insensitive to changes in light intensity and initial 1,2-DCA dose, which indicates that the efficiency of the aqueous electron in degrading 1,2-DCA does not depend on light intensity and initial 1,2-DCA concentration.

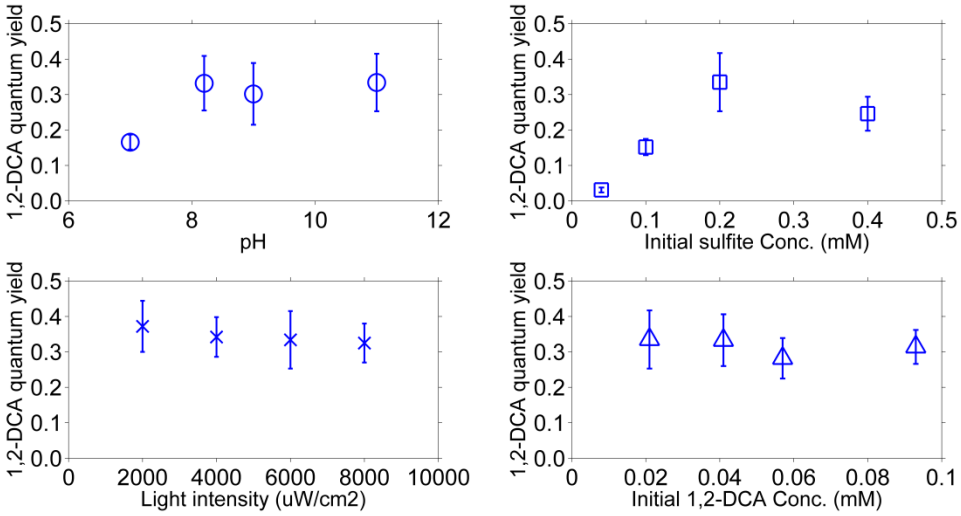

Figure 17. The effects of process variables on the quantum yield of 1,2-DCA degradation by the sulfite/UV ARP.

6. MECHANISTIC MODELING OF THE DEGRADATION OF 1,2-DCA AND VC WITH THE SULFITE/UV ARP

6.1. Mechanistic Modeling of the Degradation of 1,2-DCA With the Sulfite/UV ARP

6.1.1. Model development

The mechanism of 1,2-DCA degradation with the sulfite/UV ARP has been discussed and kinetics of degradation has been quantified using a pseudo-first-order model. The effects of experimental variables on the first-order rate constants have been described by a simple kinetic model that assumes production of reactive species and their reaction with 1,2-DCA and unspecified scavengers. However, the sulfite/UV ARP system involves more complex reactions than described by this simple model, such as reactions between 1,2-DCA and different reactive species, reactions of reactive species with themselves and other compounds in solution (scavengers). Therefore, it would be useful to have a more complex model that better describes the mechanisms of the system and such a model was developed. A total of 32 compounds and 77 reactions were considered in the mechanistic model with program details shown in Appendix D.

Some of the most important reactions in the mechanistic model are listed in Eqs. (6.1)-(6.3). Eq. (6.1) describes the absorption of UV light by the sulfite ion that produces the sulfite radical and the aqueous electron. In this mechanistic model, only the sulfite ion (SO_3^{2-}) is considered to be effective in absorbing light and producing reactive

species. At neutral or acid pH, light absorption by S(IV) species could be mainly due to the existence of metabisulfite ($S_2O_5^{2-}$), because the bisulfite (HSO_3^-) absorbs little light. There is no evidence for the production of reactive species when irradiating a solution of metabisulfite or bisulfite, thus the mechanistic model assumes that they do not produce any reactive species. Eq. (6.2) describes the reaction between the aqueous electron and 1,2-DCA, which is the first step in 1,2-DCA degradation. Eq. (6.3) describes the reaction between the aqueous electron and the intermediate produced by the first degradation step (i.e. the radical of $\bullet CH_2CH_2Cl$). The rate constant for this reaction will be designated as $k_{6.3}$.

$$SO_3^{2-} + h\nu \rightarrow SO_3^{\bullet -} + e_{aq}^- \tag{6.1}$$

$$e_{aq}^- + ClCH_2CH_2Cl \rightarrow Cl^- + \cdot CH_2CH_2Cl \tag{6.2}$$

$$e_{aq}^- + \cdot CH_2CH_2Cl \rightarrow \text{Products} + Cl^- \tag{6.3}$$

The mechanistic model consists of material balance equations (Eq. 6.4) that describes the concentration change of a compound in a completely mixed batch reactor.

$$\frac{dC_i}{dt} = \Sigma r_i \tag{6.4}$$

where C_i is the concentration of compound i, Σr_i is the sum of rates of production minus rates of removal of compound i in the sulfite/UV ARP system.

For example, to derive the concentration change of 1,2-DCA, all reactions related with 1,2-DCA production or degradation are considered. As demonstrated in Section 4, the degradation of 1,2-DCA with the sulfite/UV ARP is believed to be mainly caused by the reaction with aqueous electron (reaction 70 in the mechanistic model). However, the mechanistic model also considers the reaction between the H atom and 1,2-DCA (reaction 72 in the mechanistic model). Thus, the overall expression of the change in 1,2-DCA concentration can be described by Eq. (6.5), where k_j represents the rate constant for reaction j, C_{DCA} is the concentration of 1,2-DCA, $C_{e,aq}$ is the concentration of aqueous electron and C_H is the concentration of H atom.

$$\frac{dC_{DCA}}{dt} = -k_{70}C_{e,aq}C_{DCA} - k_{72}C_H C_{DCA} \tag{6.5}$$

The mechanistic model requires values of rate constants for all reactions as well as the quantum yield of the photochemical reaction that produces reactive species (Eq. 6.1). Some values are available in the literature (provided in Appendix D); however, the values for the rate constant ($k_{6.3}$) for the reaction between the aqueous electron and the intermediate (Eq. 6.3) are not available. In addition, the quantum yield of sulfite needs to be identified. Thus an iterative method of sequential non-linear regression was applied to search for the best values of sulfite quantum yield (Φ) and the rate constant ($k_{6.3}$) that gave the best fits to experimental data. The unknown coefficients were specified at

specific values across a range and simulations conducted at all combinations of values. The weighted sum of squares error (WSSE) was calculated for each simulation and was used as the objective function to search for the best values of Φ and $k_{6.3}$ that minimize the value of WSSE (Eq. 6.6).

$$\text{WSSE} = \Sigma\left(\frac{C_{i,exp} - C_{i,mod}}{C_{initial,exp}}\right)^2 \tag{6.6}$$

where $C_{i,exp}$ is the 1,2-DCA concentration measured during an experiment at sampling time i, $C_{i,mod}$ is the simulated concentration of 1,2-DCA at corresponding time and $C_{intial,exp}$ is the initial concentration of 1,2-DCA measured at time zero (before experiment starts).

The values of Φ and $k_{6.3}$ in Table 9 were determined by fitting 13 sets of kinetic data for 1,2-DCA degradation. The search range for the quantum yield was from 0 to 1 with an increment of 0.01 and the search range for the rate constant was from 10 to 1 E20 with 100 logarithmically spaced values. The model predictions were made by solving the set of material balance equations using Matlab function "ode15s" and program details are shown in Appendix D.

Results show that the values of Φ are within a range from 0.05 to 0.46. The rate constant ($k_{6.3}$) varies from 10 to 1 E10 $M^{-1}s^{-1}$ under different conditions, which would indicate quite different reactivities between the aqueous electron and intermediates in various experiments. However, the wide range of values obtained for $k_{6.3}$ raises

questions about their reliability, so conclusions about the meaning of their variation are limited.

The quantum yield is an intrinsic property of the sulfite ion when it receives irradiation at a specific wavelength, thus it should be a constant under similar experimental conditions. The sulfite quantum yield for experiments conducted at various solution pH, sulfite doses, light intensities and initial 1,2-DCA concentrations would be expected to be a constant. However, values of Φ range from 0.05 to 0.46. This indicates that the mechanistic model may not include all possible reactions that degrade the targets or consume aqueous electrons. Thus in the regression the model attempts to adjust the value of quantum yield to make up the deficiency of lacking specific reactions that can describe the real degradation mechanism.

Table 9. Values of sulfite quantum yield (Φ) and rate constant ($k_{6.3}$) for reaction between the aqueous electron and an intermediate (Eq. 6.3)

pH	Sulfite Conc. (mM)	UV intensity ($\mu W/cm^2$)	Initial 1,2-DCA Conc. (mM)	Sulfite Quantum Yield (Φ)	Rate Constant ($k_{6.3}$, $M^{-1}s^{-1}$)	Minimum value of WSSE	Standard error $\sqrt{\frac{WSSE}{n-2}}$
7.0	0.2	6000	0.02	0.13	2 E8	0.010	0.033
8.2	0.2	6000	0.02	0.19	9 E6	0.010	0.033

Table 9. Continued

pH	Sulfite Conc. (mM)	UV intensity ($\mu W/cm^2$)	Initial 1,2-DCA Conc. (mM)	Sulfite Quantum Yield (Φ)	Rate Constant ($k_{6.3}$, $M^{-1}s^{-1}$)	Minimum value of WSSE	Standard error $\sqrt{\frac{WSSE}{n-2}}$
9.0	0.2	6000	0.02	0.17	10	0.009	0.034
11.0	0.2	6000	0.02	0.18	10	0.010	0.033
11.0	0.04	6000	0.02	0.05	2 E9	0.027	0.055
11.0	0.1	6000	0.02	0.10	1 E8	0.002	0.013
11.0	0.4	6000	0.02	0.15	8 E7	0.004	0.021
11.0	0.2	2000	0.02	0.22	5 E6	0.011	0.033
11.0	0.2	4000	0.02	0.36	3 E9	0.004	0.020
11.0	0.2	8000	0.02	0.34	1 E9	0.031	0.059
11.0	0.2	6000	0.04	0.39	7 E9	0.012	0.037
11.0	0.2	6000	0.06	0.18	3 E7	0.004	0.022
11.0	0.2	6000	0.09	0.46	1 E10	0.005	0.024

The rate constant ($k_{6.3}$) between the aqueous electron and the intermediate ($\bullet CH_2CH_2Cl$) could vary under different conditions. However, there could be other intermediates being produced that also react with aqueous electron. Therefore, the

mechanistic model simplifies the reactions between aqueous electron and all intermediates into one reaction and this may result in a wide range of values of the rate constant at different experimental conditions.

Another round of regressions was conducted to search for better values of the rate constants ($k_{6.3}$), but they used a constant value of 0.22 for the sulfite quantum yield (Φ), which is the average of values in Table 9. The search range for $k_{6.3}$ was from 10 to 1E20 with 200 logarithmically spaced values. Results are shown in Table 10.

With a constant value of quantum yield, the variation in the values of rate constants ($k_{6.3}$) decreases substantially (compare Table 10 with Table 9). This indicates that the mechanistic model describes well most of the experiment data by assuming a constant quantum yield and using one reaction to describe all possible reactions between the aqueous electron and any intermediates. It is also noticed that the values of the rate constant ($k_{6.3}$) at lower sulfite concentrations are much larger than those obtained in higher sulfite doses. This is the result of the model attempting to fit slower degradation of 1,2-DCA observed at lower sulfite doses. The model increases $k_{6.3}$ so that the concentration of the aqueous electron is reduced, resulting in slower degradation of 1,2-DCA.

Table 10. Values of rate constant ($k_{6.3}$) between the aqueous electron and an intermediate (Eq. 6.3)

pH	Sulfite Conc. (mM)	UV intensity ($\mu W/cm^2$)	Initial 1,2-DCA Conc. (mM)	Rate Constant ($k_{6.3}$, $M^{-1}s^{-1}$)	Minimum value of WSSE	Standard error $\sqrt{\frac{WSSE}{n-2}}$
7.0	0.2	6000	0.02	2 E10	0.019	0.046
8.2	0.2	6000	0.02	1 E8	0.019	0.046
9.0	0.2	6000	0.02	2 E8	0.037	0.068
11.0	0.2	6000	0.02	1 E8	0.027	0.055
11.0	0.04	6000	0.02	6 E13	1.545	0.414
11.0	0.1	6000	0.02	6 E13	0.038	0.062
11.0	0.4	6000	0.02	1 E9	0.021	0.046
11.0	0.2	2000	0.02	6 E7	0.011	0.033
11.0	0.2	4000	0.02	1 E8	0.006	0.024
11.0	0.2	8000	0.02	1 E8	0.066	0.086
11.0	0.2	6000	0.04	9 E7	0.015	0.041
11.0	0.2	6000	0.06	2 E8	0.020	0.047
11.0	0.2	6000	0.09	7 E7	0.008	0.030

6.1.2. Fitting degradation data of 1,2-DCA

The values of sulfite quantum yield (0.22) and rate constants ($k_{6.3}$) in Table 10 were used in model simulations that are compared with all the experimental data. Values for the other coefficients are provided in Appendix D and the simulation results are shown in Figure 18-Figure 21.

The mechanistic model fits the degradation data well at various pH conditions as shown in Figure 18. The rate constants applied to obtain the best fit varies from 1 E8 to 2 E10 M^{-1} s^{-1}at different pH.

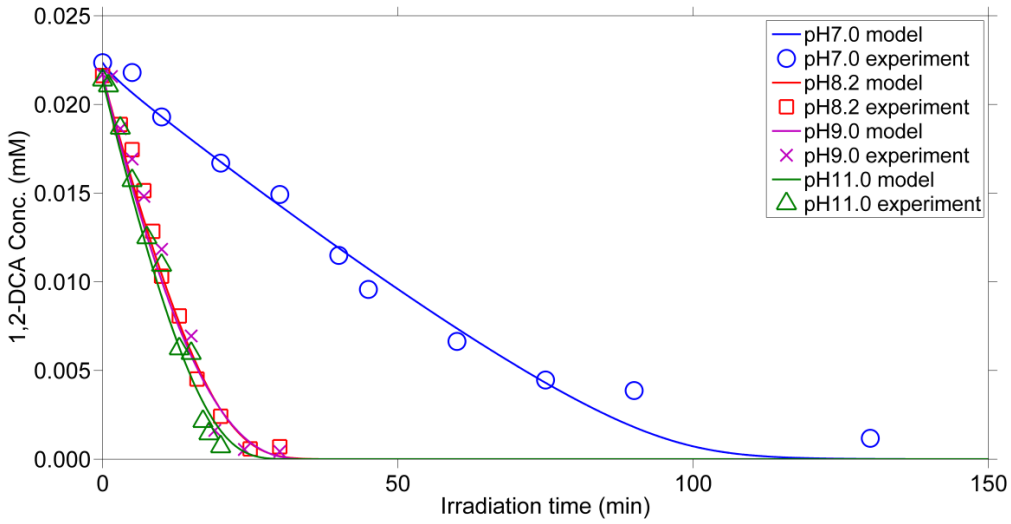

Figure 18. Mechanistic model simulation of 1,2-DCA degradation at various pH.

The mechanistic model fits the degradation data well at sulfite doses higher than 0.2 mM (Figure 19). However, it does not predict the degradation kinetics well at lower sulfite doses. At the lowest sulfite dose (0.04 mM), the model substantially overestimates the degradation of 1,2-DCA. A possible explanation for this is that the

value of the sulfite quantum yield used in the simulation is not suitable for low sulfite doses. A value of 0.050 was calculated in the initial regressions at a sulfite dose of 0.04 mM (Table 9), which is the smallest one among all experimental conditions. The sulfite quantum yield used to generate the model predictions shown in Figure 19 is 0.22, which is about 4.6 times higher than the value previously obtained. An acceptable fit to the data cannot be achieved by only adjusting the value of $k_{6.3}$, and this could be caused by the real sulfite quantum yield in this condition (0.04 mM sulfite dose) being lower than the value used in the simulation (0.22). This would mean that the quantum yield depends on the sulfite concentration. However, this is contrary to previous analysis that the quantum yield should be independent of the sulfite concentration. Therefore, the poor fitting is more likely to be caused by the model describing reactions between the aqueous electron and a number of intermediates in terms of a reaction with only one intermediate. This simplification could make the simulated concentration of aqueous electron higher than the actual concentration present in the solution, so the simulated degradation of 1,2-DCA would be faster than the real degradation and all 1,2-DCA would be removed in the simulation before the sulfite is exhausted. Thus, this mechanistic model did not describe the observed plateau in the 1,2-DCA concentration that was probably caused by consumption of sulfite in the experiment. The fitting for the degradation data at 0.1 mM sulfite dose shows that the model predicts the first several data points well, but fails to predict the later stage of the degradation. It also suggests that when sulfite concentration was simulated to drop to some level (around 0.075 mM, indicated by the simulated sulfite concentration at 50 minutes), the model cannot produce accurate predictions.

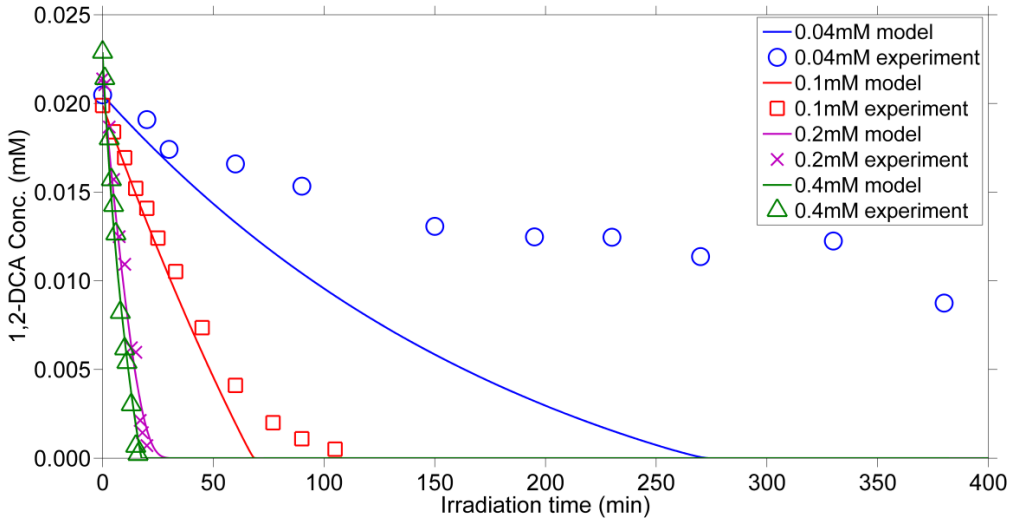

Figure 19. Mechanistic model simulation of 1,2-DCA degradation at various sulfite doses.

The mechanistic model prediction fits the degradation data well at different UV light intensities as shown in Figure 20. The rate constant ($k_{6.3}$) ranges from 6 E7 to 1 E8 M^{-1} s^{-1}. Compared with the large variation in rate constants that was obtained at different sulfite doses, the relatively constant values of $k_{6.3}$ at different light intensities indicates that intermediates species are not sensitive to the change in UV light intensity.

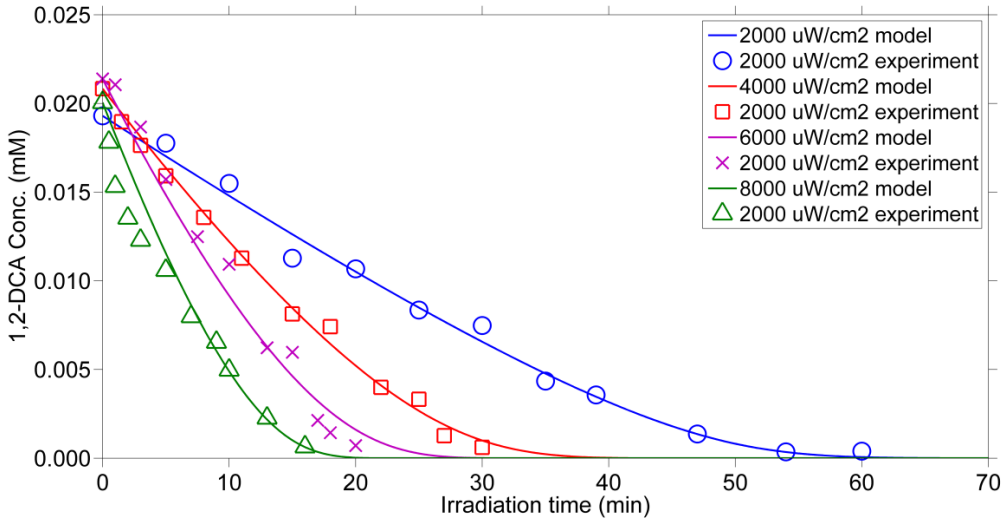

Figure 20. Mechanistic model simulation of 1,2-DCA degradation at various UV light intensities.

The mechanistic model can predict the degradation of 1,2-DCA well when its initial concentration varies as shown by Figure 21. The rate constant ($k_{6.3}$) ranges from 7 E7 to 2 E8 M^{-1} s^{-1} over the range in initial concentrations considered.

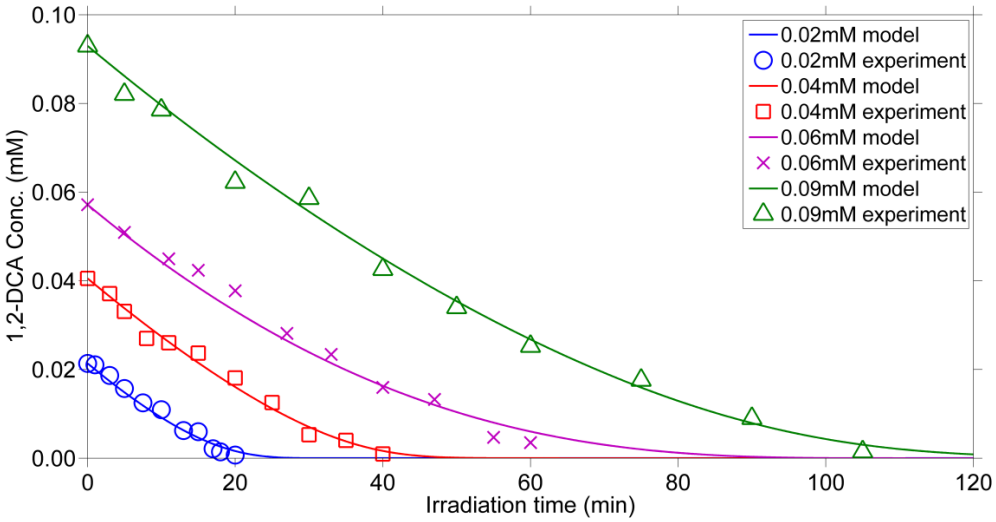

Figure 21. Mechanistic model simulation of 1,2-DCA degradation at various initial 1,2-DCA concentrations.

The model also predicts the experimental data well when aqueous electron scavengers (nitrate, nitrous oxide) were applied, as shown in Figure 22. The fitting was conducted with the quantum yield of 0.22 and the rate constant of 2 E8 M^{-1} s^{-1}. These values are the ones obtained for the same experimental conditions, but without presence of nitrate or nitrous oxide. The values of WSSE are 0.004 and 0.001 for the data obtained with nitrate and nitrous oxide, respectively.

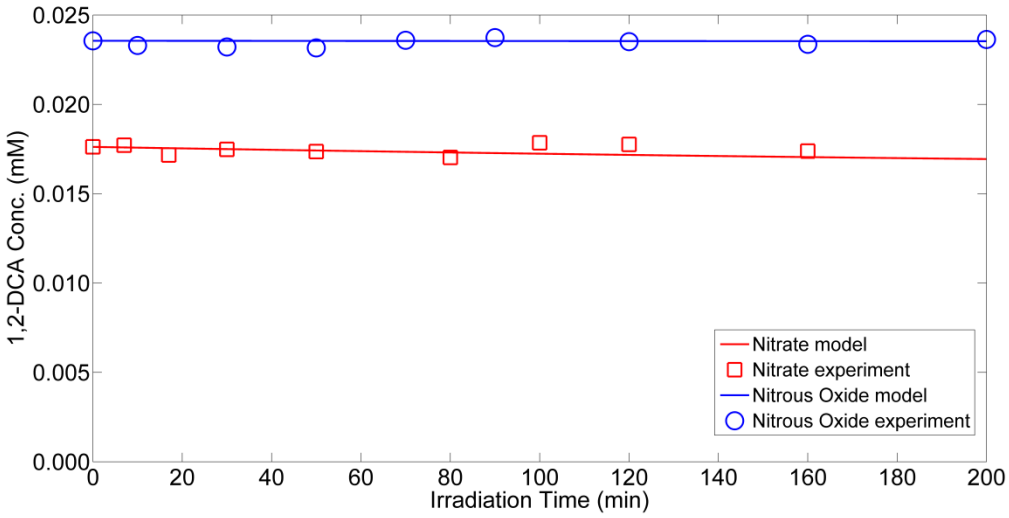

Figure 22. Mechanistic model simulation of 1,2-DCA degradation with nitrate or nitrous oxide as aqueous electron scavengers

6.2. Mechanistic Modeling for the Degradation of VC with the Sulfite/UV ARP

6.2.1. Model development

The mechanistic model was also applied to predict the degradation of VC by the sulfite/UV ARP. VC is considered to be degraded in two steps (Section 4). First, the VC molecule is attacked by the sulfite radical and forms an intermediate sulfonate radical, e.g.. $^{\cdot}SO_3^{-}CH_2CHCl\bullet$). Then, the aqueous electron reacts with the intermediate to produce chloride and organic products. This mechanism is expressed by Eq. (6.7) and (6.8).

$SO_3^{\bullet-}$ + VC → radical intermediate rate constant $k_{6.7}$ (6.7)

e_{aq}^- + radical intermediate → products +Cl^- rate constant $k_{6.8}$ (6.8)

The sulfite quantum yield, the rate constant ($k_{6.7}$) for the reaction between sulfite radial and VC (Eq. (6.7)), and the rate constant ($k_{6.8}$) of the reaction between the aqueous electron and the radical intermediate (Eq. (6.8)) are unknown parameters that need to be determined. Since the sulfite quantum yield has been identified using data for 1,2-DCA degradation, and the degradations of VC were conducted with similar sulfite doses and pH, the value of 0.22 was used as the sulfite quantum yield in the model for degradation of VC.

The value of $k_{6.7}$ should be constant at all experimental conditions. However, the value of $k_{6.8}$ could vary at various experiments since the intermediates could be different at different experimental conditions. Eq.(6.8) is intended to represent a number of similar reactions and $k_{6.8}$ is an overall rate constant that could represents the net effect of several similar reactions. The determinations of $k_{6.7}$ and $k_{6.8}$ were performed in two stages. First, a reasonable assumption for the value of $k_{6.8}$ was assumed and used to search for the best value of $k_{6.7}$. The rate constant ($k_{6.3}$) between the aqueous electron and intermediates for 1,2-DCA degradation was determined to be 2 E8 M^{-1} s^{-1} at pH 9 and this is the pH condition for most of the VC degradation experiments. It is assumed that the rate constant for the reaction between the aqueous electron and the radical intermediate in VC degradation has similar value, so a value of 2 E8 M^{-1} s^{-1} is used for

$k_{6.8}$ to search for the best $k_{6.7}$ that minimize the value of WSSE. A total of 11 data sets were fitted and the range for $k_{6.7}$ was from 10 to 1 E20 M^{-1} s^{-1} with 100 logarithmically spaced values. Results are shown in Table 11.

Table 11. Values of rate constant ($k_{6.7}$) between sulfite radial and VC

pH	Sulfite Conc. (mM)	UV intensity ($\mu W/cm^2$)	Initial VC Conc. (mM)	Rate Constant ($k_{6.7}$) between sulfite radical and VC ($M^{-1}s^{-1}$)	WSSE	Standard error $\sqrt{\frac{WSSE}{n-2}}$
9.0	0.16	4000	0.016	2 E5	0.012	0.719
11.0	0.16	4000	0.016	1 E5	0.007	0.702
9.0	0.016	4000	0.016	1 E5	0.114	0.804
9.0	0.079	4000	0.016	7 E4	0.027	0.753
9.0	0.95	4000	0.016	4 E5	0.010	0.715
9.0	0.16	2000	0.016	2 E5	0.008	0.703
9.0	0.16	6000	0.016	2 E5	0.016	0.733
9.0	0.16	8000	0.016	2 E5	0.021	0.739
9.0	0.95	4000	0.018	6 E5	0.010	0.720
9.0	0.95	4000	0.028	4 E5	0.009	0.714
9.0	0.95	4000	0.019	1 E6	0.041	0.763

The values of $k_{6.7}$ range from 7 E4 to 1 E6 M^{-1} s^{-1} and have an average value of 3 E5 M^{-1} s^{-1}. This average value was used in simulations to determine the value of $k_{6.8}$ that gives the minimum value of WSSE. At pH 5 and pH 7, the quantum yield could be much different from the value of 0.233 that was determined for alkaline sulfite solutions. Thus, for the experimental data sets at pH 5 and 7, both the sulfite quantum yield and $k_{6.8}$ were set as unknown variables. Results are shown in Table 12.

Table 12. Values of rate constant ($k_{6.8}$) between aqueous electron and intermediates in the VC degradation

pH	Sulfite Conc. (mM)	UV intensity ($\mu W/cm^2$)	Initial VC Conc. (mM)	Rate Constant ($k_{6.8}$) between aqueous electron and intermediates ($M^{-1}s^{-1}$)	WSSE	Standard error $\sqrt{\frac{WSSE}{n-2}}$
5.0*	0.16	4000	0.016	1 E11	0.031	0.762
7.0*	0.16	4000	0.016	7 E8	0.010	0.720
9.0	0.16	4000	0.016	3 E 10	0.031	0.754
11.0	0.16	4000	0.016	10	0.355	0.856
9.0	0.016	4000	0.016	2 E9	0.130	0.809
9.0	0.079	4000	0.016	3 E13	0.212	0.834
9.0	0.95	4000	0.016	10	0.009	0.713
9.0	0.16	2000	0.016	4 E11	0.039	0.762
9.0	0.16	6000	0.016	4 E14	0.095	0.801

Table 12. Continued

pH	Sulfite Conc. (mM)	UV intensity ($\mu W/cm^2$)	Initial VC Conc. (mM)	Rate Constant ($k_{6.8}$) between aqueous electron and intermediates ($M^{-1}s^{-1}$)	WSSE	Standard error $\sqrt{\frac{WSSE}{n-2}}$
9.0	0.16	8000	0.016	3 E14	0.170	0.820
9.0	0.95	4000	0.018	10	0.149	0.825
9.0	0.95	4000	0.028	10	0.038	0.765
9.0	0.95	4000	0.019	10	0.128	0.808

* sulfite quantum yield applied are 0.93 and 0.24 for the experiment conducted at pH 5.0 and pH 7.0

The rate constants shown in Table 12 have large variations, ranging from 10 to 4 E14. This could be the result of the simplification in the model of describing reactions between the aqueous electron and all intermediates as a reaction with one intermediate that consumes one aqueous electron. This simplification may not be appropriate for the VC degradation and it limits the ability of the model to predict VC degradation well. More reactions that consume the aqueous electron or sulfite radical or both, should be included in the model. However, this may be difficult because less information is available to quantify these possible reactions.

6.2.2. Fitting degradation data of VC

The values of coefficients shown in Table 12 were used to simulate concentrations of 1,2-DCA under all experimental conditions and the results are shown in Figure 23-Figure 26.

The mechanistic model fits the VC degradation data well at various pH (Figure 23), except for the data at pH 11. The sulfite represents nearly all of the sulfite species at pH 9 and 11, so it could be assumed that there would be similar degradation behavior. However, the degradation data present significant differences at pH 9 and pH 11 and the model overestimates the rates of degradation at both pH. It is possible that quite different intermediates are produced at pH 11 compared to pH 9 and that they have much different reactivities towards the aqueous electron. However, these reactions cannot be well predicted by adjusting the rate constant in Eq. (6.8) and little evidence can be found to support this assumption.

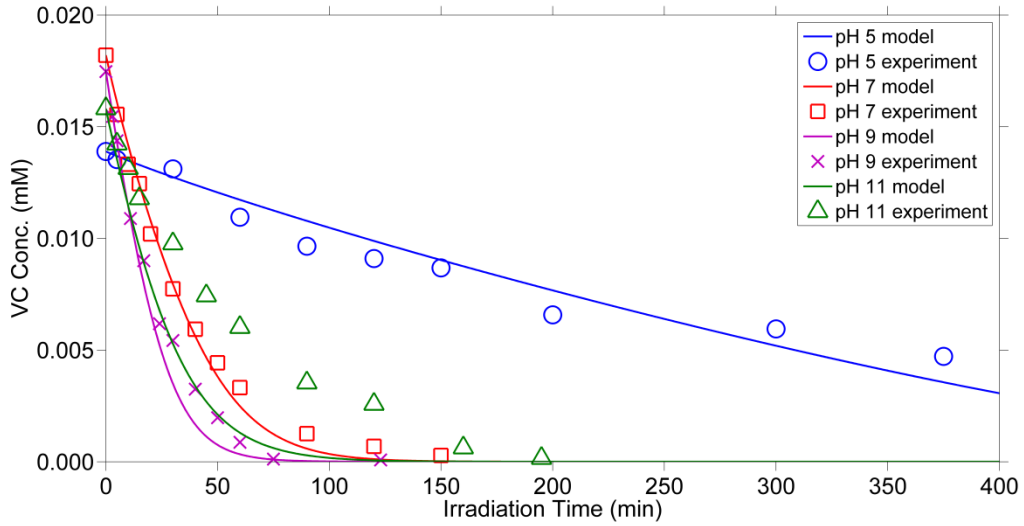

Figure 23. Mechanistic model simulation of VC degradation at various pH.

The model fits the VC degradation data well at various sulfite doses as shown in Figure 24, except for the data at a sulfite dose of 0.079 mM, in which the model overestimates the degradation rate of VC. The most likely reason for this is that the mechanistic model simplifies various reactions between the aqueous electron and different intermediates as one reaction. This simplification will ignore some reactions that consume the aqueous electron and result in an overestimate of the actual concentration of aqueous electron. Thus, the simulation shows a more rapid removal of VC observed without showing any plateau in the degradation curve.

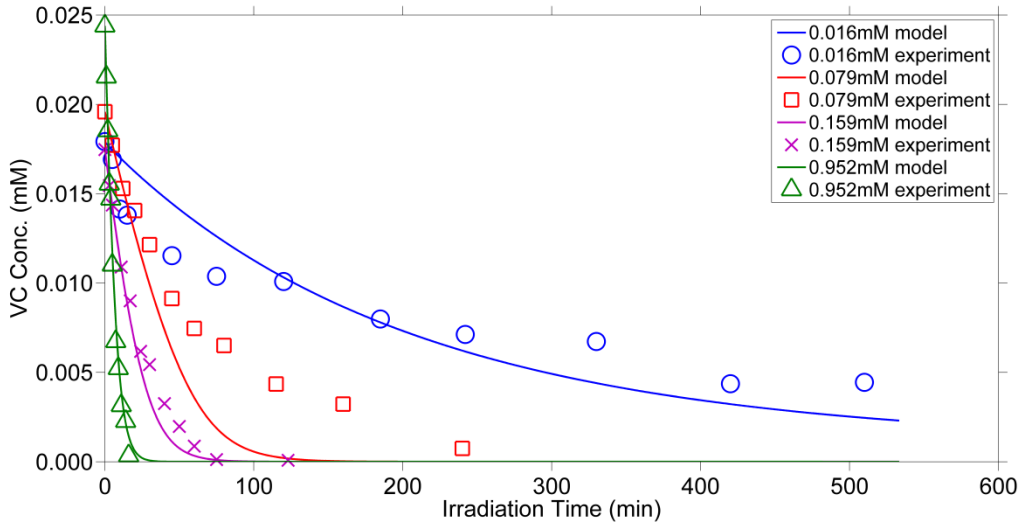

Figure 24. Mechanistic model simulation of VC degradation at various sulfite doses.

The model tends to predicts more rapid VC degradation than observed at various light intensities as shown in Figure 25. The most likely reason is that the model does not include all reactions that consume the sulfite radical. Based on the results from scavenging experiments, the model assumes a degradation mechanism in which the sulfite radical reacts with VC to form intermediates and the aqueous electron reacts with the intermediates to produce end products. However, it is possible that some intermediates also consume the sulfite radical, but the model fails to track these reactions. Therefore, the model would predict a higher concentration of sulfite radical than actually exists, which would lead to overestimating the rate of VC degradation.

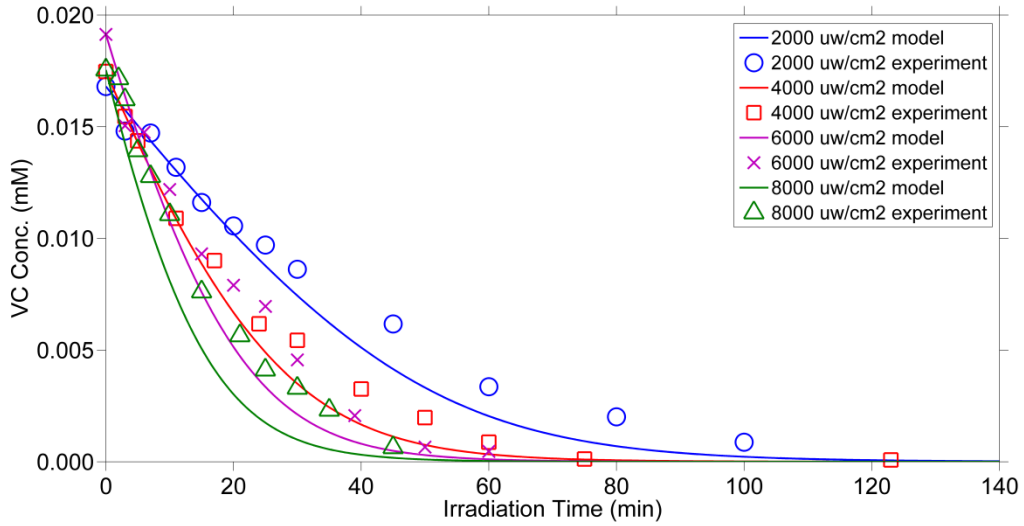

Figure 25. Mechanistic model simulation of VC degradation at various UV light intensities.

The model tends to predict slower VC removals than observed, as shown in Figure 26. The underestimation is more obvious at the highest VC doses. This could also be caused by failing to include important reactions or using inaccurate values of rate constants. This behavior indicates that the model needs some improvements to better describe VC degradation.

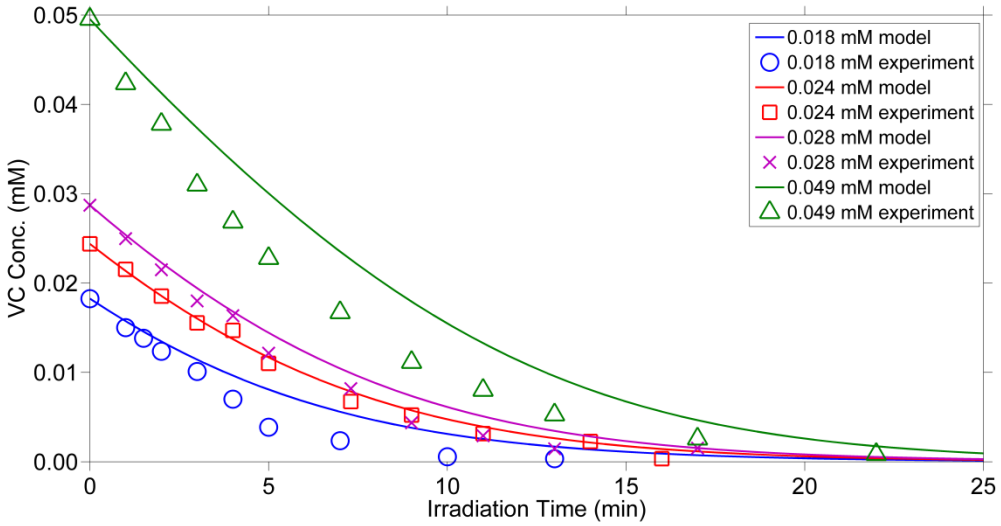

Figure 26. Mechanistic model simulation of VC degradation at various initial VC concentrations.

The model can predict the experiment data with nitrate or nitrous oxide well, as shown in Figure 27. This supports the assumption that the sulfite radical, but not the aqueous electron, degrades VC.

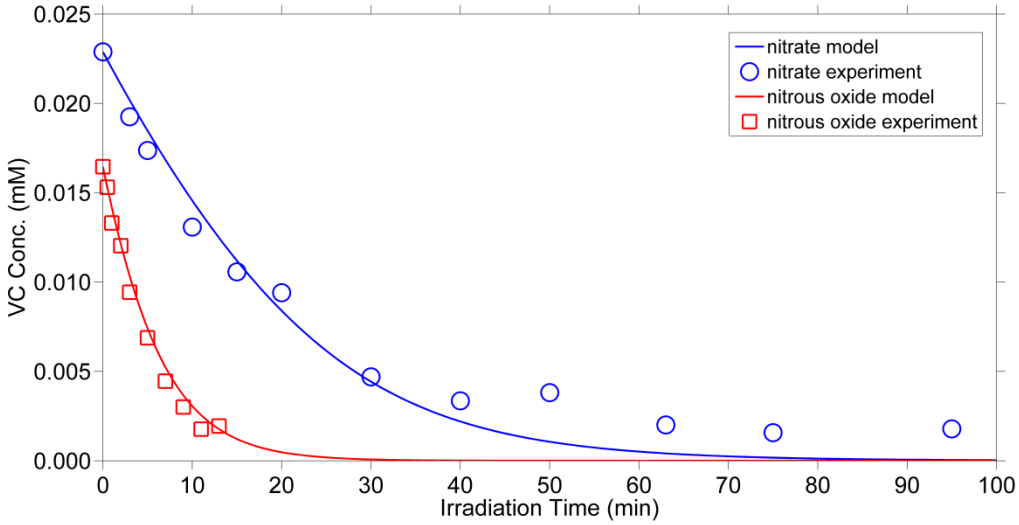

Figure 27. Mechanistic model simulation of VC degradation with nitrate or nitrous oxide as aqueous electron scavengers.

7. CONCLUSIONS

This research demonstrated the effectiveness of various Advanced Reduction Processes (ARPs) for the degradation of chlorinated organics, such as vinyl chloride (VC) and 1,2-dichloroethane (1,2-DCA). The degradation kinetics for these contaminants treated by a specific ARP, the sulfite/UV ARP, was further investigated. An empirical pseudo-first order model was applied to describe the kinetic data and help quantify the dependence of degradation kinetics on several process variables. The understanding of the degradation mechanisms resulting from this analysis supported development of a mechanistic model that simulated complex reactions occurring in the sulfite/UV ARP. Specific conclusions can be drawn based on the experimental results as follows.

First, the degradation of VC was successful with various ARPs that combined UV irradiation at 253.7 nm with different reducing reagents (dithionite/sulfite/sulfide/ferrous iron). The degradation kinetics was substantially promoted in the ARPs compared to direct photolysis (only UV, no reagents). This enhancement is due to reactions between VC and reactive species that are produced when these reducing reagents receive UV irradiation. These reactive species include sulfur dioxide radical, sulfite radical, aqueous electron and hydrogen atom. The effect of solution pH, sulfite dose, UV light intensity and initial VC dose on the degradation kinetics was further explored with the sulfite/UV ARP. A pseudo-first-order model was applied and the rate constants were compared at various experimental conditions.

Generally higher pH leads to faster VC degradation and this is due to the variation of sulfite species with changes in solution pH. Increasing sulfite dose and UV light intensity resulted in linear increases in the pseudo-first-order rate constant. The variation in initial VC dose has little influence on the rate constant. Nitrate or nitrous oxide was added as aqueous electron scavengers and results of these experiments identified that the sulfite radical is the reactive species causing VC degradation. The aqueous electron probably reacts with intermediate products, thereby affecting distribution of products. The efficiency of the sulfite/UV ARP was expressed as quantum yield for VC and the effects of various process variables on it were evaluated. A mechanistic model including 32 compounds and 77 reactions was developed and fit to the VC degradation data. The model made reasonably good predictions of VC degradation, but still needs to be improved in order to obtain more accurate fittings.

Second, complete degradation of 1,2-DCA was achieved with the same ARPs examined in experiments on VC degradation. The degradation kinetics of 1,2-DCA degradation with the sulfite/UV ARP followed a pseudo-first-order decay model and the rate constants were determined at all experimental conditions. Increasing pH increases the degradation rate at low and neutral pH, but it has little effect at higher pH. Higher sulfite doses and light intensities generally promote 1,2-DCA degradation in a linear manner as predicted by a simple model that considers production of reactive species and their reaction with the target compound and unspecified scavengers. The pseudo-first-order rate constants decrease slightly at higher initial 1,2-DCA concentrations, as predicted by the simple model. Experiments with scavengers of aqueous electrons

showed that the degradation of 1,2-DCA is mainly due to the aqueous electron but not the sulfite radical. The dechlorination efficiency varies with the solution pH and more than 90% dechlorination was achieved at pH 11.0. The quantum yield of 1,2-DCA was compared at all experimental conditions. The mechanistic model could predict most of the 1,2-DCA degradation data well, except the data at the lowest sulfite dose.

Third, the technology of ARPs has been applied to both VC and 1,2-DCA degradation and the results demonstrate the ability of these processes to effectively degrade chlorinated aliphatic compounds. The affinity of the sulfite radical for VC is probably associated with its double bond, which implies that it will probably be important in degrading other chlorinated alkenes, while the aqueous electron will be more important in degrading chlorinated alkanes.

Fourth, application of these ARPs in treatment systems is promising given the rapid degradation kinetics and detoxification efficiency. The results of applying the sulfite/UV ARP technology suggests that it is a way to utilize sulfur dioxide gas to degrade contaminants while reducing the cost of desulfurization.

Fifth, this technology needs to be tested at pilot scale with continuous flow systems. Some practical considerations such as the installation of UV source, control of the oxygen level and water mixing, should be considered in engineering applications. It will be important in such applications to consider the effects of scavengers of reactive species that are present in the water to be treated. It may be advantageous to apply appropriate pretreatments to remove scavengers (such as nitrate or dissolved oxygen),

otherwise either the degradation efficiency of targets will be compromised or more reagents (e.g. sulfite) will be consumed.

REFERENCES

Ahmed M, Peterka DS, Suits AG. The photodissociation of the vinyl radical (C2H3) at 243 nm studied by velocity map imaging. J Chem Phys 1999; 110: 4248-4253.

Airey PL, Dainton FS. The photochemistry of aqueous solutions of Fe (II). I. photoelectron detachment from ferrous and ferrocyanide ions. Proc R Soc London, Ser. A 1966; 291: 340-352.

Al-Malack MH, Sheikheldin SY. Effect of solar radiation on the migration of vinyl chloride monomer from unplasticized PVC pipes. Water Res 2001; 35: 3283-3290.

Andreas T, Silke K, Yuri K, Aharon G. Chloroethene dehalogenation with ultrasonically produced air-stable nano iron. Ultrason Sonochem 2009; 16: 617-621.

Aochi YO, Farmer WJ. Role of microstructural properties in the time dependent sorption/desorption behavior of 1,2-dichloroethane on humic substances. Environ Sci Technol 1997; 31: 2520-2526.

ATSDR. Toxicological profile for 1,2-dichloroethane. U.S. Department of Health and Human Services, Public Health Service, Atlanta,GA, 2001.

ATSDR. Toxicological profile for vinyl chloride. U.S. Department of Health and Human Services, Public Health Service, Atlanta,GA, 2006.

Barbash JE, Reinhard M. Abiotic dehalogenation of 1,2-dichloroethane and 1,2-dibromoethane in aqueous-solution containing hydrogen-sulfide. Environ Sci Technol 1989; 23: 1349-1358.

Begley JF, Czarnecki M, Kemen S, Verardo A, Robb AK, Fogel S, et al. Oxygen and ethene biostimulation for a persistent dilute vinyl chloride plume. Ground Water Monit R 2012; 32: 99-105.

Bejankiwar R, Lalman JA, Seth R, Biswas N. Electrochemical degradation of 1,2-dichloroethane (DCA) in a synthetic groundwater medium using stainless-steel electrodes. Water Res 2005; 39: 4715-4724.

Borowska ZK, Mauzerall DC. Efficient near ultraviolet light induced formation of hydrogen by ferrous hydroxide. Orig Life Evol Biosph 1987; 17: 251-9.

Bradley PM, Chapelle FH. Anaerobic mineralization of vinyl chloride in Fe(III)-reducing, aquifer sediments. Environ Sci Technol 1996; 30: 2084-2086.

Bradley PM, Chapelle FH. Effect of contaminant concentration on aerobic microbial mineralization of DCE and VC in stream-bed sediments. Environ Sci Technol 1998; 32: 553-557.

Bradley PM, Chapelle FH. Methane as a product of chloroethene biodegradation under methanogenic conditions. Environ Sci Technol 1999; 33: 653-656.

Bradley PM, Chapelle FH. Acetogenic microbial degradation of vinyl chloride. Environ Sci Technol 2000; 34: 2761-2763.

Butler EC, Hayes KF. Kinetics of the transformation of trichloroethylene and tetrachloroethylene by iron sulfide. Environ Sci Technol 1999; 33: 2021-2027.

Buxton GV, Greenstock CL, Helman WP, Ross AB. Critical review of rate constant for reactions of hydrated electrons, hydrogen atoms and hydroxyl radicals. J Phys Chem Ref Data 1988; 17: 513-886.

Chawla OP, Arthur NL, Fessenden RW. electron spin resonance study of the photolysis of aqueous sulfite solutions J Phys Chem 1973; 77: 772-776.

Chen RH, Avotinsh Y, Freeman GR. Solvent effects on the reactivity of solvated electrons with ions in isobutanol/water mixed-solvents. Canadian Journal of Chemistry-Revue Canadienne De Chimie 1994; 72: 1083-1093.

Cheng CJ, Lin TH, Chen CP, Juang KW, Lee DY. The effectiveness of ferrous iron and sodium dithionite for decreasing resin-extractable Cr(VI) in Cr(VI)-spiked alkaline soils. J Hazard Mater 2009a; 164: 510-6.

Cheng XP, Yang GY, Mu TC, Guo XK, Wang XL. Absorption of vinyl chloride by room temperature ionic liquids. Clean 2009b; 37: 245-248.

Chu W, Jia J. The photodegradation and modeling of a typical NAPL trichloroethene, by monochromatic UV irradiations. Environ Sci Technol 2009; 43: 1455-9.

Croue JP, Reckhow DA. Destruction of chlorination byproducts with sulfite. Environ Sci Technol 1989; 23: 1412-1419.

Cupples AM, Spormann AM, McCarty PL. Growth of a dehalococcoides-like microorganism on vinyl chloride and cis-dichloroethene as electron acceptors as determined by competitive PCR. Appl Environ Microbiol 2003; 69: 953-959.

Deister U, Neeb R, Helas G, Warneck P. Temperature dependence of the equilibrium CH2(OH)2 + HSO3- = CH2(OH)SO3- + H2O in aqueous solution. J Phys Chem 1986; 90: 3213-3217.

Dinglasan-Panlilio MJ, Dworatzek S, Mabury S, Edwards E. Microbial oxidation of 1,2-dichloroethane under anoxic conditions with nitrate as electron acceptor in mixed and pure cultures. FEMS Microbiol Ecol 2006; 56: 355-64.

Dogliott.L, Hayon E. Flash photolysis study of sulfite thiocyanate and thiosulfate ions in solution. J Phys Chem 1968; 72: 1800-1807.

Dzhabiev TS, Tarasov BB. Photochemical decomposition of an aqueous-solution of sodium sulfide. J Photochem Photobiol A: Chem 1993; 72: 23-27.

Elsner M, Chartrand M, Vanstone N, Couloume GL, Lollar BS. Identifying abiotic chlorinated ethene degradation: characteristic isotope patterns in reaction products with nanoscale zero-valent iron. Environ Sci Technol 2008; 42: 5963-70.

EPA US. 2011 Edition of the drinking water standards and health advisories, Washington, DC, 2011.

Fischer M, Warneck P. Photodecomposition and photooxidation of hydrogen sulfite in aqueous solution. J Phys Chem 1996; 100: 15111-15117.

Freedman DL, Herz SD. Use of ethylene and ethane as primary substrates for aerobic cometabolism of vinyl chloride. Water Environ Res 1996; 68: 320-328.

Fu J, Zhang ZM, Tang JY, Zeng QF, An SQ, Zhu HL. Photoreduction of reactive brilliant red X-3B by ultraviolet irradiation/potassium borohydride/sodium bisulfite. J Environ Eng-ASCE 2010; 136: 1314-1319.

Getoff N. Decomposition of biological resistant pollutants in water by irradiation. Radiat Phys Chem 1990; 35: 432-439.

Grodkowski J, Neta P. Ferrous ions as catalysts for photochemical reduction of CO2 in homogeneous solutions. J Phys Chem 2000; 104: 4475-4479.

Guo L, Wang B, Huang W, Wu F, Huang J. Photocatalytic degradation of diphenolic acid in the presence of beta-cyclodextrin under UV light. 2009 International Conference on Environmental Science and Information Application Technology, 2009, 322-324.

Gurtler R, Moller U, Sommer S, Muller H, Kleinermanns K. Photooxidation of exhaust pollutants. Chmosphere 1994; 29: 1671-1682.

Gwinn MR, Johns DO, Bateson TF, Guyton KZ. A review of the genotoxicity of 1,2-dichloroethane (EDC). Mutat Res 2011; 727: 42-53.

Hara K, Sayama K, Arakawa H. UV photoinduced reduction of water to hydrogen in Na2S, Na2SO3, and Na2S2O4 aqueous solutions. J Photochem Photobiol A: Chem 1999; 128: 27-31.

Hartmans S, Bont JAMd. Aerobic vinyl chloride metabolism in mycobacterium aurum L1. Appl Environ Microbiol 1992; 58: 1220-1226.

Hata J, Miyata N, Kim ES, Takamizawa K, Iwahori K. Anaerobic degradation of cis-1,2-dichloroethylene and vinyl chloride by clostridium sp. strain DC1 isolated from landfill leachate sediment. J Biosci Bioeng 2004; 97: 196-201.

Hayon E, Treinin A, Wilf J. Electronic-spectra, photochemistry, and autoxidation mechanism of sulfite-bisulfite-pyrosulfite systems - SO2-, SO3-, SO4-, and SO5-Radicals. J Am Chem Soc 1972; 94: 47-57.

He JZ, Ritalahti KM, Aiello MR, Loffler FE. Complete detoxification of vinyl chloride by an anaerobic enrichment culture and identification of the reductively dechlorinating population as a dehalococcoides species. Appl Environ Microbiol 2003; 69: 996-1003.

Huang CC, Lo SL, Tsai SM, Lien HL. Catalytic hydrodechlorination of 1,2-dichloroethane using copper nanoparticles under reduction conditions of sodium borohydride. J Environ Monitor 2011; 13: 2406-2412.

Khriachtchev L, Pettersson M, Isoniemi E, Rasanen M. 193 nm photolysis of H2S in rare-gas matrices: luminescence spectroscopy of the products. J Chem Phys 1998; 108: 5747-5754.

Kielhorn J, Melber C, Wahnschaffe U, Aitio A, Mangelsdorf I. Vinyl chloride: still a cause for concern. Environ Health Perspect 2000; 108: 579-88.

Klan P, Wirz J. Photochemistry of organic compounds: Wiley, 2009.

Kocamemi BA, Cecen F. Cometabolic degradation and inhibition kinetics of 1,2-dichloroethane (1,2-DCA) in suspended-growth nitrifying systems. Environ Technol 2010; 31: 295-305.

Koester R, Asmus KD. Die Reaktionen chlorierter aethylene mit hydratisierten elektronen und OH-radikalen in waessriger Loesung. Z. Naturforsch. Teil B 1971; 26: 1108 - 1116.

Korolev VV, Bazhin NM. Photolysis of ferrous-ions in sulfuric-acid solutions. High Energ Chem 1978; 12: 353-356.

Kotonarou A, Mills G, Hoffmann MR. Oxidation of hydrogen sulfide in aqueou solution by ultrasonic irradiation. Environ Sci Technol 1992; 26: 2420-2428.

Koziollek P, Bryniok D, HJ. K. Ethene as an auxiliary substrate for the cooxidation of cis-1, 2-dichloroethene and vinyl chloride. Arch Microbiol 1999; 172: 240-246.

Le NB, Coleman NV. Biodegradation of vinyl chloride, cis-dichloroethene and 1,2-dichloroethane in the alkene/alkane-oxidising mycobacterium strain NBB4. Biodegradation 2011; 22: 1095-1108.

Lee MD, Odom JM, Buchanan RJ, Jr. New perspectives on microbial dehalogenation of chlorinated solvents: insights from the field. Annu Rev Microbiol 1998; 52: 423-52.

Li CT, Yang RB, Shih ML, Tsai PJ, Hsieh LT, Chen CY. Reaction mechanism of 1,2-dichloroethane/O2/Ar in the cold plasma environment. Chem Eng J 2003; 92: 177-184.

Li K, Stefan MI, Crittenden JC. UV photolysis of trichloroethylene: product study and kinetic modeling. Environ Sci Technol 2004; 38: 6685-93.

Li W, Lu S, Qiu Z, Lin K. Clofibric acid degradation in UV(254)/H(2)O(2) process: effect of temperature. J Hazard Mater 2010; 176: 1051-1057.

Li X, Ma J, Liu G, Fang J, Yue S, Guan Y, et al. Efficient reductive dechlorination of monochloroacetic acid by sulfite/UV process. Environ Sci Technol 2012; 46: 7342-9.

Lin C, Jou C-JG, Wang C-L. Visible-light-sensitized dechlorination of perchloroethlene. Water Environ Res 2009; 81: 76-81.

Lin YH, Chiu TC, Hsueh HT, Chu H. N-doped TiO(2) photo-catalyst for the degradation of 1,2-dichloroethane under fluorescent light. Appl Surf Sci 2011; 258: 1581-1586.

Linkous CA, Huang CP, Fowler JR. UV photochemical oxidation of aqueous sodium sulfide to produce hydrogen and sulfur. J Photochem Photobiol A: Chem 2004; 168: 153-160.

Liu X, Yoon S, Batchelor B, Abdel-Wahab A. Degradation of vinyl chloride by the sulfite/UV advanced reduction process (ARP): effects of process variables and a kinetic model. Sci Total Environ 2013a; 454-455: 578-583.

Liu X, Yoon S, Batchelor B, Abdel-Wahab A. Photochemical degradation of vinyl chloride with an advanced reduction process (ARP)–effects of reagents and pH. Chem Eng J 2013b; 215-216: 868–875.

Luo Y-R. Bond Dissociation Energies. In: Haynes WM, Lide DR, editors. CRC handbook of chemistry and physics. Boca Raton, FL: CRC Press/Taylor and Francis, 2012.

MacCrehan WA, Jensen JS, Helz GR. Detection of sewage organic chlorination products that are resistant to dechlorination with sulfite. Environ Sci Technol 1998; 32: 3640-3645.

Makarov SV. Novel trends in chemistry of sulfur-containing reductants. Usp Khim 2001; 70: 996-1007.

Mayhew SG. The redox potential of dithionite and SO-2 from equilibrium reactions with flavodoxins, methyl viologen and hydrogen plus hydrogenase. Eur J Biochem 1978; 85: 535-47.

McKenna CE, Gutheil WG, Song W. A method for preparing analytically pure sodium dithionite. Dithionite quality and observed nitrogenase-specific activities. Biochim Biophys Acta 1991; 1075: 109-17.

Melsheimer J, Schlogl R. Identification of reaction products of mild oxidation of H2S in solution and in solid state by UV-vis spectroscopy. Fresenius J Anal Chem 1997; 357: 397-400.

Mertens R, Sonntag Cy. Photolysis (A=254 nm) of tetrachloroethene in aqueous solutions. J Photochem Photobiol A: Chem 1995; 85: 1-9.

Murov SL, Carmichael I, Hug GL. Handbook of photochemistry. New York: Marcel Dekker Inc., 1993.

Neta P, Huie RE. Free-radical chemistry of sulfite. Environ Health Perspect 1985; 64: 209-17.

Ohlsson PI, Blanck J, Ruckpaul K. Reduction of lactoperoxidase by the dithionite anion monomer. Eur J Biochem 1986; 158: 451-4.

Ozawa T, Kwan T. ESR studies on the reactive character of the radical anions, SO2, SO3 and SO4 in aqueous solution. Polyhedron 1983; 2: 1019-1023.

Ozawa T, Kwan T. ESR studies on the reactions of the sulphite radical anion, SO3, with olefinic compounds in aqueous solutions. Polyhedron 1986; 5: 1531-1536.

Pirard SL, Pirard JP, Heyen G, Schoebrechts JP, Heinrichs B. Experimental procedure and statistical data treatment for the kinetic study of selective hydrodechlorination of 1,2-dichloroethane into ethylene over a Pd-Ag sol-gel catalyst. Chem Eng J 2011; 173: 801-812.

Popat SC, Deshusses MA. Kinetics and inhibition of reductive dechlorination of trichloroethene, cis-1,2-dichloroethene and vinyl chloride in a continuously fed anaerobic biofilm reactor. Environ Sci Technol 2011; 45: 1569-1578.

Pukhovskaya SG, Guseva LZ, Makarov SV, Naidenko EV. A new procedure for the spectrophotometric determination of nitrogen(II) oxide in solutions. J Anal Chem 2005; 60: 21-23.

Ranguelova K, Bonini MG, Mason RP. (Bi)sulfite oxidation by copper, zinc-superoxide dismutase: sulfite-derived, radical-initiated protein radical formation. Environ Health Perspect 2010; 118: 970-5.

Rasche ME, Hyman MR, Arp DJ. Factors limiting aliphatic chlorocarbon degradation by nitrosomonas europaea: cometabolic inactivation of ammonia monooxygenase and substrate specificity. Appl Environ Microbiol 1991; 57: 2986-94.

Sano T, Kutsuna S, Negishi N, Takeuchi K. Effect of Pd-photodeposition over TiO2 on product selectivity in photocatalytic degradation of vinyl chloride monomer. J Mol Catal A: Chem 2002; 189: 263-270.

Shalygin AS, Malysheva LV, Paukshtis EA. Mechanism of 1,2-dichloroethane dehydrochlorination on the acid sites of oxide catalysts as studied by IR spectroscopy. Kinet Catal 2011; 52: 305-315.

Shi XL, Shi. Generation of SO3.bul- and OH radicals in SO32- reactions with inorganic environmental pollutants and its implications to SO32- toxicity. J Inorg Biochem 1994; 56: 155-165.

Smidt H, de Vos WM. Anaerobic microbial dehalogenation. Annu Rev Microbiol 2004; 58: 43-73.

Smits THM, Assal A, Hunkeler D, Holliger C. Anaerobic degradation of vinyl chloride in aquifer microcosms. J Environ Qual 2011; 40: 915-922.

Song H, Carraway ER. Reduction of chlorinated ethanes by nanosized zero-valent iron: kinetics, pathways, and effects of reaction conditions. Environ Sci Technol 2005; 39: 6237-45.

Stookey LL. Ferrozine - a new spectrophotometric reagent for iron. Anal Chem 1970; 42: 779-781.

Sun Q, Feitz AJ, Guan J, Waite TD. Comparison of the reactivity of nansized zero-valent iron (nZVI) particles produced by borohydride and dithionite reduction of iron salts. Nano 2008; 3: 341-349.

Tiehm A, Schmidt KR, Pfeifer B, Heidinger M, Ertl S. Growth kinetics and stable carbon isotope fractionation during aerobic degradation of cis-1,2-dichloroethene and vinyl chloride. Water Res 2008; 42: 2431-2438.

Vilve M, Vilhunen S, Vepsalainen M, Kurniawan TA, Lehtonen N, Isomaki H, et al. Degradation of 1,2-dichloroethane from wash water of ion-exchange resin using fenton's oxidation. Environ Sci Pollut Res Int 2010; 17: 875-884.

Wei YT, Wu SC, Chou CM, Che CH, Tsai SM, Lien HL. Influence of nanoscale zero-valent iron on geochemical properties of groundwater and vinyl chloride degradation: a field case study. Water Res 2010; 44: 131-140.

Wei YT, Wu SC, Yang SW, Che CH, Lien HL, Huang DH. Biodegradable surfactant stabilized nanoscale zero-valent iron for in situ treatment of vinyl chloride and 1,2-dichloroethane. J Hazard Mater 2012; 211: 373-380.

Xie Y, Cwiertny DM. Use of dithionite to extend the reactive lifetime of nanoscale zero-valent iron treatment systems. Environ Sci Technol 2010; 44: 8649-8655.

Yamazaki S, Tanimura T, Yoshida A. Reaction mechnism of photocatalytic degradation of chlorinated ethylenes on porous TiO2 pellets: Cl radical-initiated mechnism. J Phys Chem-US 2004; 108: 5183-5188.

Yano T, Tschuikowroux E. Photo-decomposition of 1,1-difluoro-1,2-dichloroethane at 147 nm. J Phys Chem-US 1979; 83: 2572-2578.

Yiin BS, Walker DM, Margerum DW. Non-metal redox kinetics: general-acid-assisted reactions of chloramine with sulfite and hydrogen sulfite. Inorg Chem 1987; 26: 3435-3441.

Yuan MH, Lin YY, Chang CY, Chang CC, Shie JL, Wu CH. Atmospheric-pressure radio-frequency discharge for degradation of vinyl chloride with Pt/Al2O3 catalyst. IEEE Trans Plasma Sci 2011; 39: 1092-1098.

Zhang WX. Nanoscale iron particles for environmental remediation: an overview. J Nanopart Res 2003; 5: 323-332.

Zhao HP, Schmidt KR, Lohner S, Tiehm A. Robustness of an aerobic metabolically vinyl chloride degrading bacterial enrichment culture. Water Sci Technol 2011; 64: 1796-1803.

Zhao S, Ma H, Wang M, Cao C, Xiong J, Xu Y, et al. Study on the mechanism of photo-degradation of p-nitrophenol exposed to 254 nm UV light. Environ Health Perspect 2010; 180: 86-90.

Zuo YG, Deng YW. Iron(II)-catalyzed photochemical decomposition of oxalic acid and generation of H2O2 in atmospheric liquid phases. Chemosphere 1997; 35: 2051-2058.

Zuo YG, Zhan J. Effects of oxalate on Fe-catalyzed photoxidation of dissolved sulfur dioxide in atmospheric water. Atmos Environ 2005; 39: 27-37.

Zuo YG, Zhan J, Wu TX. Effects of monochromatic UV-visible light and sunlight on Fe(III)-catalyzed oxidation of dissolved sulfur dioxide. J Atmos Chem 2005; 50: 195-210.

APPENDIX A. SUPPLEMENTARY DATA FOR SECTION 2

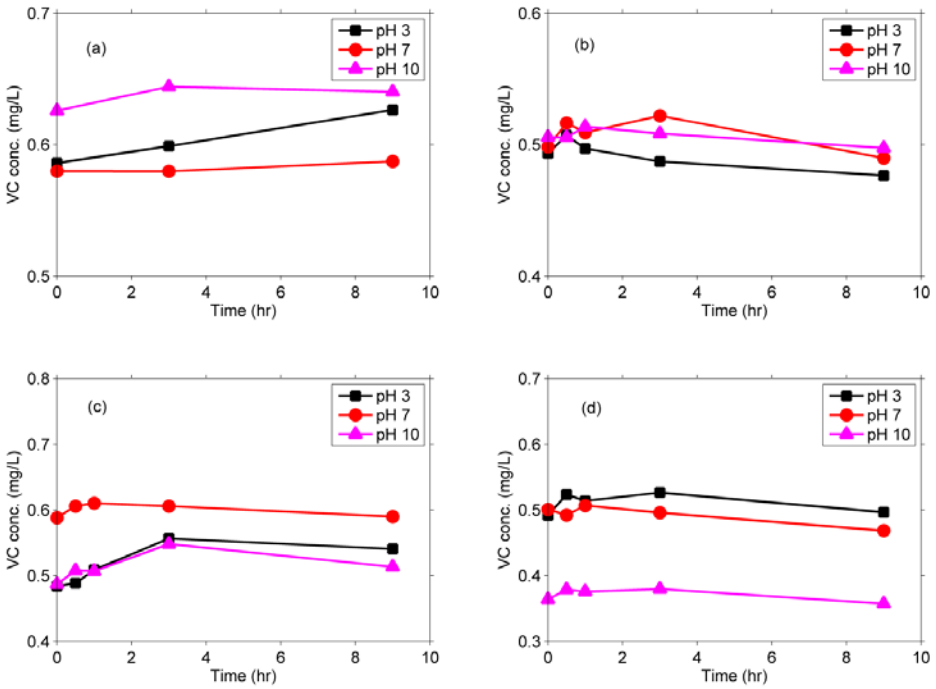

Figure 28. Control experiments at pH 3, 7 and 10 with VC and a reagent of (a) dithionite (b) sulfite (c) sulfide (d) ferrous iron

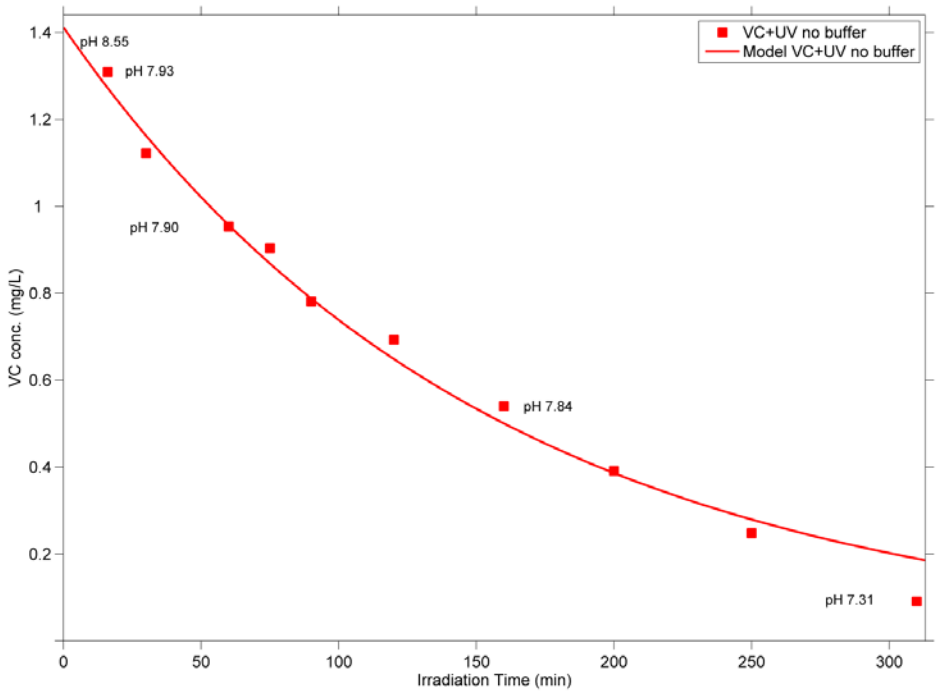

Figure 29. pH changes during direct photolysis of VC

A.1. Rate of Light Absorption of a Particular Wavelength by Dissolved Species

Nomenclature

I = light flux (Einstein/m^2-s)

$\varepsilon_{ln,i}$ = molar absorptivity (M^{-1} m^{-1}) of compound i (defined on natural logarithm basis, differs from molar absorptivity used with Beer-Lambert law for absorbance by factor of 2.303, $\varepsilon_{ln} = 2.303\ \varepsilon_{bl}$, where ε_{bl} is the decadic molar absorptivity used with the Beer-Lambert law, i.e. $I=I_0 10^{-\varepsilon C x}$)

L = total thickness of reactor in direction of light path (m)

A = area of reactor perpendicular to light path (m^2)

V = volume of reactor (m^3)

C_i = concentration of compound i (mole/m^3)

In this study, compound i could be VC or a reagent that is used to produce radical. The rate of light absorption by any compound dissolved in the water can be related to the change of light intensity that results from absorption by that compound with the use of a steady-state material balance. Conducting the balance over a differential element of thickness "dx" where light is passing in the x direction, shows that the volumetric rate of light absorption is equal to the gradient of the light intensity:

$$0 = AI_x - AI_{x+dx} + 0 - Adx\, r_{light}$$

where r_{light} is the overall rate of absorption of light (Einstein/m^3-s)

$$r_{light} = (AI_x - AI_{x+dx})/Adx$$

$$r_{light} = - dI/dx$$

The rate of light absorption is also proportional to light intensity as assumed in the Beer-Lambert law:

$$-dI/dx = \varepsilon_{ln,i} C_i I$$

This can be solved to give:

$$I = I_0 \exp(-\varepsilon_{ln,i} C_i x)$$

Therefore, $r_{light} = - dI/dx = \varepsilon_{ln,i} C_i I = \varepsilon_{ln,i} C_i I_0 \exp(-\varepsilon_{ln,i} C_i x)$

If there are more than one compound that absorb light in the solution, light intensity will be influenced by all compounds, so

$I = I_0 \exp(-\varepsilon_{ln,all} C_{all} x)$

Where $\varepsilon_{ln,all} C_{all} = \sum \varepsilon_{ln,i} C_i$

So the rate of light absorption by compound i should be expressed as:

$r_{light} = \varepsilon_{ln,i} C_i I_0 \exp(-\varepsilon_{ln,all} C_{all} x)$

Note that the rate of light absorption (r_{light}) is a function of position (x), so it depends on position in the reactor, because the light intensity changes within the reactor. In many cases, measurements will be made on the average reaction rate in the reactor, not on the rate at a specific point in the reactor, so it will be useful to calculate an average rate and an average light intensity.

Then the average rate of light absorption by compound i is $r_{light,avg} = \varepsilon_{ln,i} C_i I_{avg}$

The average light intensity can be calculated with the assumption that the reactor is well mixed, so that the concentrations are the same everywhere in the reactor and that length of the light path is constant through all parts of the reactor (i.e. typically this will result with the two faces of the reactor are of equal area and the light enters perpendicularly to them).

$$I_{avg} = \frac{\int_0^L I dx}{\int_0^L dx}$$

where L = thickness of reactor in direction of light path

$$I_{avg} = \frac{\int_0^L I_0 \exp\left(-\varepsilon_{\ln,all} C_{all} x\right) dx}{\int_0^L dx}$$

Assume that $\varepsilon_{ln,all}C_{all}$ is constant throughout the system, i.e. that the system is completely mixed so that the concentration is the same everywhere.

$$I_{avg} = \frac{I_0 \left| \frac{\exp\left(-\varepsilon_{\ln,all} C_{all} x\right)}{-\varepsilon_{\ln,all} C_{all}} \right|_0^L}{\left| x \right|_0^L}$$

$$I_{avg} = \frac{I_0 \left(-\frac{\exp\left(-\varepsilon_{\ln,all} C_{all} L\right)}{\varepsilon_{\ln,all} C_{all}} + \frac{1}{\varepsilon_{\ln,all} C_{all}} \right)}{L}$$

$$I_{avg} = \frac{I_0 \left(1 - \exp\left(-\varepsilon_{\ln,all} C_{all} L\right)\right)}{\varepsilon_{\ln,all} C_{all} L}$$

Then the average rate of light absorption ($r_{light,avg}$) by compound i can be expressed by

$$r_{light,avg} = \varepsilon_{ln,i} C_i I_{avg} = \frac{\varepsilon_{\ln,i} C_i I_0 \left(1 - \exp\left(-\varepsilon_{\ln,all} C_{all} L\right)\right)}{\varepsilon_{\ln,all} C_{all} L}$$

A.2. Calculate the Reaction Rate of Eq. (2.8) in Section 2

$$A + h\nu \rightarrow R \qquad (2.8)$$

When a reagent (A) absorbs light it can produce radicals. The rate of radical formation is proportional to the rate of light absorption by the reacting species, with the proportionality factor being the quantum yield (φ). If Eq. (2.8) is the reaction of a reagent absorbing light to product radical, then the reaction rate ($r_{rxn,8}$) is

$$r_{rxn,8} = \varphi\, r_{light,A,avg}$$

where $r_{rxn,8}$ = reaction rate of Eq. (2.8), (mole/m^3-s),

φ =quantum yield of the reagent that absorbs light to produce radical (mole/Einstein).

$r_{light,A,avg}$ = the average rate of light absorption by reagent A (Einstein/m^3-s)

Based on the analysis of average rate of light absorption ($r_{light,avg}$) in section 2, the reaction rate of Eq. (2.8) is

$$r_{rxn,8} = \varphi\, r_{light,A,avg} = \frac{\varphi \varepsilon_{ln,A} C_A I_0 \left(1 - \exp\left(-\varepsilon_{ln,all} C_{all} L\right)\right)}{\varepsilon_{ln,all} C_{all} L}$$

In this study, the major light absorbing species in the solution are VC and the reagents. The light being absorbed by water is so low and it is not considered here. Therefore,

$$\varepsilon_{ln,all}C_{all} = \varepsilon_{ln,A}C_A + \varepsilon_{ln,VC}C_{VC}$$

and the reaction rate of Eq. (2.8) is

$$r_{rxn,} = \varphi\, r_{light,A,avg} = \frac{\varphi\varepsilon_{ln,A}C_A I_0\left(1-\exp\left(-\varepsilon_{ln,all}C_{all}L\right)\right)}{\varepsilon_{ln,all}C_{all}L}$$

$$= \frac{\varphi\varepsilon_{ln,A}C_A I_0\left(1-\exp\left(-(\varepsilon_{ln,A}C_A + \varepsilon_{ln,VC}C_{VC})L\right)\right)}{(\varepsilon_{ln,A}C_A + \varepsilon_{ln,VC}C_{VC})L}$$

Based on the Beer-Lambert law, when absorbance increases, that means the molar absorptivity of the reagent increases if concentration and path length is kept constant. A general plot of $r_{rxn,8}$ vs. $\varepsilon_{ln,A}$ in Figure 30 shows that the reaction rate of equation (2.8) will increase if $\varepsilon_{ln,A}$ increases. To generate Figure 30, the following values are assumed:

Φ=1, C_A=1, I_0=1, $\varepsilon_{ln,VC}C_{VC}$=0.5, L=1

The change in above values won't change the trend of the curve so the conclusion is still valid in other values of the parameters applied to generate the curve in Figure 30.

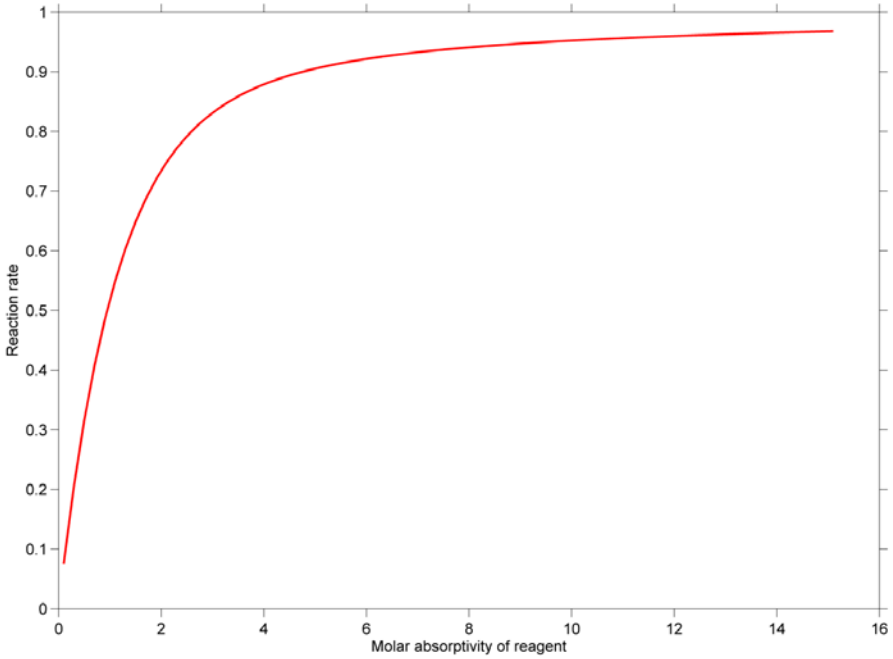

Figure 30. The effect of change in molar absorptivity on reaction rate

A.3. Rates of Production of Radicals

The rates of production of radicals/products can be calculated in the normal way using stoichiometric coefficients that give the ratio of the molar rate of production of radical/products per overall rate of reaction. For production of product radical specie "R" using stoichiometric coefficient s(R) = moles R produced per mole reaction (2.8)

$$r_R = s(R)^* r_{rxn,8}$$

where r_R is the rate of production of radical "R"

The increase in absorbance leads to increase in reaction rate of Eq. (2.8) (r_{rxn}), and since the rate of production of radical (r_R) is proportional to the reaction rate of Eq. (2.8), thus the increase in absorbance leads to the increase in the rate of production of radical.

APPENDIX B. SUPPLENMENTATY DATA FOR SECTION 3

B.1. Rate of Light Absorption of a Particular Wavelength by Dissolved Species

Nomenclature

I = light flux (Einstein/m^2-s)

$\varepsilon_{ln,i}$ = molar absorptivity (M^{-1} m^{-1}) of compound i (defined on natural logarithm basis, differs from molar absorptivity used with Beer-Lambert law for absorbance by factor of 2.303, $\varepsilon_{ln} = 2.303\ \varepsilon_{bl}$, where ε_{bl} is the decadic molar absorptivity used with the Beer-Lambert law, i.e. $I=I_0 10^{-\varepsilon C x}$. In this study, $\varepsilon_{ln,A}$, $\varepsilon_{ln,VC}$ are the weighted average of molar absorptivity of sulfite and VC)

L = total thickness of reactor in direction of light path (m)

A = area of reactor perpendicular to light path (m^2)

V = volume of reactor (m^3)

C_i = concentration of compound i (mole/m^3) (In this study, $C_{sulfite}$ is the sulfite concentration and C_{VC} is the VC concentration)

The rate of light absorption by any compound dissolved in the water can be related to the change of light intensity that results from absorption by that compound with the use of a steady-state material balance. Conducting the balance over a differential element of thickness "dx" where light is passing in the x direction, shows that the volumetric rate of light absorption is equal to the gradient of the light intensity:

$$0 = AI_x - AI_{x+dx} + 0 - Adx\, r_{light} \quad \text{(B.1)}$$

where r_{light} is the overall rate of absorption of light (Einstein/m^3-s)

$$r_{light} = (AI_x - AI_{x+dx})/Adx = - dI/dx \quad \text{(B.2)}$$

The rate of light absorption is also proportional to light intensity as assumed in the Beer-Lambert law:

$$-dI/dx = \varepsilon_{ln,i} C_i\, I \quad \text{(B.3)}$$

This can be solved to give:

$$I = I_0 \exp(-\varepsilon_{ln,i} C_i\, x) \quad \text{(B.4)}$$

Therefore, the overall rate of light absorption by the reagent i is

$$r_{light} = - dI/dx = \varepsilon_{ln,i} C_i\, I = \varepsilon_{ln,i} C_i\, I_0 \exp(-\varepsilon_{ln,i} C_i\, x) \quad \text{(B.5)}$$

If there are more than one compound that absorb light in the solution, light intensity will be influenced by all compounds, so

$$I = I_0 \exp(-\alpha_{all} x) \quad \text{(B.6)}$$

where $\alpha_{all}=\sum\varepsilon_{ln,i}C_i$

So the rate of light absorption by compound i should be expressed as:

$$r_{light,i}= \varepsilon_{ln,i}C_i I_0 \exp(-\alpha_{all} x) \quad \text{(B.7)}$$

Note that the rate of light absorption ($r_{light,i}$) is a function of position (x), so it will vary at different locations in the reactor, because the light intensity varies within the reactor. In many cases, measurements will be made on the average reaction rate in the reactor, not on the rate at a specific point in the reactor, so it will be useful to calculate an average rate and an average light intensity.

Then the average rate of light absorption by compound i is

$$r_{light,i,avg} = \varepsilon_{ln,i}C_i I_{avg} \quad \text{(B.8)}$$

B.2. Derivation of the Average Light Intensity as a Function of Influent Light Flux and Dissolved Species

The average light intensity can be calculated with the assumption that the reactor is well mixed, so that the concentrations are the same everywhere in the reactor and that length of the light path is constant through all parts of the reactor (i.e. typically this will

result with the two faces of the reactor are of equal area and the light enters perpendicularly to them).

$$I_{avg} = \frac{\int_0^L I dx}{\int_0^L dx} \tag{B.9}$$

where L = thickness of reactor in direction of light path

$$I_{avg} = \frac{\int_0^L I_0 \exp\left(-\alpha_{\text{all}} x\right) dx}{\int_0^L dx} \tag{B.10}$$

Assume that the reactor is completely mixed so that α_{alll} is constant throughout the system. This leads to the following derivations.

$$I_{avg} = \frac{I_0 \left| \frac{\exp\left(-\alpha_{\text{all}} x\right)}{-\alpha_{\text{all}}} \right|_0^L}{\left| x \right|_0^L} \tag{B.11}$$

$$I_{avg} = \frac{I_0 \left(-\frac{\exp\left(-\alpha_{\text{all}} L\right)}{\alpha_{\text{all}}} + \frac{1}{\alpha_{\text{all}}} \right)}{L} \tag{B.12}$$

$$I_{avg} = \frac{I_0\left(1-\exp\left(-\alpha_{all}L\right)\right)}{\alpha_{all}L} \tag{B.13}$$

In this study, both VC and sulfite absorb UV light thus the average light intensity can be expressed as

$$I_{avg} = \frac{I_0\left(1-\exp\left(-(\varepsilon_{ln,A}C_A + \varepsilon_{ln,VC}C_{VC})L\right)\right)}{(\varepsilon_{ln,A}C_A + \varepsilon_{ln,VC}C_{VC})L} \tag{B.14}$$

B.3. Derivations of the Kinetic Model

A kinetic model was developed to explain the effect of pH, sulfite dose, light intensity and initial VC concentration on the degradation rate constant of VC.

Table 13. Process kinetics and stoichiometry for VC degradation by sulfite/UV ARP

	Reactions	Rate equations	Sulfite	R	VC	S
(a)	Sulfite+hν→R	$r_1=\varphi_1 I_{avg} \varepsilon_{ln,sulfite} C_{sulfite}$	-1	1		
(b)	VC+ hν→P_1	$r_2= \varphi_2 I_{avg} \varepsilon_{ln,VC} C_{VC}$			-1	
(c)	VC+R→P_2	$r_3=k_3 * C_{VC} * C_R$		-1	-1	
(d)	S+R→P_3	$r_4=k_4 * C_s * C_R$		-1		-1

Table 13. Continued

Nomenclature:

R= reactive species such as sulfite radical, hydrated electron or hydrogen atom

S= scavengers that could react with radicals or hydrated electrons

P_1, P_2, P_3=products of reaction (b), (c) and (d) in Table 13.

r_1, r_2, r_3, r_4= reaction rates of reactions (a) ~ (d) in Table 13.

φ_1, $\varphi_{2=}$quantum yield of sulfite or VC

$\varepsilon_{ln,sulfite}$, $\varepsilon_{ln,VC}$= molar absorptivity of sulfite or VC ($M^{-1}cm^{-1}$, defined on natural logarithm basis, differs from molar absorptivity used with Beer-Lambert law for absorbance by factor of 2.303, $\varepsilon_{ln} = 2.303\ \varepsilon_{bl}$, where ε_{bl} is the decadic molar absorptivity used with the Beer-Lambert law, i.e. $I=I_0 10^{-\varepsilon Cx}$)

$C_{sulfite}$, C_{VC}, C_R, C_s= molar concentrations of sulfite, VC, reactive species and scavenger

I_{avg}=average light intensity in the solution ($\mu w/cm^2$)

k_3, k_4=the rate constant of reaction (c) and (d) in Table 13.

In Table 13, reactions (a) ~ (d) are considered as the basic processes in the degradation of VC by sulfite/UV ARP system. Reaction (a) describes the process that sulfite solution absorbs light and produces radicals or hydrated electrons. Reaction (b) describes the direct photolysis of VC. Reaction (c) shows the photochemical degradation of VC caused by the radicals or hydrated electrons. Reaction (d) is a summary of other

reactions that may consume radicals/hydrated electrons by possible scavengers in the solution.

The rate of reaction (a) is proportional to the rate of light absorption by the reacting species, with the proportionality factor being the quantum yield (φ). Thus the reaction rate of Eq. (a) can be expressed as

$$r_1 = \varphi_1 r_{light,sulfite,avg} = \varphi_1 I_{avg} \varepsilon_{ln,sulfite} C_{sulfite} \quad \text{(B.15)}$$

The rate of reaction (b) can be derived with same method and is expressed as

$$r_2 = \varphi_2 I_{avg} \varepsilon_{ln,VC} C_{VC} \quad \text{(B.16)}$$

At steady state, the change of concentration of radical is assumed as zero. So the material balance of radical in the batch reactor can be shown as

$$dC_R/dt = r_1-(r_3+r_4) = 0 \quad \text{(B.17)}$$

Then the rate of reaction (a) can be expressed as

$$r_1=r_3+r_4= k_3C_{VC} C_R + k_4C_SC_R \quad \text{(B.18)}$$

The concentration of reactive species can be developed by combining Eq. (B.15) and (B.18) and is shown by Eq. (B.19)

$$C_R=r_1/(k_3C_{VC}+ k_4C_S)= \varphi_1 I_{avg} \varepsilon_{ln,sulfite} C_{sulfite} /(k_3C_{VC}+ k_4C_S) \quad (B.19)$$

The degradation rate of VC (r_{VC}) can be expressed as

$$dC_{VC}/dt =-r_2-k_3C_{VC}C_R$$

$$=-\varphi_2 I_{avg}\varepsilon_{ln,\,VC}C_{VC} - k_3C_{VC} (\varphi_1 I_{avg} \varepsilon_{ln,sulfite} C_{sulfite}) /(k_3C_{VC}+ k_4C_S) \quad (B.20)$$

In this study, all degradation of VC is assumed as a pseudo-first-order decay to compare all the rate constants with different influence factors. Therefore, the expression of the rate constant by the simple mechanistic model can be made by comparing pseudo-first order decay model ($dC_{vc} / dt= -k_{obs} C_{vc}$) and Eq. (B.20), and is shown by Eq. (B.21)

$$k_{obs}= \varphi_2 I_{avg} \varepsilon_{ln,VC} + k_3\varphi_1 I_{avg} \varepsilon_{ln,sulfite} C_{sulfite} /(k_3C_{VC}+ k_4C_S) \quad (B.21)$$

In this study, the major light absorbing species in the solution are VC and the reagents. The light being absorbed by water is so low and it is not considered here.

In this study, the absorbances of solutions in all experimental conditions were measured below 0.05. The low absorbance of solution indicates that about 90% of influent light is going through the reactor without being absorbed. The averaged light

intensity (I_{avg}) can be assumed same as the light intensity entering the reactor (I_0). Therefore, the degradation rate constant of VC can be simplified and is shown in Eq. (B.22)

$$k_{obs}= \varphi_2 I_0 \varepsilon_{ln,VC} C_{VC} + k_3 C_{VC} (\varphi_1 I_0 \varepsilon_{ln,sulfite} C_{sulfite}) /(k_3 C_{VC}+ k_4 C_S) \quad (B.22)$$

B.4. Calculation of Efficiency (φ_r) of Reactive Species Reacting with VC

$$\varphi_r = \text{moles of VC degraded / mole of reactive species produced} = r_{vc,\,avg}/ r_R \quad (B.23)$$

where $r_{vc,\,avg}$ is the averaged rate of VC degradation and r_R is the rate of reactive species production

B.4.1. Calculation of averaged rate of VC degradation

$$r_{vc,\,avg}= \sum k_{obs} Ct/n \quad (B.24)$$

where k_{obs} (s^{-1}) is the simulated degradation rate constant of VC at specified experimental condition, Ct (mol/m^3) is the concentration of VC measured at time t and n it the total number of Ct.

B.4.2. Rates of production of reactive species

The production of reactive species can be shown in Eqs. (B.25) and (B.26).

$$SO_3^{2-} + h\nu \rightarrow SO_3^{\bullet-} + e_{aq}^- \quad \text{(B.25)}$$

$$HSO_3^- + h\nu \rightarrow SO_3^{\bullet-} + H^\bullet \quad \text{(B.26)}$$

The rate of production of reactive species (sulfite radical, hydrated electron or H atom) can be calculated in the way using stoichiometric coefficient (S_R) that relates the rate of reactive species production and the rate of sulfite destruction. The value of S_R is defined as moles of reactive species produced per mole of sulfite destruction. The rate of sulfite destruction (r_1) has been shown by Eq. (B.15), thus the rate of reactive species production can be expressed as

$$r_R = S_R * r1 = S_R \, \varphi_1 \, I_{avg} \, \varepsilon_{ln,sulfite} \, C_{sulfite} \quad \text{(B.27)}$$

The averaged degradation rate of VC, rate of production of reactive species and the efficiencies of reactive species reacting with VC are summarized in the Table 14. Here we assume the sulfite radical is the only species that causes VC degradation, so the value of S_R is 1. If the hydrated electron or H atom also works for VC degradation, the

value of S_R will be greater than 1 and the value of efficiency (φ_r) will be lower than corresponding value listed in Table 14.

Table 14. Efficiency (φ_r) of reactive species reacting with VC

Initial VC conc. (mg/L)	$r_{vc,\ avg}$ (mol/m^3-s)	r_R (mol/m^3-s)	φ_r
1.14	3.7E-5 ±18%	1.3E-4	0.28±18%
1.52	3.2E-5 ±12%	1.3E-4	0.25±12%
1.79	3.7E-5 ±13%	1.3E-4	0.28±13%
3.10	6.1E-5 ±4.6%	1.3E-4	0.47±4.6%

APPENDIX C. SUPPLENMENTARY DATA FOR SECTION 4

C.1. Rate of Light Absorption of a Particular Wavelength by Dissolved Species

Nomenclature

I = light flux (Einstein/m^2-s)

$\varepsilon_{ln,i}$ = molar absorptivity (M^{-1} m^{-1}) of compound i (defined on natural logarithm basis, differs from molar absorptivity used with Beer-Lambert law for absorbance by factor of 2.303, $\varepsilon_{ln} = 2.303\ \varepsilon_{bl}$, where ε_{bl} is the decadic molar absorptivity used with the Beer-Lambert law, i.e. $I=I_0 10^{-\varepsilon C x}$.)

L = total thickness of reactor in direction of light path (m)

A = area of reactor perpendicular to light path (m^2)

V = volume of reactor (m^3)

C_i = concentration of compound i (mole/m^3)

The rate of light absorption by any compound dissolved in the water can be related to the change of light intensity that results from absorption by that compound with the use of a steady-state material balance. Conducting the balance over a differential element of thickness "dx" where light is passing in the x direction, shows that the volumetric rate of light absorption is equal to the gradient of the light intensity:

$$0 = AI_x - AI_{x+dx} + 0 - Adx\ r_{light} \qquad (C.1)$$

where r_{light} is the overall rate of absorption of light (Einstein/m^3-s)

$$r_{light} = (AI_x - AI_{x+dx})/Adx = - dI/dx \quad (C.2)$$

The rate of light absorption is also proportional to light intensity as assumed in the Beer-Lambert law. For a system in which only one compound absorbs light:

$$-dI/dx = \varepsilon_{ln,i} C_i I \quad (C.3)$$

This can be solved to give:

$$I = I_0 \exp(-\varepsilon_{ln,i} C_i x) \quad (C.4)$$

Therefore, the overall rate of light absorption by the reagent i is

$$r_{light} = - dI/dx = \varepsilon_{ln,i} C_i I = \varepsilon_{ln,i} C_i I_0 \exp(-\varepsilon_{ln,i} C_i x) \quad (C.5)$$

If several compounds absorb light, the light intensity at any point will be influenced by the concentrations of all the compounds that absorb light, so

$$I = I_0 \exp(-\alpha_{all} x) \quad (C.6)$$

where $\alpha_{all}=\sum\varepsilon_{ln,i}C_i$

In this case, the rate of light absorption by compound i should be expressed as:

$$r_{light,i}= \varepsilon_{ln,i}C_i\ I_0\ \exp(-\alpha_{all}\ x) \qquad (C.7)$$

Note that the rate of light absorption ($r_{light,i}$) is a function of position (x), so it will vary at different locations in the reactor, because the light intensity varies within the reactor. In many cases, measurements will be made on the average concentrations in the reactor and these will be used to evaluate average rates of removal in the reactor, so it will be useful to calculate an average rate and an average light intensity.

Then the average rate of light absorption by compound i is

$$r_{light,i,avg} = \varepsilon_{ln,i}C_i\ I_{avg} \qquad (C.8)$$

C.2. Derivation of the Average Light Intensity as a Function of Influent Light Flux and Dissolved Species

The average light intensity can be calculated with the assumption that the reactor is well mixed, so that the concentrations are the same everywhere in the reactor and that length of the light path is constant through all parts of the reactor. This will typically result when the two faces of the reactor are of equal area and the light enters perpendicularly to them.

$$I_{avg} = \frac{\int_0^L I dx}{\int_0^L dx} \tag{C.9}$$

where L = thickness of reactor in direction of light path

$$I_{avg} = \frac{\int_0^L I_0 \exp\left(-\alpha_{\text{all}} x\right) dx}{\int_0^L dx} \tag{C.10}$$

Since the reactor is completely mixed and concentrations are the same throughout the reactor, α_{all} is constant throughout the system.

$$I_{avg} = \frac{I_0 \left| \frac{\exp\left(-\alpha_{\text{all}} x\right)}{-\alpha_{\text{all}}} \right|_0^L}{\left| x \right|_0^L} \tag{C.11}$$

$$I_{avg} = \frac{I_0 \left(-\frac{\exp\left(-\alpha_{\text{all}} L\right)}{\alpha_{\text{all}}} + \frac{1}{\alpha_{\text{all}}} \right)}{L} \tag{C.12}$$

$$I_{avg} = \frac{I_0 \left(1 - \exp\left(-\alpha_{\text{all}} L\right)\right)}{\alpha_{\text{all}} L} \tag{C.13}$$

In this study, only sulfite absorbs UV light, so the average light intensity can be expressed as

$$I_{avg} = \frac{I_0\left(1-\exp\left(-\varepsilon_{\ln,SO_3^{2-}}\ C_{SO_3^{2-}} L\right)\right)}{\varepsilon_{\ln,SO_3^{2-}}\ C_{SO_3^{2-}} L} \qquad \text{(C.14)}$$

C.3. Derivations of the Basic Kinetic Model

A kinetic model was developed to explain the effect of pH, sulfite dose, light intensity and initial 1,2-DCA concentration on the degradation rate constant of 1,2-DCA.

Table 15. Process kinetics and stoichiometry for 1,2-DCA degradation by UV-activated ARP

	Reactions	Rate equations	Reagent	R	DCA	S
(a)	Reagent+hν→R	$r_1=\varphi_1\ I_{avg}\ \varepsilon_{ln,reagent}\ C_{reagent}$	-1	1		
(b)	DCA+R→P_1	$r_2=k_2 * C_{DCA} * C_R$		-1	-1	
(c)	S+R→P_2	$r_3=k_3 * C_s * C_R$		-1		-1

Nomenclature:

Reagent=reagent that produces reactive species

R= reactive species such as sulfite radical or hydrated electron

DCA= the target contaminant of 1,2-DCA

S= scavengers that could react with sulfite radicals or hydrated electrons

Table 15. Continued

P_1, P_2=products

r_1, r_2, r_3= reaction rates of reactions (a) ~ (c)

$\varphi_{1=}$quantum yield of reagent

$\varepsilon_{ln,reagent}$= molar absorptivity of reagent (defined on natural logarithm basis, differs from molar absorptivity used with Beer-Lambert law for absorbance by factor of 2.303, ε_{ln} = 2.303 ε_{bl}, where ε_{bl} is the decadic molar absorptivity used with the Beer-Lambert law, i.e. $I=I_0 10^{-\varepsilon C x}$)

$C_{reagent}$, C_{DCA}, C_R, C_s= molar concentrations of reagent, 1,2-DCA, reactive species and scavenger

k_2, k_3=second order rate constant of reaction (b) and (c)

In Table 15, reactions (a) to (c) are considered as the basic processes in the degradation of 1,2-DCA by the sulfite/UV ARP. Since the control experiments showed little degradation of 1,2-DCA when only UV or sulfite was applied, their direct reactions with 1,2-DCA are not considered here. Reaction (a) describes the process in which the reagent (sulfite ion, SO_3^{2-}) absorbs light and produces a reactive species. This process actually produces two reactive species (sulfite radicals and aqueous electrons), either one of which could be the reactive specie for a given contaminant. Reaction (b) shows the photochemical degradation of 1,2-DCA caused by the reactive species. Reaction (c) is a

summary of other reactions that may consume the reactive species by possible scavengers in the solution.

The rate of reaction (a) is proportional to the rate of light absorption by the reagent, with the proportionality factor being the quantum yield (φ). The rate of light absorption by the reagent has been developed in Eq. (C.8).Thus the reaction rate of Eq. (a) can be expressed as

$$r_1 = \varphi_1 \, r_{light,sulfite,avg} = \varphi_1 \, I_{avg} \, \varepsilon_{ln,reagent} \, C_{reagent} \qquad (C.15)$$

At stationary conditions, the change of concentration of reactive species is assumed to be negligible relative to the rates of production and consumption of the reactive species. Therefore, the material balance of reactive species in the batch reactor can be shown as

$$dC_R/dt = r_1-(r_2+r_3) = 0 \qquad (C.16)$$

Then the rate of reaction (a) can be expressed as

$$r_1=r_2+r_3= k_2C_{DCA} \, C_R + k_3C_SC_R \qquad (C.17)$$

The concentration of the reactive species can be developed by combining Eq. (C.15) and (C.17) and is shown by Eq. (C.18)

$$C_R = r_1/(k_2 C_{DCA} + k_3 C_S) = \varphi_1 I_{avg} \varepsilon_{ln,reagent} C_{reagent} /(k_2 C_{DCA} + k_3 C_S) \quad (C.18)$$

The degradation rate of 1,2-DCA (r_{DCA}) can be expressed as

$$dC_{DCA}/dt = -r_2 = -k_2 C_{DCA} C_R = - k_2 C_{DCA} \varphi_1 I_{avg} \varepsilon_{ln,reagent} C_{reagent} /(k_2 C_{DCA} + k_3 C_S) \quad (C.19)$$

In this study, the degradation of 1,2-DCA was assumed to follow a pseudo-first-order decay model. This was done to facilitate the evaluation of process variables on degradation kinetics. Therefore, the kinetic model was used to predict effects of various factors on the pseudo-first order rate coefficient.

$$k_{obs} = k_2 \varphi_1 I_{avg} \varepsilon_{ln,reagent} C_{reagent} /(k_2 C_{DCA} + k_3 C_S) \quad (C.20)$$

In this study, the major light absorbing species in the solution are the sulfite species. The light being absorbed by water is very low and it is not considered here. The absorbances of all sulfite solutions used in these experiments were below 0.05. This indicates that about 90% of influent light is passing through the reactor without being absorbed. Therefore, average light intensity (I_{avg}) can be reasonably approximated by the light intensity entering the reactor (I_0). Therefore, the expression for the pseudo-first-order rate constant can be simplified as shown in Eq. (C.21)

$$k_{obs} = k_2 \varphi_1 I_0 \varepsilon_{ln,reagent} C_{reagent} /(k_2 C_{DCA} + k_3 C_S) \quad (C.21)$$

C.4. Calculation of Efficiency (φ) of Reactive Species Reacting with 1,2-DCA

φ= quantum yield for 1,2-DCA degradation/ quantum yield of reactive species $= (r_{DCA,\,avg}/r_{photon})/ (r_R/r_{photon}) = r_{DCA,\,avg}/ r_R$ (C.22)

where $r_{DCA,\,avg}$ is the average rate of 1,2-DCA degradation, r_{photon} is the rate of photon absorption and r_R is the production rate of reactive species.

(1) Calculation of average rate of 1,2-DCA degradation

$$r_{DCA,\,avg} = \sum k_{obs} C_t / n \quad \text{(C.23)}$$

where k_{obs} (s^{-1}) is the simulated pseudo-first order rate constant of 1,2-DCA at specified experimental condition, C_t (mol/m^3) is the concentration of 1,2-DCA measured at time t and n is the total number of C_t.

(2) Rates of photon absorption

The absorption of photons can be shown in Eq. (C.24).

$$SO_3^{2-} + h\nu \rightarrow SO_3^{\bullet -} + e_{aq}^- \quad \text{(C.24)}$$

The rate of production of reactive species (sulfite radical or aqueous electron) can be calculated in the way using stoichiometric coefficient (S_R) that relates the rate of reactive species production and the rate of sulfite destruction. The value of S_R is defined

as moles of reactive species produced per mole of sulfite destruction. Thus the rate of reactive species production can be expressed as

$$r_R = S_R * r1 = S_R \, \varphi_1 \, I_0 \, \varepsilon_{ln,reagent} \, C_{reagent} \qquad (C.25)$$

The average degradation rate of 1,2-DCA, rate of production of reactive species and the efficiencies of reactive species reacting with 1,2-DCA are summarized in the Table 16.

Table 16. Efficiency (φ) of reactive species reacting with 1,2-DCA

Initial 1,2-DCA conc. (mM)	$r_{DCA,\,avg}$ (mol/m^3-s)	r_R (mol/m^3-s)	φ
0.021	1.76E-05	3.90E-05	0.45
0.041	1.80E-05	3.90E-05	0.46
0.057	1.53E-05	3.90E-05	0.39
0.093	1.64E-05	3.90E-05	0.42

C.5. Pseudo-First-Order Degradation Rate Constant

Table 17. Values of pseudo-first order rate constants at all experimental conditions

pH	Sulfite Conc. (mM)	UV intensity ($\mu W/cm^2$)	Initial 1,2-DCA Conc. (mM)	Rate Constant (k_{obs}, min^{-1})
7.0	0.2	6000	0.02	0.019±0.0024
8.2	0.2	6000	0.02	0.086±0.020
9.0	0.2	6000	0.02	0.087±0.025
11.0	0.2	6000	0.02	0.099±0.024
11.0	0.04	6000	0.02	0.0019±0.00045
11.0	0.1	6000	0.02	0.024±0.0037
11.0	0.4	6000	0.02	0.14±0.027
11.0	0.2	2000	0.02	0.041±0.0079
11.0	0.2	4000	0.02	0.070±0.012
11.0	0.2	8000	0.02	0.14±0.023
11.0	0.2	6000	0.04	0.052±0.012
11.0	0.2	6000	0.06	0.031±0.0064
11.0	0.2	6000	0.09	0.021±0.0033

APPENDIX D. MECHNISTIC MODELING

Matlab Program for Mechanistic Modeling in the Degradation of 1,2-DCA/VC with the Sulfite/UV ARP

This program calculates sulfite ion quantum yield and rate constant ($k_{6.3}$)

```
clear all
clc
tic;
%input kinetic experiment data
data=load('dcainit0.09.txt');% import data from txt file
t_min_exp= data(:,1);  % time in minutes
vc_exp= data(:,2); % VC or 1,2-DCA concentration in mM

q1 = 0.0:0.01:1;        %sulfite quantum yield
k1 = logspace(1,20,100);        %reaction rate constant of eaq with
•CH2CH2Cl•-  or reaction rate constant of SO3•- with target
err_old = 10e10;
err_mat=zeros(length(q1),length(k1));

%calculate combination of quantum yield and reaction rate constant that
gives least sum of squared errors for the target and sulfite
concentrations, normalized by the respective initial concentrations
%c(:,28) is VC and c(:,29) is 1,2-DCA. c_mod_vc and c_exp could be 1,2-
DCA
%if the simulation is to calculate DCA parameters
i=1;

for q1 = 0.0:0.01:1
    j=1;
    for k1 = logspace(1,20,100)

        arpsim254_input_xu(q1,k1);
        [t,c]=arpsim254_run_xu;
        t_min=t./60;

        c_mod_vc=interp1(t_min,c(:,29),t_min_exp);

  err = sum(((vc_exp./1000-c_mod_vc)./(vc_exp(1)/1000)).^2);

         if(err < err_old)
```

```
          err_old = err;
          min_values =[q1,k1];
          end;

        err_mat(i,j) = err;
        j=j+1;


    end
    i=i+1
end

toc;

min_values
min(min(err_mat))
```

Input values and reactions in the mechanistic model

```
function dummy=arpsim254_input_xu(q1,k1)
% m-file to organize input for kinetic model that simulate radical
% reactions occuring in advanced reduction processes; 8/17/2010 by BB
% Variables:

% s = (n x m+1) matrix of stoichiometric coefficients
% c0 = (1 x m) matrix of initial concentrations of species
% k = (1 x n) matrix of rate coefficients

% Initialize matrices
n= 77;            % number of reactions
m= 32;            % number of species
c0=zeros(m,1); % initial concentrations, M
s=zeros(n,m);  % stoichiometric coefficients
k=zeros(1,n); % rate constants, can be second order (L/mol-s) or first-
order (1/s)
mol_abs=zeros(1,m);

% Initialize Variables
tstop = 9600;    % time to stop simulation (s)
ph = 7 ;% pH of solution
r_vol =1.7e-5; % volume of reactor (m^3)
I0 = 1.272e-4; % light flux entering reactor (einstein/m^2-s) (2.12 e-5
E/m^2-s/(mw/cm^2) att 253.7 nm)
r_area= 1.7e-3; % area of reactor perpindicular to light, m^2
h_nu_av= 4.715e5; % light energy = h*nu*Av =h c/lambda * Av, J/einstein
(=4.715E5 J/E for 253.7 nm)
k1co3=10^-6.352; % first acid dissosciation constant for carbonic acid,
VMinteq Ver. 3
k2co3=10^-10.329; % second acid dissosciation constant for carbonic
acid,VMinteq Ver. 3
```

```
k1so3=10^-1.85; %first acid dissosciation constant for sulfurous
acid,VMinteq Ver. 3
k2so3=10^-7.19; %second acid dissosciation constant for sulfurous acid,
VMinteq Ver. 3
kw=10^-13.997; % dissociation constant for water, VMinteq Ver. 3
abs_coef_water = 1.59; % absorption coefficient (ln based) for water
(m-1)ref: Hale and Querry, 1973.
q_yield_so3= q1;% quantum yield of reaction producing sulfite radical
anion and e; value of 0.39 from
                  % Fischer 1996
q_yield_vc= 0.57;% this value is calculated as the initial quantum
yield of VC from direct photolysis experiments at pH9, it will be used
to calculate rate constant k in eq(76)
%specify options for ODE solver (Relative error tolerance, absolute
error
%tolerance, and specify that all concentrations be non-negative)
options=odeset('RelTol', 1e-6, 'AbsTol', 1e-9, 'NonNegative', [1:m]);


% c0, initial concentations of all species, (M)
c0(1)=0;  % OH'
c0(2)=0;  % H2O2
c0(3)=0;  % eaq-
c0(4)=0;  % H'
c0(5)=0;  % H2
c0(6)=10^-ph;   % H+
c0(7)=kw/c0(6); % OH-
c0(8)=0;  % HO2'
c0(9)=0;  % HO2-'
c0(10)=0; % HO2^-
c0(11)=0; % H2O2+
c0(12)=0; % OH-'  note: a radical, not hydroxide ion
c0(13)=0; % O2
c0(14)=0; % O^2-
c0(15)=0; % O2^-'
c0(16)=0; % O2^2-
c0(17)=0; % O-'
c0(18)=0; % HCO3-
c0(19)=k2co3*c0(18)/c0(6); % CO32-
c0(20)=0; % CO3-'
c0(21)=0; % NO3-
c0(22)=0; % NO32-
c0(23)=0; % Cl-
c0(24)=0; % ClOH
c0(25)=c0(6)*c0(18)/k1co3; % H2CO3
c0(26)= 2e-4; % total sulfite (H2SO3+SO2, HSO3-, SO32-)
c0(27)=0; % sulfite radical anion, SO3-'
c0(28)=0; % VC
c0(29)=2.236e-5; % 1,2-DCA
c0(30)=0; % N2O, nitrous oxide
c0(31)=0; % •CH2CH2Cl
c0(32)=0; % (SO3-)-CH2-CHCl•
```

```
% Specifiy reaction listed below that should be ignored (will set k=0);
% added 7/2012 by BB
kzero=[]; % enter reaction number from list below for reactions to
ignore

% Specify species that should remain at constant concentration,
regardless
% of reactions; added 7/12/2012 by BB
c_const=[6 7]; % enter species number to be held constant;
               %H+ (#6) and OH- (#7) should be constant because rate
constants
               %calculated using ionization fractions for sulfite


% Calculate variables that depend on others
alpha2_so3=k1so3*k2so3/(c0(6)^2+c0(6)*k1so3+k1so3*k2so3); % second
ionization fraction for SO3
mol_abs(26) = 4170*alpha2_so3; % molar abs for SO3 at 254 nm, ln-basis;
source is measurement (18.1 M^-1 cm^-1, decadic)
                               % made by Bhanu Prakash (11/4/2010)
                               % assumes HSO3 does not absorb at 254 nm
mol_abs(28)=106;      %unit: (M^-1 m^-1). molar absorptivity of VC from
measurements, (0.46M^-1 cm^-1,decadic)
r_l = r_vol/r_area; % calculate depth of reactor in direction of light
path
I0_l=I0/r_l; % ratio of incident light intensity to thickness of
reactor (Einstein/m^3-s).


% Specify reactions, stoichiometric coefficients and rate equations
%(1) OH' + H2 --> H' + H2O     (k = 4.2*10^7 M-1 s-1)Ref: Buxton,  et
al., 1988
%     1    5      4
    s(1,1)=-1;s(1,5)=-1;s(1,4)=1;
    k(1)=4.2e7;

%(2) OH' + H2O2 --> HO2' + H2O      (k = 2.7*10^7 M-1 s-1)Buxton,  et
al., 1988
%     1      2       8
    s(2,1)=-1; s(2,2)=-1; s(2,8)=1;
    k(2)=2.7e7;

%(3) OH' + O2^-' --> O2 + OH-     (k = 8.0*10^9 M-1 s-1)Ref: Buxton,
et al., 1988
%     1     15      13   7
    s(3,1)=-1; s(3,15)=-1; s(3,13)=1; s(3,7)=1;
    k(3)=8.0e9;

%(4) OH' + HO2' --> H2O + O2     (k = 6.0*10^9 M-1 s-1)Ref: Buxton,  et
al., 1988
%      1     8              13
    s(4,1)=-1; s(4,8)=-1; s(4,13)=1;
```

```
    k(4)=6.0e9;

%(5) OH' + OH' --> H2O2     (k = 5.5 *10^9 M-1 s-1)Ref: Buxton,  et
al., 1988
%     1     1       2
    s(5,1)=-2; s(5,2)=1;
    k(5)=5.5e9;

%(6) OH' + OH- --> O-' + H2O     (k = 1.3*10^10 M-1 s-1) Ref: Buxton,
et al., 1988
%     1     7       17
    s(6,1)=-1; s(6,7)=-1;
    k(6)=1.3e10;

%(7) OH' + H2O2+ --> H+ + H2O     (k = 1.2*10^10 M-1 s-1)Ref: Buxton,
et al., 1988
%     1     11       6
    s(7,1)=-1; s(7,11)=-1; s(7,6)=1;
    k(7)=1.2e10;

%(8) OH' + O-' --> HO2^-     (k = 2.0*10^10 M-1 s-1)Ref: Buxton,  et
al., 1988
%     1     17      10
    s(8,1)=-1; s(8,17)=-1; s(8,10)=1;
    k(8)=2.0e10;

%(9) OH' + HO2^- --> HO2' + OH-     (k = 7.5*10^9 M-1 s-1) Ref: Buxton,
et al., 1988
%     1     10       8      7
    s(9,1)=-1; s(9,10)=-1; s(9,8)=1; s(9,7)=1;
    k(9)=7.5e9;

%(10) eaq- + H' + H2O --> H2 + OH-      (k = 2.5*10^10 M-1 s-1)Ref:
Buxton,  et al., 1988
%       3     4            5    7
    s(10,3)=-1; s(10,4)=-1; s(10,5)=1; s(10,7)=1;
    k(10)=2.5e10;

%(11) eaq- + eaq- + 2H2O --> 2 OH- + H2 (k = 5.5*10^9 M-1 s-1)Ref:
Buxton,  et al., 1988
%      3      3                7     5
    s(11,3)=-2; s(11,7)=2; s(11,5)=1;
    k(11)=5.5e9;

%(12) eaq- + H2O2 --> OH' + OH-     (k = 1.1*10^10 M-1 s-1)Ref: Buxton,
et al., 1988
%      3      2        1    7
    s(12,3)=-1; s(12,2)=-1; s(12,1)=1; s(12,7)=1;
    k(12)=1.1e10;

%(13) eaq- + O2 --> O2^-'     (K = 1.9*10^10 M-1 s-1)Ref: Buxton,  et
al., 1988
```

```
%      3      13     15
    s(13,3)=-1; s(13,13)=-1; s(13,15)=1;
    k(13)=1.9e10;

%(14) eaq- + O2^-' --> O2^2-     (k = 1.3*10^10 M-1 s-1)Ref: Buxton,
et al., 1988
%      3      15       16
    s(14,3)=-1; s(14,15)=-1; s(14,16)=1;
    k(14)=1.3e10;

%(15) eaq- + H+ --> H'    (k = 2.3*10^10 M-1 s-1)Ref: Buxton,  et al.,
1988
%      3     6      4
    s(15,3)=-1; s(15,6)=-1; s(15,4)=1;
    k(15)=2.3e10;

%(16) eaq- + H2O  --> H' + OH- (k = 1.9*10^1 s-1)Ref: Buxton,  et al.,
1988
%      3              4     7
    s(16,3)=-1; s(16,4)=1; s(16,7)=1;
    k(16)=1.9e1*55.5;  % value of 19 is 2nd order const, convert to 1st
order constant with 55.5 M H2O, 6/18/12

%(17) eaq- + HO2^- --> products     (k = 3.5*10^9 M-1 s-1)Ref: Buxton,
et
%al., 1988; Buxton does not show products, but Zele uses OH' and 2OH-
%although it is not balanced
%      3      10
    s(17,3)=-1; s(17,10)=-1;
    k(17)=3.5e9;

%(18) eaq- + OH' --> OH-    (k = 3.0*10^10 M-1 s-1) Ref: Buxton,  et
al., 1988
%      3      1       7
    s(18,3)=-1; s(18,1)=-1; s(18,7)=1;
    k(18)=3.0e10;

%(19) eaq- + O'- + H2O --> 2OH-     (k = 2.2*10^10 M-1 s-1)Ref: Buxton,
et
%al., 1988; water not in Buxton, but needed for balance
%      3     17             7
    s(19,3)=-1; s(19,17)=-1; s(19,7)=2;
    k(19)=2.2e10;

%(20) H' + O2 --> HO2'     (k = 2.1*10^10 M-1 s-1)Ref: Buxton,  et al.,
1988
%     4    13      8
    s(20,4)=-1; s(20,13)=-1; s(20,8)=1;
    k(20)=2.1e10;

%(21) H' + O2^-' --> HO2^-'     (k = 2.0*10^10 M-1 s-1, Ref?)
%     4     15       9
```

```
    s(21,4)=-1; s(21,15)=-1; s(21,9)=1;
    k(21)=2.0e10;

%(22) H' + H' --> H2     (k = 7.8*10^9 M-1 s-1)Ref: Buxton,  et al.,
1988
%     4    4      5
    s(22,4)=-2; s(22,5)=1;
    k(22)=7.8e9;

%(23) H' + OH' --> H2O     (k = 7.0*10^9 M-1 s-1)Ref: Buxton,  et al.,
1988
%     4     1
    s(23,4)=-1; s(23,1)=-1;
    k(23)=7.0e9;

%(24) H' + HO2' --> H2O2     (k = 1.0*10^10 M-1 s-1)Ref: Buxton,  et
al., 1988
%     4     8        2
    s(24,4)=-1; s(24,8)=-1; s(24,2)=1;
    k(24)=1.0e10;

%(25) H' + H2O2 --> H2O + OH'    (k = 9.0*10^7 M-1 s-1)Ref: Buxton,  et
al., 1988
%     4     2              1
    s(25,4)=-1; s(25,2)=-1; s(25,1)=1;
    k(25)=9.0e7;

%(26) H' + OH- --> eaq- + H2O     (k = 2.2*10^7 M-1 s-1)Ref: Buxton,
et al., 1988
%     4     7       3
    s(26,4)=-1; s(26,7)=-1; s(26,3)=1;
    k(26)=2.2e7;

%(27) H' + H2O -->  H2 + OH'  (k = 1.0*10^1 s-1)Ref: Buxton,  et al.,
1988 (assume first-order, unrecomended value, too low to measure
accurately)
%     4             5     1
    s(27,4)=-1; s(27,5)=1; s(27,1)=1;
    k(27)=1.0e1;

%(28) O-' + H2O --> OH' + OH- (k = 1.8*10^6 s-1)Ref:Buxton,  et al.,
1988 (assume first-order)
%     17             1     7
    s(28,17)=-1; s(28,1)=1; s(28,7)=1;
    k(28)=1.8e6;

%(29) O-' + HO2^- --> O2^-' + OH-     (k = 4.0*10^8 M-1 s-1)Ref:
Buxton,  et al., 1988
%      17    10       15     7
    s(29,17)=-1; s(29,10)=-1; s(29,15)=1; s(29,7)=1;
    k(29)=4.0e8;
```

```
%(30) O-' + H2 --> H' + OH-     (k = 8.0*10^7 M-1 s-1)Ref: Buxton,  et
al., 1988
%     17    5      4     7
    s(30,17)=-1; s(30,5)=-1; s(30,4)=1; s(30,7)=1;
    k(30)=8.0e7;

%(31) O-' + H2O2 --> O2^-' + H2O     (k = 5.0*10^8 M-1 s-1)Ref: Buxton,
et al., 1988
%     17     2        15
    s(31,17)=-1; s(31,2)=-1; s(31,15)=1;
    k(31)=5.0e8;

%(32) O-' + O2^-' + H2O --> 2OH- + O2     (k = 6.0*10^8 M-1 s-1)Ref:
Buxton,  et al., 1988
%     17     15       7      13
    s(32,17)=-1; s(32,15)=-1; s(32,7)=2; s(32,13)=1;
    k(32)=6.0e8;

%(33) HO2' + O2^-' + H2O --> O2 + H2O2 + OH-     (k = 9.7*10^7 M-1 s-1)
Ref: Zele et al., 1998
%      8      15             13    2      7
    s(33,8)=-1; s(33,15)=-1; s(33,13)=1; s(33,2)=1; s(33,7)=1;
    k(33)=9.7e7;

%(34) HO2' + HO2' --> H2O2 + O2     (k = 8.3*10^5 M-1 s-1)Ref: Zele et
al., 1998
%      8      8        2     13
    s(34,8)=-2; s(34,2)=1; s(34,13)=1;
    k(34)=8.3e5;

%(35) HO2' --> H+ + O2^-'     (k = 8.0*10^5 M-1 s-1)Ref: Zele et al.,
1998
%      8        6    15
    s(35,8)=-1; s(35,6)=1; s(35,15)=1;
    k(35)=8.0e5;

%(36) H+ + O2^-' --> HO2'     (k = 4.5*10^10 M-1 s-1)Ref: Zele et al.,
1998
%     6    15        8
    s(36,6)=-1; s(36,15)=-1; s(36,8)=1;
    k(36)=4.5e10;

%(37) H+ + OH- --> H2O     (k = 1.4*10^11 M-1 s-1) Ref: from Laidler
1965 in Stumm and Morgan, p. 71
%      6    7
    s(37,6)=-1; s(37,7)=-1;
    k(37)=1.4e11;

%(38) H+ + HO2^-' --> H2O2     (k = 2.0*10^10 M-1 s-1)Ref: Zele et al.,
1998
%      6    10         2
    s(38,6)=-1; s(38,10)=-1; s(38,2)=1;
```

```
    k(38)=2.0e10;

%(39) H2O2 --> H+ + HO2^-'     (k = 3.6*10^-2 M-1 s-1)Ref: Zele et al.,
1998
%      2        6    10
    s(39,2)=-1; s(39,6)=1; s(39,10)=1;
    k(39)=3.6e-2;

%(40) hold for future addition


%(41) HCO3- + eaq- --> products     (k = 1.0*10^6 M-1 s-1) Ref: Buxton
et al. 1988 (give value as maximum)
%      18      3
    s(41,18)=-1; s(41,3)=-1;
    k(41)=1.0e6;

%(42) HCO3- + H' --> products     (k = 4.4*10^4 M-1 s-1)Ref: Buxton et
al. 1988
%      18     4
    s(42,18)=-1; s(42,4)=-1;
    k(42)=4.4e4;

%(43) HCO3- + OH' --> CO3-' + H2O     (k = 8.5*10^6 M-1 s-1) Ref:
Buxton et al., 1988
%       18    1        20
    s(43,18)=-1; s(43,1)=-1; s(43,20)=1;
    k(43)=8.5e6;

%(44) CO32- + eaq- --> products     (k = 3.9*10^5 M-1 s-1)Ref: Buxton
et al., 1988
%      19      3
    s(44,19)=-1; s(44,3)=-1;
    k(44)=3.9e5;

%(45) CO32- + OH' --> CO3-' + OH-     (k = 3.9*10^8 M-1 s-1)Ref: Buxton
et al., 1988
%     19       1       20      7
    s(45,19)=-1; s(45,1)=-1; s(45,20)=1; s(45,7)=1;
    k(45)=3.9e8;

%(46) CO3-' + OH' --> products     (k = 3.0*10^9 M-1 s-1)Ref: Zele et
al., 1998
%      20      1
    s(46,20)=-1; s(46,1)=-1;
    k(46)=3.0e9;

%(47) NO3- + eaq- --> NO32-'     (k = 9.7*10^9 M-1 s-1)Ref: Buxton et
al., 1988
%      21     3         22
    s(47,21)=-1; s(47,3)=-1; s(47,22)=1;
```

```
    k(47)=9.7e9;

%(48) NO3- + H' --> products     (k = 1.4*10^6 M-1 s-1)Ref: Buxton et
al., 1988
%      21    4
    s(48,21)=-1; s(48,4)=-1;
    k(48)= 1.4e6;

%(49) NO32-' + O2 --> O2^-' + NO3-     (k = 2*10^8 M-1 s-1) Neta et al.
1988
%      22     13      15      21
    s(49,22)=-1; s(49,13)=-1; s(49,15)=1; s(49,21)=1;
    k(49)=2e8;

%(50) Cl- + eaq- --> products     (k = 1.0*10^6 M-1 s-1)Ref: Buxton et
al. 1988 (give value as maximum)
%      23    3
    s(50,23)=-1; s(50,3)=-1;
    k(50)=1.0e6;

%(51) Cl- + OH' --> ClOH-     (k = 4.3*10^9 M-1 s-1)Ref: Buxton et al.
1988
%     23     1       24
    s(51,23)=-1; s(51,1)=-1; s(51,24)=1;
    k(51)=4.3e9;

%(52) ClOH- --> Cl- + OH'     (k = 6.1*10^9 M-1 s-1) Zele et al., 1998
%      24       23    1
    s(52, 24)=-1; s(52,23)=1; s(52,1)=1;
    k(52)=6.1e9;

%(53) H20 --> H+ + OH-   (k = 1.4 * 10^-3 M s-1 (zeroth order); to
match rxn (37) with equilibrium constant 1e-14
%             6     7
    s(53,6)=1; s(53,7)=1;
    k(53)=1.4e-3;

%(54) H+ + HCO3- --> H2CO3 (k = 4.7*10^10 M-1 s-1; from Laidler 1965 in
Stumm and Morgan, p. 71
%     6     18        25
    s(54,6)=-1; s(54,18)=-1; s(54,25)=1;
    k(54)=4.7e10;

%(55) H2CO3 --> H+ + HCO3-     (k= 2.1 E4 s-1, calculated with
equilibrium constant and rate constant for reaction (55)
%      25       6     18
    s(55,25)=-1; s(55,6)=1; s(55,18)=1;
    k(55)=2.1e4;

%(56) H+ + CO32- --> HCO3-     (k=5*10^10 M-1 s-1; assumed value near
that for reaction (55))
%      6     19       18
```

```
    s(56,6)=-1; s(56,19)=-1; s(56,18)=1;
    k(56)=5e10;

%(57) HCO3- --> H+ + CO32-     (k = 2.4, calculated with equilibrium
constant and value of rate constant for rxn (57)
%      18        6     19
    s(57,18)=-1; s(57,6)=1; s(57,19)=1;
    k(57)=2.4;

%(58) SO32- + light --> SO3-' + eaq-  (rate calculated using quantum
yield, absorbtivity and light intensity
%      26                27     3      note: species 26 is TotSO3
    s(58,26)=-1; s(58,27)=1; s(58,3)=1;

%(59) SO32- + eaq- --> products    (k<1.5e6) Buxton et al., 1988;
original
%reference Anbar 1968-jphyschem reports k<1.3e6; Anbar 1968-advchemser
says
%"Sulphate and sulphite ions are non-reactive (k < 10^6 l.mole-1 sec-
1))
% Zagorski 1971 says k < 1.5e-6 M-1s-1
% as of 7/13/2012 do not use this reaction, BB
%      26      3                     note: species 26 is TotSO3
%    s(59,26)=-1; s(59, 3)=-1;
%    k(59)=1.5e6*alpha2_so3;  % modify rate constant for pH
(alpha2_so3=SO32-/TotSO3)



%(60)  SO32- + OH' = SO3-' + OH-  k=5.5e9, Buxton et al., 1988
%       26     1      27      7         note: species 26 is TotSO3
    s(60,26)=-1; s(60,1)=-1; s(60,27)=1; s(60,7)=1;
    k(60)=5.5e9*alpha2_so3; % modify rate constant for pH
(alpha2_so3=SO32-/TotSO3)

%(61)  HSO3- + OH' = SO3-' + H2O  k=4.5e9, Buxton et al., 1988
%       26      1      27      7   note: species 26 is TotSO3
    s(60,26)=-1; s(60,1)=-1; s(60,27)=1; s(60,7)=1;
    k(60)=5.5e9*(1-alpha2_so3);% modify rate constant for pH (1-
alpha2_so3=HSO32-/TotSO3)

%(62)  SO32- + O-' + H2O = SO3-' + 2OH-   k=3e8 Buxton et al., 1988
Note
%Buxton does not show OH- and water, but is needed for balance (do not
add
%H+ on left hand side to avoid having it affect kinetics)
%       26     17         27      7   note: species 26 is TotSO3
    s(62,26)=-1; s(62, 17)=-1; s(62,27)=1; s(62,7)=2;
    k(62)=3e8*alpha2_so3;% modify rate constant for pH
(alpha2_so3=SO32-/TotSO3)
```

```
%(63) SO3-' + eaq- --> SO32-  (k=2.1e9; Buxton et al., 1988 and 1982HOR
in NRDL/NIST Soln. Chem. database; Buxton has OH- as additional
product, even though it is not balanced
%      27      3        26
    s(63,27)=-1; s(63,3)=-1; s(63,26)=1;
    k(63)=2.1e9;

%(64) SO3-' + SO3-' --> S2O62-   k=1.8e8; 1992WAY/MCE1525-1530 in
NRDL/NIST online database; 1.1E8 Fischer, 1996
%      27      27
    s(64,27)=-2;
    k(64)=1.8e8;

%(65) SO3-' + SO3-' + H2O --> SO42- + SO32- + 2 H+
k=2.3e8;%1992WAY/MCE1525-1530 in NTIS online database; 2.0E8 Fischer,
1996
%      27      27                      26       6
    s(65,27)=-2; s(65,26)=1; s(65,6)=2;
    k(65)=2.3e8;

%(66) SO3-' + CO3-' --> CO2 + SO42-  k = 5.5 e8; 1978LIL/HAN225-
227,NRDL/NIST
%       27      20
    s(66,27)=-1; s(66,20)=-1;
    k(66)=5.5e8;

%(67) SO3-' + O2 --> SO5-'    k = 1.5e9 1984HUI/NET566505669, =2.3E9
1990BUX/SAL245-250B, =1.1E9 1989HUI/CLI361-370 NRDL/NIST, avg=1.6E9
Neta et al., 1988
%      27      13
    s(67,27)=-1; s(67,13)=-1;
    k(67)=1.6e9;

%(68) SO3-' + VC --> (SO3-)-CH2-CHCl•
%      27      28         32
    s(68,27)=-1; s(68,28)=-1; s(68,32)=1;
    k(68)=0;   % arbitrary number

%(69) eaq + (SO3-)-CH2-CHCl•  -->product+ Cl-
%      3           32                    23
    s(69,3)=-1; s(69,32)=-1; s(69,23)=1;
    k(69)=0;   % arbitrary number


%(70) eaq + 1,2-DCA --> •CH2CH2Cl+ Cl-   k=6.4e8 ; 1990GET432-439 from
NIST
%      3      29             31    23
    s(70,3)=-1; s(70,29)=-1; s(70,31)=1;s(70,23)=1;
    k(70)=6.4e8;

%(71) SO3-' + 1,2-DCA --> products
%      27        29
```

```
    s(71,27)=-1; s(71,29)=-1;
    k(71)=0;

%(72) H•+ 1,2-DCA --> Cl- + ·CH2CH2Cl + H+   k=2.3e6;  1990GET432-439
from NIST
%      4     29       23       31       6
    s(72,4)=-1; s(72,29)=-1; s(72,23)=1; s(72,31)=1;s(72,6)=1;
    k(72)=2.3e6;

%(73) eaq-  + N2O + H2O --> N2 + OH• + OH-   k11=9.1E9 M-1s-1  ;
Buxton1988
%      3      30                  1      7
     s(73,3)=-1; s(73,30)=-1; s(73,1)=1; s(72,7)=1;
     k(73)= 9.1e9;

%(74) •OH + VC  --> HOCH2CHCl  k=1.2e10 ; 1971KOE/ASM1108-1116 from
NIST
%      1    28
     s(74,1)=-1; s(74,28)=-1;
     k(74)= 1.2e10;

%(75) •OH + 1,2-DCA --> H2O + CH2ClCHCl• k=7.9e8 1990GET432-439 or
k=2.0e8 1988LAL/SCH773-785
%      1     30
     s(75,1)=-1; s(75,30)=-1;
     k(75)= 7.9e8;
%(76) UV light + VC --> products
%                28
    s(76,28)=-1;

%(77) eaq +•CH2CH2Cl --> products + Cl-  k value is a constant
%      3        31                  23
    s(77,3)=-1; s(77,31)=-1; s(77,23)=1;
    k(77)=k1;
% Set k=0 for reactions to be ignored
k(kzero)=0;



% Note: when new reactions are added, value of n (number of reactions)
must be changed



% Model Notes
% 1. Coefficients in the "s" matrix are obtained from the above
equations.  They are used to determine the second-order
% rate equations and to determine the material balance equations, with
one exception.  That exception is water.
% Water is shown in reactions to provide balanced stoichiometry, but
does not play role in reactions.
```

```
%
% 2. pH is assumed constant, but stoichiometric coefficints are
included
% for production and loss of H+ and OH-, so that changes in pH can be
modeled more
% easily in the future.
% old
%save(file_name, 'n', 'm', 'c0', 's', 'k', 'tstop', 'ph', 'r_vol',
'I0', 'r_area', ...
%      'h_nu_av', 'rtol', 'atol', 'r_l', 'mol_abs', 'abs_coef_water',
...
%      'I0_l', 'q_yield_so3', 'options');

  save('data_input', 'n', 'm', 'c0', 's', 'k', 'tstop', 'ph', 'r_vol',
'I0', 'r_area', ...
      'h_nu_av', 'r_l', 'mol_abs', 'abs_coef_water', ...
      'I0_l', 'q_yield_so3', 'q_yield_vc', 'options', 'c_const');
```

This function calculates the derivatives of concentration with respect to time

```
function dcdt=arpsim254_deriv_xu(t,c,n,m,k,s,mol_abs,abs_coef_water,
I0_l, q_yield_so3,r_l,q_yield_vc, c_const)
% This function calculates the derivatives of concentration with
respect to time for a model that describe
% reactions of radicals in water.
% Modified on 8/11/2010 from ebeam_deriv3
%
% initialize matrices
r=zeros(1,n); % rates of reactions


% Calculate variables
% calculate total absorption coefficinet using molar absorptivities and
% molar concentrations
abs_coef=mol_abs*c+abs_coef_water;
%
% calculate first-order rate constant for rxn 58 (form radicals from
SO3)
% assumes well mixed reactor
k(58)= q_yield_so3*mol_abs(26)*I0_l/abs_coef*(1-exp(-
abs_coef*r_l))*0.001; % 0.001 m^3/L photolysis of sulfite
k(76)= q_yield_vc*mol_abs(28)*I0_l/abs_coef*(1-exp(-
abs_coef*r_l))*0.001;% 0.001 m^3/L, direct photolysis of VC

% calculate rates of reactions
i=zeros(1, n);
j=zeros(1, m);
r=k;

for i=1:1:n;
```

```
   for j=1:1:m;
      if s(i, j) < 0;
         r(i) = r(i)*c(j)^-s(i, j);
      end
   end
end


% calculate derivative from rates of reactions and stoichiometry
dcdt = r*s;
dcdt = dcdt'; % transpose to obtain required column vector

% set derivatives equal to zero for species to be held constant; added
% 7/2012 by BB
dcdt(c_const)=0;

%temp
%if t>10000
%    r.*s(:,26)'
%    c(3)
%    c(26)
%    c(27)
%
%    pause
%end
%end temp
end
```

This program calls ode15s to run the mechanistic model

```
function [t,c]=arpsim254_run_xu
% function to simulate reactions resulting from reaction of radicals
% modified from run_ebeam3.m, which was used to simulate batch
irradiation by electron beam
% Bill Batchelor, modified from run_ebeam3 on 8/11/2010
%
% load values for
n,m,c0,s,k,tstop,ph,r_vol,I0,r_area,h_nu_av,r_l,mol_abs,
%                 abs_coef_water,I0_l,q_yield_so3, options
load data_input;

 tspan = [0:tstop/1000:tstop];
% tspan=[0:tstop];
tic;    % start timer

% call ODE solver
[t, c]=ode15s(@arpsim254_deriv_xu, tspan, c0, options,n, m, k, s,
mol_abs, ...
    abs_coef_water, I0_l, q_yield_so3, r_l, q_yield_vc, c_const);

toc  % stop timer, print time of execution
```

This program generates the plot for experimental data and simulated data

```
% this file will generate the plot with both experimental data and
modeled
% curve
arpsim254_input_xu_plot_DCA; % the file that generates the modeled data
with best values of q and k
[t,c]=arpsim254_run_xu;
t_min=t./60;  %(unit as minutes)
plot(t_min,c(:,29)*1000) % makes plot of 1,2-DCA compound using mM
units
hold on
data=load('dcasul0.1.txt');% import data from txt file
plot(data(:,1),data(:,2))
% calculate the fit error with the following commands
t_min_exp=data(:,1);
c_exp=data(:,2);
c_mod=interp1(t_min,c(:,29),t_min_exp); %calculate modeled DCA
concentration at experiment time
err=sum((c_exp./1000-c_mod).^2)    % sum error squar
werr=sum(((c_exp./1000-c_mod)./(c_exp(1)/1000)).^2)  % weighted sum
error square
```